The Hong Kong Polytechnic University

Department of Land Surveying and Geo-Informatics

Development of Geographic Image Cognition Approach for Land Degradation Assessment with Hyperion Images

Jing Wang

A thesis submitted in partial fulfillment of the requirements for the degree of Doctor of Philosophy

January, 2010

CERTIFICATE OF ORIGINALITY

I hereby declare that this thesis is my own work and that, to the best of my knowledge and belief, it reproduces no material previously published or written, nor material that has been accepted for the award of any other degree or diploma, except where due acknowledgement has been made in the text.

_____(Signed)

_____Wang Jing_____(Name of student)

Abstract

Land degradation is a major problem world-wide. The degradation process is much related to the soil characteristics, topography, vegetation, land types, land use, climate, and human activities. Quantification of land degradation is difficult mainly due to the ambiguously expressed knowledge and the lack of appropriate information. However, there is a pressing need for an objective intelligent methodology of monitoring and assessment of land degradation at a regional scale. This research is to develop an approach of geographic image cognition (GEOIC) to study land degradation and explore its applications by combining hyperspectral images, geographic information and multi-source data/information. The approach is developed based on the methodology of object-based image analysis (OBIA) and realized through the segmentation of land degradation spectral response units (DSRUs) using the diagnostic indicators related to land degradation. The approach was tested and validated in a study area, located in an agriculture-pasture mixed region in the edge of Loess Plateau area with complex physical and geographical situations and widely distributed land degradation.

In this research, the definition, conceptual issues, theoretical underpinning, and the framework of the GEOIC approach were first proposed. Its applications in mapping soil organic matter (SOM) and assessment of land degradation were investigated with the data collected in the study area. The GEOIC for the study of land degradation is to simulate the function and process of the visual interpretations of geoscience experts, and to extract spatial feature, spatial object and spatial pattern of land degradation from remote sensing images and multi-source information. Its realization was done through the DSRU segmentation by land type classification with integrating Hyperion images, geographic information, vegetation, soil, DEM and local information. The developed approach can improve the accuracy of the extraction of land degradation information. The research is the first attempt to apply the approach of GEOIC in the extraction of land degradation information. Moreover, the research provides a methodology of determining the diagnostic indicators related to land degradation and their combinations. The method of determining the diagnostic indicators from local farmers' perception and from the comparison among

different combinations of the diagnostic indicators was also proposed. The results showed that the overall classification accuracy was improved by 11.5% when the optimal combination of diagnostic indicators was used. The higher classification accuracy was achieved at an appropriate level for GEOIC approach than at similar pixel level and for the SAM method and DSLI method. The differences among the results with the GEOIC method and the methods of DSLI and SAM are significant. .

Investigation on SOM mapping with the approach of GEOIC was also performed. The GEOIC approach based on DSRU estimation models for soil parameter mapping is of advantage. The results using Hyperion images are comparable well with the field survey results and close to the results with the Kridge interpolation of soil samples. The developed method can be used for mapping soil features at a regional scale by integrating field data, remote sensing images and various regional variables.

Acknowledgements

Table of Contents

List of Figures

List of Tables

List of Abbreviations

AK   Available Potassium

AN   Available Nitrogen

AP   Available Phosphorus

ASD   Analytical Spectral Device

ASSOD   Soil Degradation in South and Southeast Asia

BDI   Soil Biological Degradation Index

CDI   Soil Chemical Degradation Index

CEC   Cation Exchange Capacity

DDI   Soil Degradation Distance Index

DEM   Digital Elevation Model

DH   Hazard Index of Land Degradation

DRU   Desertification Response Unit

DSLI   Degraded Soil Line Index

DSRU   Land Degradation Spectral Response Unit

FAO   Food and Agriculture Organization of the United Nations

GEOBIA   Geographic Object-Based Image Analysis

GEOIC   Geographic Image Cognition

GLASOD   Global Assessment of the Status of Human-induced Soil Degradation

GLCM   Grey-Level Co-occurrence Matrix

GLDV   Grey-Level Divergence Vector

HRU   Hydrological Response Unit

IARR   Internal Average Relative Reflectance

ISODATA   Iterative Self-Organizing Data Analysis Technique

ISRIC   International Soil Reference and Information Centre

LD   Weighted Mean Index of Land Degradation

LDI   Spectral Index of Land degradation

LDPI   Land Degradation Proportion Index

MCARI   Modified Chlorophyll Absorption Ratio Index

MLR   Multiple Linear Regression

NDVI   Normalized Difference Vegetation Index

OBIA   Object-based Image Analysis

PCA   Principal Components Analysis

PDI   Soil Physical Degradation Index

PLSR   Partial Least-square Regression

PRA   Participatory Rural Appraisal

REA   Representative Elementary Area

RMS   Root Mean Square

SAM   Spectral Angle Mapping

SFI   Soil Fertility Spectral Index

SI   Salinity Index

SLI   Soil Line Index

SNR   Signal-to-Noise Ratio

SOM   Soil Organic Matter

SWIR   Short-Wave Infrared

TK   Total Potassium

TN   Total Nitrogen

TP   Total Phosphorus

UNCCD   United Nations Convention to Combat Desertification

UNEP   United Nations Environment Programme

VHSR   Very High Spatial Resolution

VNIR   Visible/Near Infrared

Chapter 1

Introduction

1.1 Monitoring of land degradation

Population, land resources, and environment are three major subjects for human being. Land resources are defined as to be used land by human being under the definite technologies within a definite period (Sivakumar and Ndiangui, 2007). Land degradation is a major issue for land resources, and must be monitored. It is difficult, however, to trace the origin of the term "land degradation". An international legally binding definition by the United Nations Convention to Combat Desertification (UNCCD) describes *"land degradation"* as *"reduction or loss of the biological productivity resulting from land uses or combination of processes, such as soil erosion, deterioration of properties of soil and long-term loss of natural vegetation"*. From the definition, land degradation implies a reduction of the potential productivity of the land (e.g., soil degradation and accelerated erosion, reduction of the quantity and diversity of natural vegetation) and results from a long history of human pressure upon land resources as well as from interactions between varying climatic characteristics and ecologically unbalanced human intervention (UNCOD, 1977; Dregne and Boyadgiev, 1983; Oldeman *et al*., 1990; Hill *et al*., 1995).

Land degradation is a major problem world-wide (Oldeman, 2000). Five global land degradation assessments, which were carried out between 1977 and 2003 and presented degradation estimates ranging 15% to 63% of global degradation, differ in the selection of measurable attributes of land degradation, in the quality of the data sets, and in their spatial coverage (Sivakumar and Ndiangui, 2007). Land degradation is also a serious issue in China. Soil erosion, land desertification, and grassland

degradation occur annually in large scale with total areas of about 10×10^3 km^2, 2.5×10^3 km^2, and 2.0×10^5 km^2, respectively. It is estimated that over one-third of terrestrial land area in China is threatened by land degradation, largely because of inappropriate land-use. Land degradation together with the population growth makes negative impacts on food production and living conditions. Therefore there is a considerable interest in the study of land degradation processes. One of the main study subjects is to monitor and assess the situation of land degradation, for which collection of all-scaled information on land degradation is required.

Land degradation is closely related to physiognomy, soil characteristics, vegetation, land types, land use/ land cover, climate, and human activities. Therefore land degradation can be estimated and measured by these diagnostic indicators obtainable with remote sensing techniques and other approaches (Dregne and Boyadgiev, 1983; Oldeman, 2000; Stroosnijder, 2005). In general, monitoring and assessment of land degradation are based on two groups of techniques/approaches: conventional soil survey techniques and remote sensing techniques. The conventional soil survey techniques usually measure soil physical and chemical parameters as well as their changes for assessing the situation of land degradation, while the remote sensing techniques generally use satellite images for land degradation classification. On the other hand, the conventional classification methods using remote sensing images are pixel-based. Most of the studies used Landsat TM and SPOT images with the spectral index method for land degradation mapping at regional scale (Escadafal *et al*., 1994, 1995; Haboudane *et al*., 2002; Wang, 2006; Omuto and Shrestha, 2007; Chen and Rao, 2008; Gao and Liu, 2008;). Some investigators developed spectral unmixing methods, spectral angle matching techniques, and geostatistic methods for land degradation classification (e.g., Van der Meer, 2001; Shrestha *et al*., 2005; Boschetti *et al*., 2007; De Jong and Van De Meer, 2007). Many studies showed that it is difficult to quantify land degradation due to several factors/reasons, such as the ambiguously expressed knowledge, benchmark, diagnostic indicators, units, and scaling of land degradation assessment, and the limitations of the techniques of image analysis and information mining. In addition, the lack of appropriate information on land characteristics, vegetation cover and soil parameters is commonly regarded as a major obstacle in this research field (Hudson, 1971; Dregne

and Boyadgiev, 1983; De Jong, 1994; Escadafal *et al*., 1995; Williams and Balling, 1996; Nicholson *et al*., 1998; Menenti *et al*., 1999; Stroosnijder, 2005; Wang, 2006; Sivakumar and Ndiangui, 2007; Chen and Rao, 2008; Gao and Liu, 2008).

Recent advances in sensor technology and digital imaging techniques, along with ever increasing spectral and spatial resolutions have made possible to develop new and intelligent methods of exploiting imaged information for decision making. The intelligent methodology of monitoring and assessment of land degradation by integrating remote sensing images, geographic information, land information and geoscience knowledge has emerged with the development of techniques of geographic image analysis.

1.2 Objectives and key issues of this research

The goal of this research is to develop an approach of Geographic Image Cognition (GEOIC) to study land degradation and initiate its applications by combining hyperspectral images, geographical information and multi-source information. The approach will be tested and validated in a study area, located in an agriculture-pasture mixed region in the edge of Loess Plateau area with complex physical and geographical situations and widely distributed land degradation. This research will complement and improve the theory and methodology for land degradation research in terms of eco-environment protection and sustainable land use. To achieve the above goal the following four main issues need addressing.

 (1) The conception, connotation, and framework of the Geographic Image Cognition (GEOIC) for the study of land degradation need to be developed, which are based on the methodology of Object-based Image Analysis (OBIA). The term G*eographic Image Cognition* (GEOIC) is used in a literal sense to mean knowing or knowledge on images using geoscience knowledge, and in an intrinsic sense to mean the objectively knowing or knowledge on remote sensing images and multi-source information using geoscience knowledge. It provides an integrated approach for the extraction of land thematic information. The approach is developed from the methodology of OBIA. In other words GEOIC is an approach of developing the

automated methods to partition remote sensing imagery and multi-source information into meaningful image-objects and to assess their spatial, spectral, geographic and temporal characteristics in order to generate thematic information. The GEOIC approach extends the application fields of the OBIA methodology. Moreover, the approach focuses not only on the extraction of thematic information, but also on mining of thematic information and the quantification of ambiguously expressed knowledge. The approach is realized through the segmentation of geo-objects or meaningful image objects with remote sensing information, geographic information, and vegetation, soil, and other ancillary information. The advantages of the GEOIC approach include its emulation of a human interpreter's ability in image interpretation and integration of different types of geo-data and a set of fuzzy-logic-based rules into an object-based analysis process.

(2) The method to select the appropriate diagnostic indicators related to land degradation and incorporate them into the GEOIC needs to be created. The GEOIC approach is an integrated approach for the extraction of land degradation information. It needs to integrate various diagnostic indicators related to land degradation. Therefore the second key issue is to develop a reliable method of choosing and determining the appropriate diagnostic indicators and the method of incorporating these indicators into the approach of GEOIC.

(3) The method for up-scaling the estimation models for soil organic matter (SOM) mapping at regional scale under the approach of GEOIC needs to be studied. There exist some problems in the application of the established estimation models between the soil parameters and spectral reflectance for the interpretation of multi-spectral or hyperspectral images without making any corrections for the change of scale. Therefore, the third key issue is to determine the appropriate up-scaling method to the estimation models and investigate an effective way to map soil parameters at regional scale.

(4) The systematic approach to the application of the GEOIC approach for extracting land degradation information needs developing. There exist a number of methods for

land degradation classification. The merits of the GEOIC approach over others need to be demonstrated.

In relation to the above-mentioned four key issues, this study mainly includes three parts:

✧ To discuss some conceptual issues and the theoretical background on GEOIC for the study of land degradation. This part aims at addressing the first key issue for developing the approach of GEOIC for land degradation study.

✧ To apply the GEOIC approach in SOM mapping related to land degradation. The aim is to investigate the up-scaling method of the estimation models for SOM mapping using hyperspectral remote sensing images and multi-source data through the segmentation of Land Degradation Spectral Response Units (DSRUs). This part focuses on exploring the applicability of the GEOIC approach for mapping SOM to address the third key issue.

✧ To apply the developed GEOIC approach in the extraction of land degradation information. DSRUs as land degradation mapping units and the diagnostic indicators for land degradation evaluation are determined from the comparison of different combinations of diagnostic indicators with the perception of local farmers. The approach is compared with the Spectral Angle Mapping (SAM) method and Degraded Soil Line Index (DSLI) method. This part aims at addressing the second and fourth key issues.

1.3 Organization of the thesis and summary of contributions

After this introduction, Chapter 2 focuses on research background and literature review about the classification and mapping methods of land degradation using multi-spectral and hyperspctral remote sensing data.

Chapter 3 discusses some conceptual issues and the theoretical underpinning of GEOIC for the study of land degradation for developing the methodology. In this chapter, some factors influencing visual cognition on images are analyzed using the results obtained from geo-experts, skilled interpreters and simple users through a

questionnaire survey. The conception, connotation, models and mathematics methodologies related to the GEOIC for the study of land degradation is also discussed from different viewpoints. The framework of the GEOIC for the study of land degradation is then proposed.

The GEOIC approach is tested and validated in a study area. Chapter 4 describes the situation of the study area and the collected data and methods of pre-processing Hyperion images in this research.

Chapter 5 is devoted to the application of the GEOIC approach in SOM mapping using the data collected in the study area. The objective of this chapter is to investigate the up-scaling method of the estimation models for mapping SOM. In this chapter, the features of soil parameters, soil types and soil spectrums, and SOM spectral responses are discussed. The up-scaling method is then developed by setting up the SOM estimation models based on DSRUs using hyperspectral remote sensing images and multi-source data through the segmentation of DSRUs.

Chapter 6 focuses on the application of the GEOIC approach for extracting land degradation information by land type classification using the data collected in the study area. The GEOIC approach is realized by the segmentation of DSRUs using Hyperion images, geographic information, vegetation, soil parameters, Digital Elevation Model (DEM) and local information. The diagnostic indicators of land degradation responding to spectrum feature, and other features of physiognomy, vegetation, and soil are determined by a comparison of the results of land degradation classification using different combinations of diagnostic indicators with the perception of local farmers. In addition, the GEOIC approach is compared with the SAM method and DSLI method using the data in the study area. The results showed a significant improvement in the accuracy of land degradation classification with the GEOIC approach and illustrated the development of a systematic approach for the quantification of ambiguously expressed information on land degradation.

Chapter 7 summarizes the findings and provides recommendations for further study.

Figure 1.1 shows the flow of the research and relations among different sub-topics and chapters in the thesis. Through a literature review on monitoring and assessment of land degradation using remote sensing images, especially using hyperspectral remote sensing images, the key issues for the development of methodology are discussed. The conception, connotation, and framework of GEOIC on studying land degradation are formulated

Because SOM is one of important diagnostic indicators related to land degradation, the second step is evaluating the potential of hyperspectral data for mapping soil parameters with the approach of GEOIC. The purpose is to find the quantitative relations between related feature parameters and the SOM contents and develop the up-scaling method of estimation models for SOM mapping at regional scale using Hyperion images and multi-source data through the segmentation of DSRUs.

Chapter 2   **Chapter 3**

| Literatures review | → | Framework of GEOIC on studying land degradation | ← | Related methods and theories |

Chapter 4

Data collection

| Soil features | Soil spectrum | Land use map | Hyperion image | Ancillary data |

Chapter 5

Registration with related data

Application in SOM mapping

| Spectral response analysis and SOM mapping | ↔ | Segmentation of land degradation spectral response units (DSRU) |

| Farmer survey | ↔ | Determining the diagnostic indicators of land degradation |

Chapter 6

Initial land degradation classification

SAM and DSLI methods

| Geoscience knowledge rules | → | Mining and extraction of information |

Mapping based on the pixel by pixel method

Conclusions by comparison

Chapter 7

Conclusions and recommendations

Figure 1.1 The research flowchart and the relations among different sub-topics and chapters

The third step is the application of the GEOIC approach for the extraction of land degradation information, which is illustrated with the example of the study area. DSRUs, as land degradation mapping units, are determined by the segmentation of Hyperion images and multi-source information. The diagnostic indicators for land degradation evaluation are also determined by the comparison of different combinations of diagnostic indicators with the perception of local farmers obtained from a farmer survey. The GEOIC approach is realized through the segmentation of DSRUs by land type classification using geoscience knowledge and local knowledge.

A comparison of the GEOIC approach with the pixel by pixel classification methods is done to demonstrate the merits of the approach of GEOIC.

This research enriches the theory and methodology for land degradation research in terms of eco-environment protection and sustainable land use. The major conclusions and achievements of the research are summarized below:

(1) This research developed the approach of GEOIC for the study of land degradation based on the methodology of OBIA. The definition, conceptual issues, and the theoretical underpinning, and the framework of the approach were proposed. The key objective of GEOIC on studying land degradation was to simulate the function and process of the visual interpretations by experts, and extract spatial feature, spatial object and spatial pattern of land degradation from remote sensing images and multi-source information. It is an approach to develop the automated methods to partition remote sensing images and multi-source data into DSRUs and to assess their spatial, spectral, geographic and temporal characteristics.

(2) This research is the first attempt to apply the approach of GEOIC in the extraction of land degradation information with remote sensing images and multi-source information. The approach was realized through the DSRU segmentation by land type classification with integrating Hyperion images, geographic information, vegetation, soil parameters, DEM and local information. Especially, the approach was tested and validated in a study area located in Hengshan County in ShaanXi province, agriculture-pasture mixed area in Loess Plateau in China. It provided a systematic way for the extraction of land degradation information with hyperspectral images at a regional scale and demonstrated the improvement in the accuracy of land degradation assessment.

(3) This research investigated and developed the SOM mapping method related to land degradation with hyperspectral images and soil spectral at a regional scale with the approach of GEOIC. The *in-situ* estimation models based on the relationship between the SOM contents and the spectral reflectance were developed by determining the sensitive bands for estimating SOM. The application of the *in-situ*

estimation models to images needs compensating for the change of scale. The DSRU estimation models were developed based on the relationship between the contents of SOM and the spectral and regional variables of DSRUs. The DSRU estimation model is not only based on some variables in *in-situ* models, but also some environmental variables to compensate for the change of scale. The method provided a way for mapping soil features at a regional scale by integrating field data, remote sensing images and regional variables.

(4) This research also provided a reliable method of integrating and determining the diagnostic indicators related to land degradation. Under the cognition mode of feature-object-pattern, DSRUs were segmented in the support of the integration of Hyperion images and multi-source information of various diagnostic indicators based on geoscience knowledge and geographic information. DSRU is an ecologically and geographically and spectrally homogeneous area with similar characteristics of physiognomy, vegetation, soil and image spectral information. It links hydrological and erosion processes with spectral response of land degradation. It is of significance not only to extract land degradation information, but also to integrate the diagnostic indicators related to land degradation. Moreover, the research firstly proposed the method of determining the diagnostic indicators related to land degradation from the local farmers' perception and from the comparison of different combinations of diagnostic indicators.

Chapter 2

Research Background and Literature

Review

According to an international legally binding definition by the United Nations Convention to Combat Desertification (UNCCD), land is described as a *"terrestrial bio-productive system that comprises soil, vegetation, other biota, and the ecological and hydrological processes that operate within the system"*. It is the result of various natural landscape forming processes and human interference. The definition and connotation of land degradation described by UNCCD are mentioned in the introduction. From the definition and connotation, the knowledge on land degradation is usually expressed ambiguously and is difficult to be quantified. It can be measured and assessed by some diagnostic indicators, such as physiognomy, soil characteristics, vegetation, land types, land use/ land cover, climate, and human activities, and with remote sensing techniques and other approaches. This chapter reviews and comments on the literature about the basic conceptual issues of land degradation, methodologies for extracting land degradation information and image classification. Based on the review and comments the objectives of this research are clearly formulated. Section 1 addresses the background on monitoring of land degradation with remote sensing. Section 2 focuses on literature review about mapping of soil parameters related to land degradation. Section 3 summarizes the methodologies of land degradation classification.

2.1 Background on monitoring of land degradation with remote sensing

2.1.1 Scale issue related to land degradation

The issues of scale related to monitoring and assessment of land degradation were studied by many researches. Monitoring and assessment of land degradation is a process of investigating the characteristics, processes and distribution of land degradation for understanding a complex landscape. It is now widely recognized that landscape is a complex system having a hierarchical structure where dominant patterns and processes exist at specific scales (O'Neill *et al*., 1991; Walsh *et al*., 1998; Wu and Marceau, 2002; Hay *et al*., 2003). To better understand and quantify monitoring and assessment of land degradation, useful concepts of scale related to remote sensing information have been developed.

Scale is the fundamental determinant of hierarchical structure (Goodchild, 2001). In general terms, scale corresponds to one's 'window of perception'. More exactly, scale refers to the spatial dimensions at which entities, patterns, and processes can be observed and characterized. Furthermore, every scale reveals information specific to its level of observation (Marceau, 1999). No single scale is sufficient for assessing the varying sized, and spatially arranged components on the planet, a society, or in any complex system. Therefore, to appropriately monitor, model, and manage these environments a multi-scale (i.e. more than a single scale) approach is necessary (Lam and Quanttrochi, 1992; Hay and Marceau, 2004). Gibson *et al*. (2000) presented the definitions for the basic terms related to the concept of scales (Table 2.1). The term scale is most commonly used in relation to the absolute or relative scale of space.

Table 2.1 Definitions of the basic terms related to the concept of scale according to

Gibson *et al*. (2000)

Term	Definition
Scale	The spatial, temporal, quantitative, or analytical dimension used to measure and study any phenomenon
Extent	The size of the spatial, temporal, quantitative, or analytical dimension of a scale
Resolution (grain)	The precision used in the measurement
Absolute scale	The distance, time, or quantity measured on an objectively calibrated measurement device
Relative scale	A transformation of an absolute scale to one that describes the functional relationship of one object or process to another (e.g., the relative distance between two locations based on the time required by an organism to move between them)

Remote sensing information refers to the pixel, gray level, texture, gray spectrum and texture analysis, dependent variables of image, image simulation and the information model (Ma, 1997). The basic geometric unit of an image is pixel. There are four scales in different forms in the conversion process from remote sensing image domain to land information domain: namely (1) cartographic scale, (2) scale of spatial extent, (3) scale of action, and (4) spatial resolution. The cartographic or map scale refers to the ratio of a distance on a map to the corresponding distance on the ground. A large-scale map covers a small area with a higher detail, while a small-scale map covers a larger area with less detail. On the contrary, the geographical or observational scale refers to the size or spatial extent of the study. A geographic large-scale study covers a large area of interest, while a geographic small-scale study covers a small area (Cohen *et al*., 2003). The operational scale refers to the level at which observation processes operate in the environment (Turner *et al*., 2003). This scale, also called scale of action, represents a level at which a certain process phenomenon is best observed. Spatial resolution refers to the smallest distinguishable parts of an object, for instance a pixel size of a raster map or remote sensing images. The processes of land degradation at various scales reflect the various spatial distributing structures of land degradation types. Monitoring and assessment of land degradation depend on the above four types of scale. The study area (or geographic observation scale) determines the data of different spatial resolution required.

Scaling means a process of transferring data or information from one scale to another scale. As noted by Jarvis (1994), scaling represents a real challenge because of the nonlinearity between processes and variables, and heterogeneity in properties that determines the rates of processes. Practically, scaling can be performed by bottom-up or top-down approach. Up-scaling is to derive information at a larger scale with the information at a smaller scale, while down-scaling is decomposing the information at one scale into its constituents at a smaller scale. The scaling methods for monitoring and assessment of land degradation are based on statistical methodologies and geographical analysis methodologies, in which the most challenges lie on spatial heterogeneity of soil and vegetation and other factors indicating land degradation (Woodcock and Strahler, 1987). The up-scaling of environmental processes simplifies landscape complexity. Such a simplification is a critical issue in land surface modeling as ecosystem simulations depend closely upon the representation of land surface heterogeneity. This may inevitably cause significant biases in model prediction because many homogeneous phenomena or changes in environmental variables at a regional scale might be heterogeneous in valley or farm scale. To partially reduce the biases in environmental model simulations, several approaches had been proposed in the past two decades to improve the representation of land surface heterogeneity in these models (Wood, 1994; Pellenq *et al*., 2003; Bo and Wang, 2003). Remote sensing offers a great potential for scaling. It provides the required data not only for up-scaling or down-scaling physical models, but also for validating their outputs. Turner *et al*. (1996) conducted a study to determine the effects of spatial scale on the results obtained from a spatially distributed biogeochemical model. The results clearly indicated the differences in the inputs and outputs as spatial resolution is coarsened. Recently, scientists have demonstrated that remote sensing is a particular case of the modifiable areal unit problem (MAUP) (Marceau *et al*., 1994). This explains the inconsistencies in the results when remote sensing data are used to produce thematic maps or as inputs into physical models, without taking into account the impacts of scale. As noted by Raffy (1992), remote sensing models are often based on a relationship between a soil-level parameter and the sensor reflectance at a given wavelength. The general practice is to apply these models to the reflectance measured from satellites on heterogeneous surfaces, without any correction to compensate for the change of scale. Therefore, it is of

considerable importance that the scale effects in remote sensing should be fully understood to avoid any arbitrary and erroneous results.

2.1.2 Mapping unit related to land degradation

Mapping unit is another major factor affecting the results of monitoring and assessment of land degradation. The mapping unit can be a nation, a region, a county, a town, a village, a field, a patch, or a pixel. The mapping unit for monitoring and assessment of land degradation should be an ecologically homogeneous tract of land at a scale. It describes the characteristics of the most obvious (mappable) land attributes: physiognomy, soil, vegetation, and land use and land cover (including human alteration of them). A landscape is supposed to be divided into many ecologically and geographically homogeneous areas with similar characteristics of physiognomy, vegetation, and soil. A homogeneous area with similar soil-vegetation pattern typically covering a hill slope or a part of a hill slope is thought to be the result of hydrological and erosion processes related to land degradation. The mapping unit affects the accuracy of the extracted land degradation information. Different spatial scale produces the results of different accuracy: with larger scale, the representation of environmental characteristics is less and the precision of monitoring and assessment of land degradation will be lower.

In the hydrology, 'naturally homogeneous areas' were introduced as a necessary tool for hydrological modeling. These 'naturally homogeneous areas' in hydrology are referred to as Representative Elementary Area (REA) or Hydrological Response Unit (HRU), assuming non-variability of the data and parameters within its delineation (De Wit *et al*., 2005). A similar concept called 'Desertification Response Units' (DRUs) was introduced in the field of land degradation research, aiming at linking hydrological and erosion processes from one temporal and spatial resolution to another (Imeson *et al*., 1995; Imeson, 2000). The classification of DRUs was based on spatial patterns of soil and vegetation because these patterns are thought to be the result of the movement of water, water availability and the redistribution of water in the landscape or the catchments. Based on these ideas, the 'Land Degradation Spectral Response Unit' (DSRUs) is proposed in this study as the unit for monitoring

and assessment of land degradation using remote sensing data. The classification of DSRU is based on spatial patterns of soil and vegetation, and spectral features and geographic information.

2.1.3 Benchmark related to land degradation

Determination of ecological benchmark is one of major topics in land degradation research. The classification of land degradation is generally based on a defined benchmark with various degrees of degradation, i.e. non-degraded land, slightly degraded land, moderately degraded land, and highly degraded land. However, the benchmark is difficult to identify in practice because of difficulty in finding a "baseline" which ecologically has not been affected by human activities. Many studies on the benchmark for land degradation evaluation were conducted. The academic ecological benchmark (or called absolute baseline) which is the top vegetation communities according to natural environment and climate was proposed by The Food and Agriculture Organization of the United Nations (FAO) and United Nations Environment Program (UNEP) (Dregne and Boyadgiev, 1983). From the ecological point of view, the changes in vegetation structure from the top vegetation communities to others are directly indicative to land degradation (Grainger, 1992). On the contrary, some researchers suggested that the baseline should be relative, which changes with time, because most vegetation communities in dry land area differ from its own vegetation communities due to climate variation and human activities (Sun and Li, 1999). They proposed that the preserved land regarded as non-degraded land in a local area was used as the relative baseline for land degradation assessment. Another group of researchers proposed the use of the average situation in a defined time period with the detailed degradation data in the area as baseline. Three kinds of theories for land degradation assessment were developed: the human-induced soil degradation based on the assessment of absolute degraded land with diagnostic indicators (representative one: the 'Global Assessment of the Status of Human-induced Soil Degradation' (GLASOD) project by the International Soil Reference and Information Centre (ISRIC) and UNEP) (Oldeman *et al*., 1990); the assessment of relative degraded land affected by human activities based on a combination of land productivity and management level (representative one: the

'Soil Degradation in South and Southeast Asia' (ASSOD) project by ISRIC, UNEP and FAO); and the comprehensive assessment of land degradation based on landscape diversity or spatial heterogeneity according to differences in soil degradation and vegetation degradation in ecological system (representative one: by Russia academic institute). Among the three theories, the theory of relative baseline was widely developed by the most of land degradation researchers at a regional scale (Wang, 2006). However, it should be noted that different factors affect the process of land degradation at different scales in different regions. The development of the methods to extract land degradation information related to land productivity and management level is a very important research area.

2.1.4 Methodology for monitoring and assessment of land degradation

Extraction of land degradation information is of importance for monitoring and assessment of land degradation situation. It involves the collection of information on climate, soil, vegetation, physiognomy, land resources and productivities, and the interpretation of all the information/data. The knowledge on land degradation is often expressed ambiguously. Consequently, land degradation can sometimes be estimated or measured directly, but often be indirectly estimated from land characteristics and/or diagnostic criteria. A diagnostic criterion, also named as land degradation evaluation indicator, is a variable serving as a basis for assessing land degradation in a given area (Doran and Parkin, 1994; Imeson, 2000; Stroosnijder, 2005; Sivakumar and Ndiangui, 2007). The variables can be land characteristics, physiognomy, soil characteristics, vegetation, land use/land cover, climate, and human activities, or function of them. There is considerable freedom in the way these various diagnostic indicators are integrated (Zonneveld, 1989). It is therefore of importance to develop a systematic approach to the evaluation of land degradation through an integration of these diagnostic indicators.

The methodologies of geo-analysis on earth surface using remote sensing images were developed in recent years. Chen and Zhao (1990) proposed an approach of geographic image analysis, which has two functions: the provision of the information that can be obtained with remote sensing and the analysis of the information that

cannot be reflected on remote sensing images according to the bi-dimension and their correlations. On the basis of the above idea, Luo (2000) proposed a concept of remote sensing intelligent geo-interpretation model. The approach of geographic image analysis focuses on extracting, coding, reserving, accessing and utilizing remote sensing information using artificial intelligence. It is a transformation process from physical and / or semantic image information to precisely defined codes or thematic mapping (Zhou *et al*., 2001; Luo, 2000). It is also a process of image interpretation and decision making by imitating geoscience experts. The models of geographic image analysis are its core (Luo *et al*., 2001). Combined with the spatial cognition behaviors and cognition psychological studies, the modes of spatial cognition were studied and the idea of GEOIC was proposed by several researchers (e.g., Lu *et al*., 2005; Luo *et al*., 2001; Zhou *et al*., 2001). Cognition is the process of objectification cognition. Spatial cognition is also named as spatial object cognition. Therefore, spatial object is the key target in the research on geographic image cognition. The object-based image analysis is the core research of geographic image cognition in remote sensing domain. These ideas and concepts were applied in the classification of land cover, land use and the spatial pattern of earthquake-induced crust deformations based on the information on spectrum, texture and spatial information in images (Luo *et al*., 2001; Lu *et al*., 2005).

The advancement of feature recognition and image analysis techniques facilitates the extraction of thematic information to support policy and decision making. As a strong driver, the availability of Very High Spatial Resolution (VHSR) data and the ever increasing use of geo-information for all kinds of spatially relevant management issues have catalyzed the development of new methods to exploit image information more 'intelligently'. The methodology of Object-Based Image Analysis (OBIA) has emerged with the development of new earth observation techniques (Baatz *et al*., 2008; Lang, 2008). The OBIA is mainly to provide adequate and automated methods for the analysis of VHSR imagery by describing the imaged reality using spectral, textural, spatial and topological characteristics. It offers a framework for machine-based interpretation of complex classes, defined by spectral, spatial and structural as well as hierarchical properties (Burnett and Blaschke, 2003; Hay *et al*., 2003; Benz *et al*., 2004). The ultimate aim of the OBIA should focus on incorporating and

developing geography-based intelligence (Blaschke *et al*., 2005; Lang, 2008). The methodology of the OBIA was developed from a predominantly pixel-spectra based model to a dynamic multi-scale object-based contextual model that attempts to emulate the way in which human interprets images. It can play a key role in image understanding (Blaschke, 2003; Lang and Langanke, 2005).

There are numerous challenges in the path from pixel to object and to intelligence which need to be addressed. Several researchers have proposed new concepts and studied the methodology of OBIA related to geographic image analysis and GEOIC. Hay and Castilla (2006) proposed the concept of *Geographic Object-Based Image Analysis* (GEOBIA) based on the previous studies on the OBIA. GEOBIA is the automated methods to partition remote sensing imagery into meaningful image-objects and assess their characteristics through spatial, spectral and temporal scales, so as to generate new geographic information in GIS-ready format. Lang and Tiede (2007) proposed the term *geon* to describe generic spatial objects that can be defined as a homogenous geo-spatial referencing unit, specifically designed for spatial-related policy making. Having studied the method of geo-analysis of remote sensing images and OBIA, one can find that there is a close relation between GEOIC and OBIA. All the above studies focused on developing the automated intelligent methods to extract thematic information to imitate the visual interpretation on images.

The idea and concept related to GEOIC can be applied in land resource researches using remote sensing images. The recent developments in the methodology for extracting land thematic information and land evaluation are to improve the precision and veracity of information extraction and evaluation through an integration of multi-source data. A new area of development is the approach of GEOIC, which integrates the models of statistics, artificial neural network and logical reasoning for intelligent processing and analysis on multi-source information combined with geoscience knowledge.

Land degradation information is one of major types of land information. Therefore, the approach of GEOIC can be applied in extracting thematic information on land degradation. The approach of GEOIC on studying land degradation should simulate

the function and process of the visual interpretation by experts and extract spatial feature, spatial object and spatial pattern of land degradation from remote sensing images based on integrating geoscience knowledge and geographic information and multi-source information on various diagnostic indicators.

Land degradation research has gained a great impetus over the last two decades. Many successful case studies were reported and several new methods were developed. However, little effort has been made towards building the conceptual foundation for the approach of GEOIC, in particular the methodological foundation of GEOIC on studying land degradation, and the method for an efficient integration of the diagnostic indicators.

2.2 Mapping of soil parameters using remote sensing images

Soil characteristics are major diagnostic indicators related to land degradation. Attention should be paid to the comprehensive responses of soil physical and chemical features to their spectral reflectance characteristics. Soil spectral data collected in lab and field were used to detect and map soil surface features by some researchers (e.g., Baumgardner *et al*., 1985; Hunt *et al*., 1987; Mulders, 2001; De Jong *et al*., 2001; Van der Meer, 2001). Several papers analyzed the absorption features in the spectral region between 0.4μm and 2.5μm wavelengths and correlated them with soil features, such as soil color, SOM, soil moisture, particle size distribution, soil texture, iron oxides and soil mineralogy (e.g., Al-Abbas *et al*., 1972; Dalal and Henry, 1986; Frazier, 1989; Escadafal, 1994; Ben-Dor and Banin, 1995; Ben-Dor *et al*., 1997; Ingleby and Crowe, 2000; Thomasson *et al*., 2001; Ben-Dor *et al*., 2002; Reeves *et al*., 2002; Liu *et al*., 2002; Cozzolino and Morón, 2006; Roder *et al*., 2008). Most of the early studies identified the relations between organic carbon content and spectral variables based on the reflectance in the visible range of the solar spectrum (Shields *et al*., 1968; Al-Abbas *et al*., 1972; Page, 1974). Some studies showed that soil chemical features and their physical structure also influenced the VIS-NIR spectra. The study by Bowers and Hanks (1965) indicated that the oxidation of organic matter would increase the spectral reflectance of soil, as well as the smaller particle size. Some studies revealed that soil reflectance decreased in the

wavelength range of 0.4μm to 2.5μm with an increase in organic matter content (Hoffer and Johannsen, 1969; Latz *et al*., 1984). Moreover major efforts were made to correlate specific spectral bands with SOM. Stoner and Baumgardner *et al*. (1985) identified five distinct soil reflectance types by spectral curve shape and the spectral absorption features related to soil constituents. Ben-Dor and Bannin (1994) used the full reflective spectrum to predict SOM and other mineralogical and chemical soil properties based on multivariate statistics. Galvão and Vitorello (1998) set up a relationship between the SOM content and soil spectral reflectance in the 0.5μm to 0.7μm region using AVIRIS data. Bocheng *et al*. (2004) studied the spectral characteristics of brown-humid soil to estimate SOM content and found that the SOM content was highly correlated with the original reflectance, the logarithm of the reciprocal reflectance in 0.447μm, the first differentiation of the logarithm of the reciprocal reflectance in bands of 0.516μm and 0.615μm. Hill and Schutt (2000) found organic matter had a strong influence on soil reflectance and proposed a method to parameterize soil reflectance spectra with the variables related to specific shape characteristics of the spectral profile. The method can be used to estimate organic carbon concentrations in soil with regular calibration of the regression models. Thomas *et al*. (2006) investigated the use of both Multiple Linear Regression (MLR) and Partial Least-Square Regression (PLSR) to construct a model, which can simultaneously estimate topsoil organic matter and texture from the images for high resolution topsoil mapping.

Recent spectroscopic studies have shown that SOM, soil types, grain size, soil moisture, and other parameters are indicative of land degradation and could be predicted with hyperspectral remote sensing technique (Shrestha *et al*., 2005). Hyperspectral remote sensing technique not only produces laboratory-like reflectance spectra with absorption bands specific to object's properties, but also helps improve the accuracy of mapping soil parameters (Pieters and Mustard, 1988; Kruse *et al*., 1993). Soil spectral data have been used to detect and map soil degradation. Several multivariate regression models have been developed (Krishnan *et al*., 1980; Leone and Sommer, 2000). Krishnan *et al*. (1980) found that four types of soil reflectance in his study had no spectral absorption features related to SOM in the range of 0.8-2.4μm wavelength and the correlation coefficients between the SOM

content and spectral reflectance in 0.623μm and 0.564μm were high. Leone and Sommer (2000) applied the multivariate statistical analysis in high resolution laboratory reflectance spectra of soil samples to assess soil degradation levels in a test site. Some studies directly mapped soil degradation using soil spectral features. De Jong (1994) assessed the soil hardening and classified the major soil types applying hyperspectral remote sensing in a Mediterranean environment. Dematte *et al*. (2004) developed a methodology based on spectral reflectance to evaluate soil types and soil tillage systems related to soil erosion. Vagen *et al*. (2005) studied a method of sensing landscape level change in soil fertility following deforestation and conversion in the highlands of Madagascar using VIS-NIR spectroscopy.

Though some of the studies were proved to be successful in estimating the relationship between the soil parameters and soil spectral reflectance in both laboratory and field environments, and in mapping soil conditions, there is not an effective way to map soil parameters at a regional scale so as to derive topsoil physical/chemical characteristics. It should be mentioned that several regression models between the soil parameters and soil spectral reflectance are rarely, or not at all, directly applied to the interpretation of multi-spectral or hyperspectral images. This is mainly due to the following two reasons:

(i)   Traditional multi-spectral satellite images such as Landsat with several bands and wide band width of 100 to 200 um do not have sensitive spectral response to soil surface features (De Jong, 1994). The established relationship cannot be transferred to the limited band set of multi-spectral images.

(ii)   The application of the model of a soil-level parameter with respect to sensor reflectance to images lacks sufficient corrections to compensate the change of scale. Relationship models, established based on detail point-based data in small area or local scale, may lead to estimation errors and un-realistic estimates of surface condition at extrapolation to a regional scale (Raffy, 1992; Raffy and Gregoire, 1998).

Many researchers have attempted to determine the most appropriate up-scaling technique for the models at different scales (Hay *et al*., 1997; Raffy and Gregoire, 1998). Hay *et al*. (1997) described a scaling technique that employs object-specific kernels to analyze and incorporate the influence of different sized, shaped, and spatially distributed objects within the up-scale images. Hay and Marceau (1998) stressed that the object-specific up-scaling ideas may provide a new framework for potential solution of a series of difficult scale issues. There are still a lot of rooms for investigating the methods of up-scaling estimation models for soil mapping with hyperspectral satellite images at regional scale.

2.3 Methodologies for land degradation classification with remote sensing images

In general, monitoring and assessment of land degradation are based on two types of data/information: conventional soil survey data and remote sensing data. The early efforts to map land degradation only based on conventional soil survey data have been criticized (UNCOD, 1977; UNEP, 1987; Hellden, 1991; Thomas and Middleton, 1994; Nicholas *et al*., 1997). Although many studies about land degradation were successfully done in field, there were no better ways to make the findings from field studies at patch-scale and valley-scale applicable in a relatively large area. Thus, there is a pressing need for an objective measure of land degradation at a regional scale by a synergy of remote sensing data and other types of information.

With the development of remote sensing technology, it was believed that remote sensing can significantly contribute to solving these problems (Hill *et al*., 1995). Soil and vegetation parameters, influenced by land degradation, proved to be detectable using numerical analysis of remote sensing images (Baumgardner *et al*., 1985). The information on vegetation cover can be directly extracted from images through a relationship between vegetation indices and vegetation cover. Some authors established the relationship between soil erodibility and the vegetation cover fraction, estimated from the vegetation indices using remote sensing images (Hudson, 1957; Hudson, 1971; Cyr *et al*., 1995; Biard and Baret, 1997; Hill *et al*., 1998; Arsenault and Bonn, 2005; Chen and Rao, 2008). The chemical and physical properties of

surface soil are reflected in the spectral responses, and therefore can be detected (Fischer, 1991; Leone and Sommer, 2000). This was discussed in section 2.2.

Most of the studies used multi-spectral images and high resolution images to map land degradation at a regional scale (Escadafal *et al.*, 1994, 1995; Haboudane *et al.*, 2002; Wang, 2006; Chen and Rao, 2008; Gao and Liu, 2008). Several indices of soil degradation, wind erosion, and water erosion with different expressions and standards were proposed to measure soil degradation, which incorporated soil physical and chemical properties, soil loss, soil deposition, soil bulk density and soil formation (Adejuwon and Ekanade, 1988; Escadafal *et al.*, 1994; Mougenot and Cailleau, 1995; Escadafal *et al.*, 1995; Menenti *et al.*, 1999; Haboudane *et al.*, 2002; Chabrillat *et al.*, 2003; Mohamed *et al.*, 2005; Nasir *et al.*, 2005; Vagen *et al.*, 2005; De Wit *et al.*, 2006). These indices were classified into five types: (i) index based on land degradation conceptual model; (ii) land degradation comprehensive index based on multi-indicators; (iii) land degradation proportion index; (iv) soil degradation distance index; and (v) index based on land degradation spectral model. Table 2.2 presents some of land degradation indices in literature. These indices were developed based on old generation remote sensing sensors and multi-spectral remote sensing data and conventional soil survey data.

Table 2.2 indices of land degradation in literature

Index types	Name	Method	algorithm	literature
Conceptual model	Hazard Index of Land Degradation (DH)	Comprehensive assessment on situation and rate of land degradation considering frangibility physical condition and human being stress	DH = DS + DR + IR + AP + PP Where DS = desertification status, DR = desertification rate, IR = inherent risk, AP = animal pressure, PP = population pressure	Menenti *et al.* (1999)
	Spectral Index of Land Degradation （LDI）	Comprehensive assessment on situation and rate of land degradation using remote sensing data and human being stress	LDI = SD + VD + C + A Where SD = (spectroscopic indicator of) soil degradation severity, VD = vegetation degradation severity, C = climate data, A = ancillary data (population)	Chabrillat *et al.* (2003)
Comprehensive index	Weighted Mean Index of Land Degradation (LD)	Weighted means of multi-indicators, such as soil, vegetation and others	$LD = \sum P_i \times M_i$ Where P_i=weight of indicator i, M_i=value of indicator i	Soil surveying
Proportion index	Land Degradation Proportion Index (LDPI)	Calculation of area of different degraded degree land using weighted means	LDPI=(percentage × area in slightly degraded land + percentage × area in moderately degraded land +percentage × area in highly degraded land)/ total area	Soil surveying
Distance index	Soil Degradation Distance Index (DDI)	Calculation the distance of soil parameters in one sample to baseline sample, based on soil surveying data	$DDI=[(P_1-P'_1)/P'_1+(P_2-P'_2)/P'_2+\ldots+(P_n-P'_n)/P'_n]\times100/n$ Where P_i=value of soil parameter at the initial stage, P_i'=value of soil parameter at the later stage	Adejuwon and Ekanade *et al.* (1988)
	Soil Physical Degradation Index (PDI)	Based on soil physical parameters using soil surveying data	PDI=CI/(%SA+(FC-WP)*100) Where SA= percentage of stable aggregates, FC= field capacity, WP= wilting point, CI= crusting index	De Paz *et al.* (2006)
	Soil Chemical Degradation Index (CDI)	Based on soil chemical parameters using soil surveying data	CDI=（Salts＋Na）/CEC Where Salts, Na, and CEC are contents of salt and sodium and cation exchange capacity	De Paz *et al.* (2006)
	Soil Biological Degradation Index (BDI)	Based on soil parameters indicative biological indicators using soil surveying data	BDI=1/SOM Where SOM= content of soil organic matter	De Paz *et al.* (2006)
Land degradation spectral model	Soil Line Index (SLI)	Based on soil line theory using ASTER data	$SLI=\tan\alpha /\tan\beta$	Mohamed *et al.* (2005)
	Salinity Index (SI, NDSI)	Based on bands algebraic calculation using several bands of IRS-1B data	$SI = \sqrt{B1\times B3}$ $NDSI = (B3 - B4)/(B3 + B4)$	Nasir *et al.* (2005)
	Soil Fertility Spectral Index (SFI)	Based on logic regression method using TM data	$SEF = \ln\dfrac{P(Yi = 1)}{1 - P(Yi = 1)} = \alpha + \sum_{k=1}^{k} \beta_k X_{ik}$	Vagen *et al.* (2005)

Moreover, most of the studies about land degradation focused on the methodologies of classification. Conventional classification methods using remote sensing images were based on pixels (De Jong, 1994; Turner *et al*., 1995; Escadafal *et al*., 1995; Tripathy, 1996; Hill and Schütt, 2000; Okin *et al*., 2001; Dehaan and Taylor, 2002; Gregory, 2003; Vagen *et al*., 2005). The classical pixel by pixel approaches have been used for the classification of land use /land cover and land degradation, such as unsupervised classification methods including K-Means etc, and supervised classification methods including maximum likelihood classifier, and nearest-mean classifier, etc. Spectral analysis approaches range from relatively simple maximum likelihood classification techniques to sophisticated ones, such as the spectral feature matching methods and spectral unmixing methods. Several researchers conducted the spectral feature matching of image spectra with selected reference spectra from a spectral library and proposed the spectral angle classifier. Some studies developed the spectral unmixing methods which determine the relative abundance of materials or end members within each pixel based on the spectral characteristics of those materials (Kruse *et al*., 1993; Boardman, 2006). The linear unmixing and the spectral angle matching techniques were also applied to assess their suitability in mapping surface features in land degradation studies (Okin *et al*., 2001; Shrestha *et al*., 2005; Pierre *et al*., 2005). Several authors proposed the spectral unmixing using a linear model and analyzing the fraction image to study soil degradation (Hill *et al*., 1995; Van der Meer, 1997; Haboudane *et al*., 2002). Hill *et al*. (1998) applied the spectral mixture analysis methodology to soil degradation mapping in semi-natural ecosystems of the Mediterranean. Omuto and Shrestha (2007) proposed a tree classification method. Johansen *et al*. (2008) quantified the indicators of riparian condition and assessed these indicators for detecting the change in riparian condition using two multi-spectral QuickBird images. The study by Gao and Liu (2008) concluded that the spatial resolution of the ASTER data exerts only a negligible effect on the mapping accuracy. However, for the spectral matching methods and the spectral unmixing methods, one must select a reference spectrum, which, however, cannot completely represent a given soil type or land cover type, because there are many factors affecting reflectance. It is very difficult to select pure spectra in spectral library to represent typical soil types or land cover types, resulting in poor precision of classification.

Hyperspectral images have made precise spectrum feature analysis and sensitive spectrum response to surface features possible (Hill *et al*., 1995, 1998). The developments of scanner systems that acquire data in many narrow-wavelength bands allow the use of almost continuous reflectance data in many fields of research, such as geological survey, mineral exploration, soil survey, land degradation monitoring, mine environment monitoring, pollution survey and water bodies monitoring (Leone and Sommer, 2000). Therefore, utilization of hyperspectral remote sensing technique to carry out detailed land degradation mapping becomes possible at a regional scale. Some investigators developed the spectral unmixing methods and the spectral angle matching techniques with hyperspectral images for land degradation mapping (e.g., Van der Meer, 2001; Goovaerts *et al*., 2005; Shrestha *et al*., 2005; Boschetti *et al*., 2007). The information on green vegetation, blasted vegetation and bare soil was interpreted to reflect the degree of desertification at a large scale by comparing AVIRIS and EO-1 Hyperion in Argentina dry lands (Gregory, 2003).

Several issues have to be tackled due to insufficient spatial information and geoscience knowledge. There is a limitation in these spectral approaches which account only for the correlation between spectral bands but neglect the correlation between neighboring pixels (Atkinson and Lewis, 2000). The traditional pixel-based spectral classification methods neglect some potentially useful spatial information and do not consider the spectral dependence between pixels and their neighbours, i.e. spatial autocorrelation. To solve the problem of neglecting spatial information, numerous studies were conducted using spatial statistics in the texture classification of land use and land cover (Haralick *et al*., 1973; Chen *et al*., 1997; Stein *et al*., 1999). Geostatistics refers to a group of techniques for the analysis of spatial data. It provides variogram and not only analyzes multivariate spatial correlation between a pixel and its neighbors for measuring image texture, but also does the spatial decomposition or image filtering of signal values (Woodcock *et al*., 1988; Rossi *et al*., 1994; Atkinson and Lewis, 2000; Curran, 2001; Goovaerts *et al*., 2005) . Some studies found that the approach based on texture measures can achieve higher accuracy depending upon the nature of the data and texture (Chica-Olmo and Abarca-Hernández, 2000; Berberoglu *et al*., 2007). Application of geostatistic

methods for classification and spectral matching were also investigated (Nazzareno and Michele, 2004; Van Der Meer, 2006; De Jong and Van De Meer, 2007; Berberoglu and Akin, 2009). Nazzareno and Michele (2004) proposed a multivariate indicator kriging approach, which integrated spatial information and various absorption band estimates from soil survey data, to classify soil degradation for Mediterranean agricultural lands. Van der Meer (2006) proposed an indicator kriging-based classifier for mapping the minerals alunite, kaolinite, illite and chlorite using airborne hyperspectral imaging spectrometer data and field spectra. However, a main problem with variogram as a measure of texture is that the homogeneous regions of different texture within an image must be large enough to allow the computation of the variogram up to a reasonable number of lags. In many cases, however, the parcels of interest in an image are too small compared with the spatial resolution of the image.

The above-mentioned pixel-based classification methods only use the spectral and texture information, and do not take advantage of the information about the shape and the spatial relations among the image regions. The current developments are to integrate spectrum, texture and spatial information in images and geographic information. The object-oriented analysis method has been developed based on fuzzy logic after image segmentation. The method was mainly used in the classification of land cover and land use and forest (Civanlar and Trussell, 1986; Kosko, 1992; Kruse *et al*., 1993; Herold *et al*., 2005; Lewinski and Polawski, 2005; Carleer and Wolef, 2006; Yu *et al*., 2006; Laliberte *et al*., 2007; Jacquin *et al*., 2008; Mallinis *et al*., 2008; Kim *et al*., 2008; Zhou *et al*., 2008). Some studies showed that the object-oriented classification approaches can produce better results than the pixel-based approaches (Manakos *et al*., 2000; Oruc *et al*., 2004; Whiteside and Ahmad, 2005; Brandtberg and Warnen, 2006; Matinfar and Sarmadian, 2007; Kamagata *et al*., 2008).

As we know, land degradation process is related to several factors, like physiognomy, soil characteristics, vegetation, land use/land cover, climate, and human activities. Therefore land degradation research must integrate and take full advantage of various types of data and information. However, the conventional methods for land

degradation classification were pixel-based, suffering from the problems as mentioned above. With the development of the OBIA methodology, the idea of GEOIC has been proposed. The GEOIC approach integrates remote sensing information, geographic information, and the knowledge on land resources and takes into account the spectral, texture, shape, and spatial relation between pixels based on fuzzy logic methods. The GEOIC is also an appropriate approach to handle the knowledge on land degradation which is frequently expressed ambiguously. Little however, has been done in this research area and further developments are highly required.

Many investigations on soil and land degradation with remote sensing images were conducted in arid and semi-arid zones that are considered particularly favorable to remote sensing techniques (e.g., Escadafal, 1994; Mathieu *et al*., 1998). But in an agriculture-pasture mixed region, like in the Loess Plateau in China (see chapter 4 for the detail), where physical geographical situation is very complex and land degradation is widely distributed, the assessment of the land degradation is much more complex. It is important to develop an approach, which is valid for such a complex situation.

Chapter 3

Some Issues About Geographic Image Cognition on Land Degradation

This chapter has five sections. The first section introduces the GEOIC and its key objective. The second section describes a conceptual framework of the GEOIC when applied for land degradation assessment, and its merits over other approaches. The third section discusses some concepts related to the GEOIC. The factors affecting image visual cognition are discussed in section 4, where a questionnaire survey was conducted and the results were analyzed. The last section devotes to a general discussion of the GEOIC approach, its theoretical underpinning, model underpinning, and methodological framework for land degradation assessment.

3.1 Introduction to GEOIC

To effectively extract land thematic information, the approach of GEOIC was developed based on the geographic image analysis and OBIA. As mentioned in Chapter 2, it is the objectification cognition on remote sensing images and multi-source information using geo-knowledge. The GEOIC, as an integrated approach, is the extension of the methodology of OBIA. Its key content is based on the methodology of OBIA as shown in Figure 3.1.

Provision of units, regionalization

Image fusion, integrating additional continuous data sources

Upscaling, downscaling

Segmentation techniques

Experiences from visual interpretation

Cognition & understanding

Assessment & proof of concepts

Integrating existing data sets + in-situ measures

Statistical measures / pattern recog.

Formalised knowledge

Spatial relationships

Change analysis, 'object fate'

Classification, interpretation

Figure 3.1 The OBIA as an integrated approach (after Lang (2008) with some modification)

The GEOIC is an approach of developing automated methods to partition remote sensing imagery and multi-source information into meaningful image-objects and assessing their spatial, spectral, geographic and temporal characteristics in order to generate thematic information. To this end the GEOIC incorporates knowledge and methods from different disciplines involved in the generation and use of geographic information.

The general objective of GEOIC is mining thematic information and quantifying ambiguously expressed knowledge (from remote sensing imagery and multi-source information), from which intelligence can be obtained. Here, *intelligence* refers to thematic information that enables users to effectively perceive, interpret and respond to some specific issue, such as global climate change, natural resources management, land use/land cover mapping, and others (Hay and Castilla, 2006; Hay and Castilla 2008). The GEOIC is regarded as an approach to replicate (and/or exceed experienced) human interpretation of remote sensing images in automated/semi-automated ways. This can result in more accurate, less subjective, and repeatable information, and reduce labor and time cost. Essentially, the GEOIC provides a way to move from simply collecting images, to creating geo-intelligence. In other words,

the GEOIC aims at extracting, mining, coding, reserving, accessing and utilizing remote sensing information and multi-source information with artificial intelligence. It is a translation process from physical and / or semantic image information to precisely defined codes or thematic mapping. It is significant to understand the mutual relationship among scale, space and experience in the process of cognition on land information.

3.2 GEOIC on studying land degradation

The approach of GEOIC connects the features in remote sensing images and multi-source information with vision, experience, knowledge and memory in human brain about land degradation, and forms symbolic expression of spatial information. There are three levels in the approach namely the spatial feature perception, the spatial object cognition and the spatial pattern cognition, among which the spatial object cognition is the core element. In other words, the approach is a process from the spatial feature perception to the spatial object cognition and to the spatial pattern cognition under the cognition mode of feature-object-pattern. It is related to information layer, physical layer and semantic layer (Luo, 2000). The information layer reflects the inherent and fundamental geo-features of two-dimensional remote sensing images and ancillary information, such as spectrum features, spatial features, and temporal features of land degradation. The physical layer is related to detailed information on geo-objects. The semantic layer describes the geographic attributes and the mutual relationships between environment variables (see Figure 3.2).
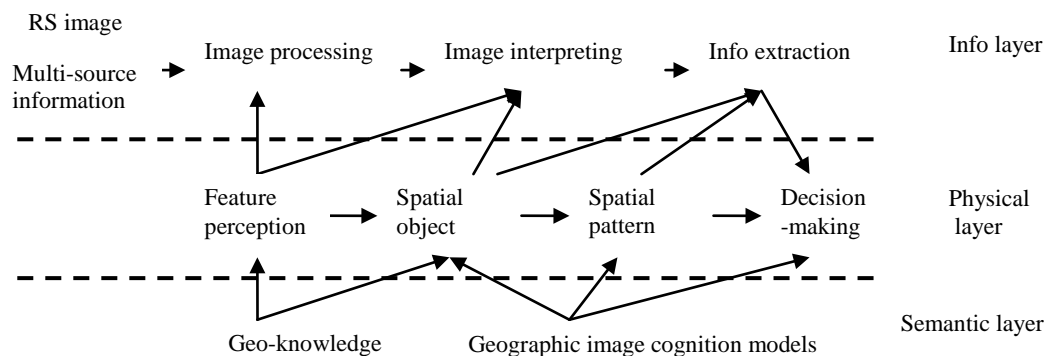
Figure 3.2 Three information layers for GEOIC (after Luo (2000) with some modification)

The GEOIC on studying land degradation is to simulate the function and process of the visual interpretation by experts, and extract spatial feature, spatial object and spatial pattern of land degradation and mine the information on land degradation from remote sensing images and multi-source information. The approach is realized through the segmentation of meaningful image objects with the support of an integration of remote sensing images and multi-source information on various diagnostic indicators, based on geoscience knowledge and geographic information. The approach provides a systematic approach for the study of land degradation (Figure 3.3). As one can see, all the diagnostic indicators related to land degradation are integrated through a *geon* concept. A *geon* concept is discussed in section 3.3. The information of diagnostic indicators was integrated and generated conditioned information, i.e. the information of meaningful image objects, which is directly used in the process of monitoring and evaluation of land degradation. By this, it enables monitoring of meta-indicators effectively to support the decision making.
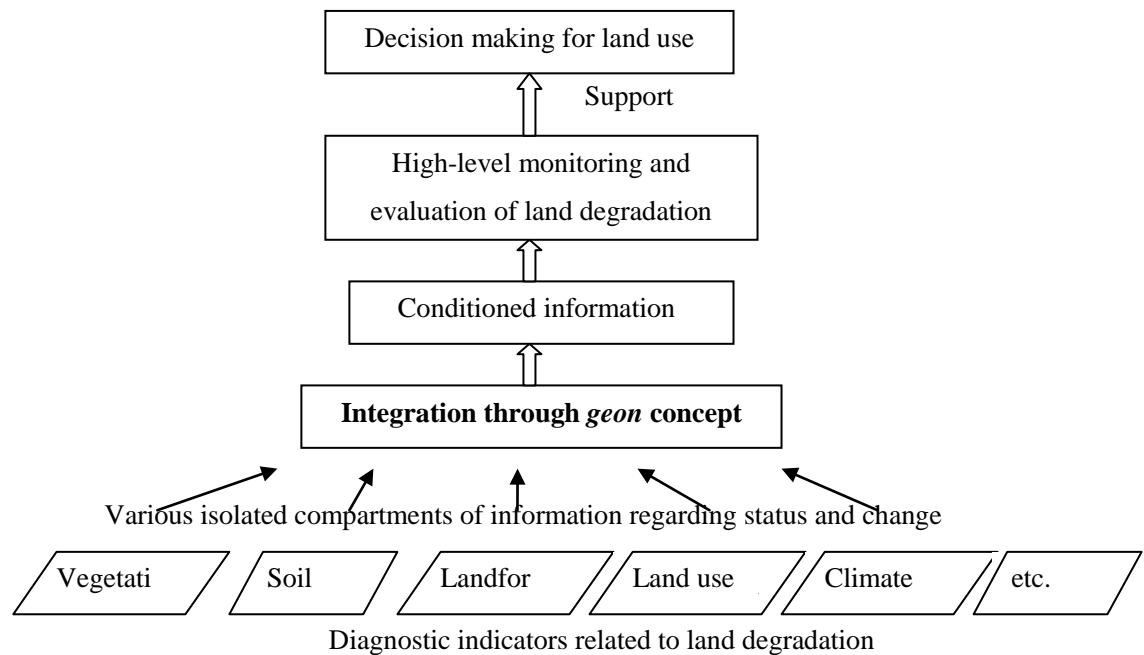
Figure 3.3 Conceptual framework of the approach GEOIC on studying land degradation

Although the GEOIC is developed from the methodology of OBIA, there are some differences between them. The GEOIC approach is an extension of OBIA methodology. It focuses not only on the extraction of thematic information, but also on mining thematic information and quantifying ambiguously expressed knowledge. Table 3.1 gives a comparison. Its applications cover a wider area, like land use and land cover classification, vegetation classification, land degradation evaluation, land quality evaluation, soil parameters mapping, and forest development, etc. The advantage of the GEOIC approach includes the emulation of a human interpreter's ability in image interpretation, and integration of different types of geo-data into an object-based analysis process and a set of fuzzy-logic-based rules.

Table 3.1 Comparison of the GEOIC approach with OBIA methodology

GEOIC approach	OBIA methodology
For mining thematic information and quantification of ambiguously expressed knowledge	For extraction of thematic information
A process of image segmentation, and classification, extraction, and mining of thematic information	A process of image segmentation, and classification and extraction of thematic information
Based on spectral and texture information, spatial relation, and geoscience knowledge and local knowledge	Based on spectral and texture information, and spatial relation
Segmentation of geo-objects or meaningful image objects, e.g. DSRU and land unit	Segmentation of image objects or meaningful image objects
Using remote sensing information, geographic information, vegetation, soil, and field survey information	Mainly using remote sensing information
Application in land use and land cover classification, vegetation classification, and land degradation evaluation, land quality evaluation, soil parameters mapping, and forest development, etc.	Application in land use and land cover classification, vegetation classification, etc.

3.3 Some concepts related to GEOIC

The term cognition in a wider sense means the act of knowing or knowledge, including feeling, consciousness, idea, imagination, memory and thought. It in some loose ways refers to the human-like processing of information. A remote sensing image is a typical, complicated and uncertain information source, which reflects the earth's surface spatial and spectral information obtained by sensors. One can hardly describe exactly what really happens if just looking at an image and suddenly 'seeing' something. But you indeed notice that if you do any kind of pattern recognition (Tarr and Cheng, 2003). Human interpretation for image cognition can derive little information if using the point-by-point approach, because less information can be derived from the brightness of individual pixels. However, one can get more information from the context and the patterns of brightness [i.e. texture], of groups of pixels, and from the sizes, shapes and arrangements of parcels of adjacent pixels (Campbell, 2002). Human interpreters also implicitly use structural knowledge in the manual classification process. They do not only consider contextual information but also information about the shape and the spatial relations between the image regions. One way to make use of this additional information is to organize the images into objects that represent the regions of similar pixels prior to the classification. In most cases, information important for the understanding of an

image is not represented in a single pixel but in meaningful image objects and their mutual relations (Blaschke, 2003). An interpreter for image cognition must often delineate, or outline, regions as they are observed in remote sensing images. In many cases the human brain can easily manage to detect and delineate features that otherwise in a machine-based way are hardly to extract (Blaschke *et al*., 2005). Indeed, image cognition is to make an explicit way, in which we deal with imaged information in various scales, we manage to relate recognized objects to each other with ease, and we understand complex scene contents readily. Image cognition can supply the information that cannot be obtained by remote sensing and analyze the information that could not be reflected by remote sensing images according to the bi-dimension and their correlations. Therefore, image cognition is the process of objectification cognition on images. Spatial cognition is also named as spatial object cognition. The core research of image cognition is spatial object cognition.

The term *geon* is proposed to describe generic spatial objects that are derived by regionalization and homogenous in terms of a varying spatial phenomenon under the influence of, and partly controlled by, policy actions (Lang and Tiede, 2007; Lang, 2008). A *geon* (from Greek *gé* = Earth and *on* = part, unit) can be defined as a homogenous geo-spatial referencing unit, specifically designed for policy-related spatial decisions. In the real world, it is close to geo-object. For geo-object, the term 'object' refers to a discrete spatial entity that has many permanent properties which endow it with an enduring identity and which differ in some way or another from the properties of its surroundings (Smith, 2001). A geographic object, or geo-object, is a bounded geographic region that can be identified for a period of time as the reference of a geographic term such as those used in map legends. It is an object of a certain minimal size (as to allow representation in a map) on or near the surface of the Earth, such as a city, a forest, a lake, a mountain, an agricultural field, a vegetation patch and so on (Smith and Mark, 1998; Castilla and Hay, 2008). In remote sensing images, *geon* is related to image-object. Image-objects are *fiat objects*. They are created by human cognition on images (Smith, 2001). Human's image cognition can identify entities that can be related to real entities in the landscape. Image cognition is a relatively new approach to the analysis of remote sensing images where the basic units, instead of being individual pixels, are image-objects. An image-object is a

discrete region in an image that is internally coherent and different from their surroundings (Benz *et al*., 2004). When an image object can be seen as a proper representation of an instance of some type of geo-object, then we can say it is a meaningful image-object, that is, a representation of a geo-object. Regarding the ontological status of image-objects, it has to be noted that they do not exist autonomously within images. Rather, they are created during the segmentation. Segmentation produces image regions, and these regions, once they are considered meaningful, become image objects; in other words an image object is a 'peer reviewed' image region; refereed by a human expert. A pixel as a technically defined unit cannot be assigned a valid corresponding real-world object, but an image object can (Castilla and Hay, 2008).

3.4 Influencing factors of image visual cognition

The aim of monitoring and evaluation of land degradation is to investigate the characteristics, processes and distribution of land degradation for better understanding a complex landscape. It is now widely recognized that landscape is a complex system with a hierarchical structure where dominant patterns and processes exist at specific scales. Remote sensing images reflect the landscape's spatial information obtained by sensors. Although the approach of GEOIC on studying land degradation is an integrated and automated one for the extraction of land degradation information, human's visual cognition on images impenetrate its whole process, including the choice of diagnostic indicators, the determination of threshold values of diagnostic indicators, membership functions, and rule sets of land degradation assessment, and the selection of validated samples, which are the base for the application of the GEOIC in the extraction of land degradation information. This also fully exhibited the connotation of image cognition with geoscience knowledge. But human's visual cognition on the environment is a common experience, easy to share, yet difficult to express in words or even rule sets. Because of the complexity and uncertainty of a landscape, image information and human's visual cognition, as well as the approach of GEOIC firstly applied in land degradation research, several factors, especially man-made factors, influence the process of image visual interpretation or image visual cognition on landscape. Most of the studies on the

influencing factors as well as their effects on visual image cognition performed the qualitative analysis only, little for quantitative analysis. We therefore conducted a questionnaire survey aiming at a quantitative analysis to supply a foundation for the determination and the selection of diagnostic indicators and validated samples.

3.4.1 Questionnaire on image visual cognition
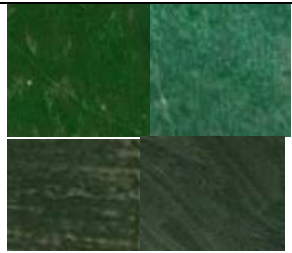
A questionnaire on image visual cognition was designed in this study and sent to 46 individuals. They consisted of geo-experts, skilled image interpreters and simple users, with the age in the range of 20-60 years and with work experience in the range of 1-20 years, including 24 females and 22 males from different institutes in China.

The questionnaire included various feature images of single land use type, such as cultivated land, forestry land, grassland, residential land, water, and sandy land, etc. It also included feature images of different types of vegetation cover, vegetation growing situation and percentage of barren land. They were chosen from medium resolution images to high resolution images of TM image, ETM$^+$ image, SPOT2 4 image, SPOT5 image and QUICKBIRD image. These feature images were not labeled by any types, name and features in the questionnaire. Tables 3.2 and 3.3 list some examples of feature images. The aim of the questionnaire is to collect the information about cognition on land use type, vegetation cover, and vegetation growth, percentage of barren land, and color and texture of feature images from geo-experts, skilled interpreters and simple users. The survey results were analyzed to show the differences in cognition abilities, influenced by experience, specialty, background knowledge, age, gender, etc, in the process of visual interpretation on images.

Table 3.2 Some examples of feature images of different land use types

	TM/ETM⁺	SPOT24+ ETM⁺	SPOT5	QUICKBIRD
Cultivated land			Irrigable Dry land	Paddy field Irrigable
Garden land				
Forestry land			Forest Open forest	Forest Open forest
Grassland		Natural	Natural Man-made	Natural Man-made
Urban Residential land				Residential Industrial
Village residential land				
Road				
Lake				Swag
River				
Salinization land				
Sandy land				
Barren land				

Table 3.3 Some examples of feature images of different vegetation situations

	Vegetation cover	Vegetation growing situation	Ratio of barren land
Type 1	High: >60%	High	High: >60%
Type 2	Medium: 30%-60%	Medium	Medium: 30%-60%
Type 3	Low: <30%	Low	Low: < 30%

3.4.2 Analysis of the survey results

Experience is important for skillful and successful image interpretation. As we know, in manual air-photo or satellite image interpretation a lot of experience is required. It mostly needs training to match the imaged false color schemes with natural phenomena and to understand certain texture or structures and the imaged features. This is because human vision is challenged when dealing with remote sensing images. Three issues distinguish the interpretation of remotely sensed images from the interpretation in our everyday experience. Firstly, remotely sensed images usually portray an overhead view – an unfamiliar perspective. Secondly, many remote sensing images use radiation outside the visible portion of the spectrum. Finally, remote sensing images often portray the earth's surface at unfamiliar scales and resolutions (Campbell, 2002). Unfortunately, even long time learning cannot prevent us from facing ambiguity when features are very like in structure or color. In

the process, experience pays an important role in image interpretation. Tables 3.4 to 3.6 and Figure 3.4. summarize the survey results. One can see that the participants with more than 5 years of work experience are better in the cognition on feature images of land use type from TM/ETM$^+$ image, fusion image of SPOT2 4 and ETM$^+$, SPOT5 image and QUICKBIRD image, and have higher percentage of correct interpretation compared with the other participants. The same group of participants is also superior in the cognition on vegetation cover, vegetation growth, and percentage of barren land. The finding was consistent with Lang's (2005) study of cognitive abilities, who pointed out the interest of a skilled interpreter may differ from that of a simple user. The former looks for certain features, whereas the latter is mainly interested in the information he wants to obtain.

Table 3.4 The correctness of cognition on feature images of land use type in four types of images by different participant groups (unit: %)

Types	Sub-types	TM/ETM$^+$	SPOT2 4+ETM$^+$	SPOT 5	QUICKBIRD
Age	<=25	64	73	42	41
	25-30	66	70	38	47
	>30	78	77	52	51
Work experience	<= 1 year	67	73	43	43
	1-5 years	63	72	41	43
	> 5 years	80	75	45	46
Specialty	RS	79	70	50	48
	GIS	69	76	52	47
	Land	63	71	43	39
	Survey	53	64	39	48
Knowledge	More RS knowledge	66	71	40	45
	A bit of RS knowledge	68	76	45	44
Total		67	73	42	45

Table 3.5 The correctness of cognition on feature images of vegetation situation by the participants with different work experience (unit: %)

Types	Vegetation cover			Vegetation growth			Ratio of barren land		
	0-30%	30-60%	>60%	High	Medium	Low	0-30%	30-60%	>60%
≤1 year	74	67	81	81	44	65	39	50	58
1-5 years	78	66	67	78	49	62	53	53	68
> 5 years	83	84	81	82	55	64	54	55	85

Table 3.6 The correctness of cognition on feature images of vegetation situation by the participants with different background knowledge (unit: %)

Types	Vegetation cover			Vegetation growth		
	0-30%	30-60%	>60%	High	Medium	Low
With more RS knowledge	81	68	71	43	46	63
With a bit RS knowledge	77	72	80	31	56	63
With geoscience knowledge	78	70	71	44	48	65
With no geoscience knowledge	81	68	81	34	53	63
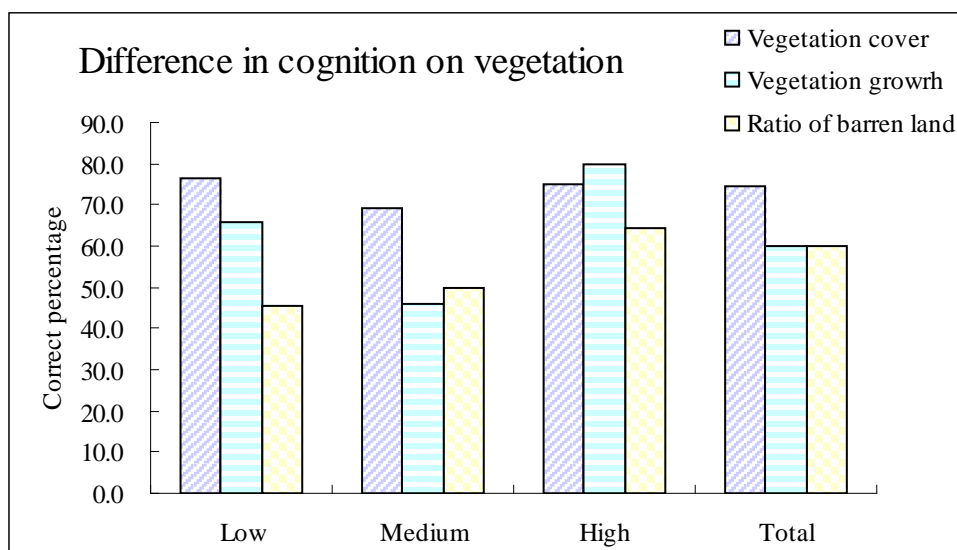
Figure 3.4 The correctness of cognition on feature images of different vegetation situation

The results showed that there was not much difference in image cognitive abilities on land use type and vegetation among the participants with different background knowledge, and no superiority for the participants with more remote sensing knowledge. The results also showed not much difference among the participants with different specialties. This suggested that the background knowledge of the participants has little influences on the image cognitive ability on feature images of single land use type.

Moreover, the results indicated that the correctness of the cognition on feature images of urban residential land, village residential land, road, lake, river, and cultivated land was higher than that of the cognition on forestry land, grassland, barren land, sandy land, and salinization land. When looking at these feature images one can identify image features of some types of land use. For example, one can

distinguish a river by its shape from other features (e.g., lakes) that have similar spectral values. This is accord with the rule of image interpretation. The results also showed that the correctness of the cognition on feature images of land use type in TM/ETM$^+$ image and fusion image of SPOT2 4 and ETM$^+$ were higher than that in images of SPOT 5 and QUICKBIRD. This is probably due to the coarse classification of land use in medium resolution images and finer classification in high resolution images. For example, feature images of cultivated land were identified in images of TM/ETM$^+$ and SPOT2 4+ETM$^+$, while irrigable land and dry land which are the sub-types of cultivated land were identified in images of SPOT 5 and QUICKBIRD. Another possible reason is that unlike a complex image including several types of land use, each chosen feature image in the questionnaire only included a single type of land use, with no context relations and background circumstances about it as reference of interpretation. So the cognitive ability on feature images of a single type of land use was not improved with high resolution images compared with the medium resolution images.

Regarding the gender the results indicated that the males did better in the cognition on feature images of vegetation cover, percentage of barren land and vegetation growth, but almost no difference in the cognition on feature images of land use type (see Figure 3.5 to 3.8). The correctness of the cognition on feature images of vegetation cover with 0-30%, 30-60% and 60-100% by the male participants was 81%, 73%, and 77%, respectively, while it was 77%, 66% and 73% by the female participants. The correctness of the cognition on feature images of vegetation cover was higher than that of the cognition on vegetation growth and the percentage of barren land. These phenomena may be explained by sex differences in cognitive abilities. The process of the cognition on feature images of vegetation cover, the percentage of barren land and vegetation growth is related not only to image features including color, texture, and shape, but also to visual–spatial abilities, such as visual perception and spatial visualization, and quantitative abilities. The process of the cognition on land use types is closely related to human memory of images of various land use types in addition to image features. Many studies concluded that there is sex differences in verbal, quantitative, and visual–spatial abilities and males are in favor in visual–spatial abilities (Maccoby and Jacklin, 1974; Linn and Pulos, 1983; Smith

and McPhee, 1987; Schiff and Oldak,1990; Eals and Silverman, 1994; Halpern, 2000). Halpern (2000) reviewed cognitive abilities, and concluded that psychometrically, measures of mathematical ability tend to be strongly correlated with spatial ability. Unlike the visual–spatial abilities, the memory of location, words, and objects is better for a female.
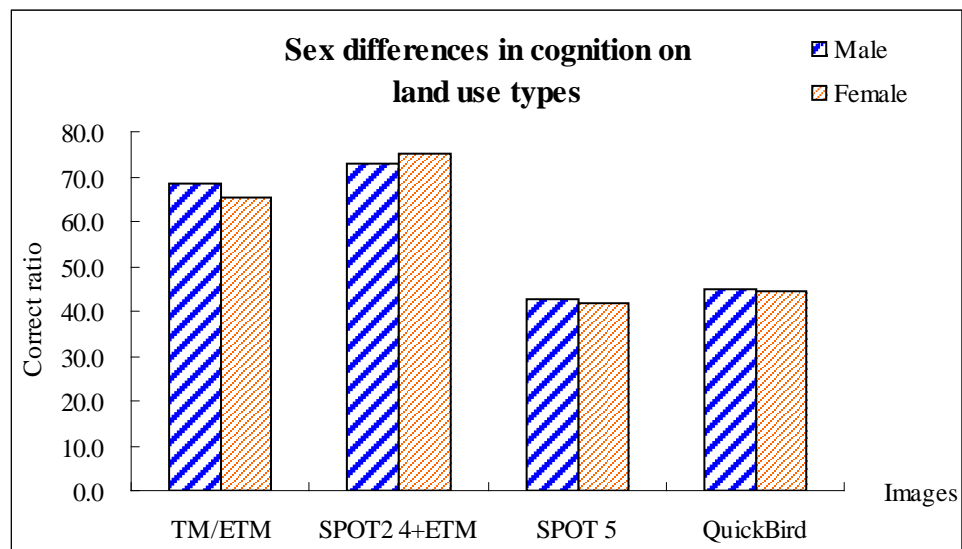
Figure 3.5 Sex differences in the cognition on feature images of land use types in four types of images
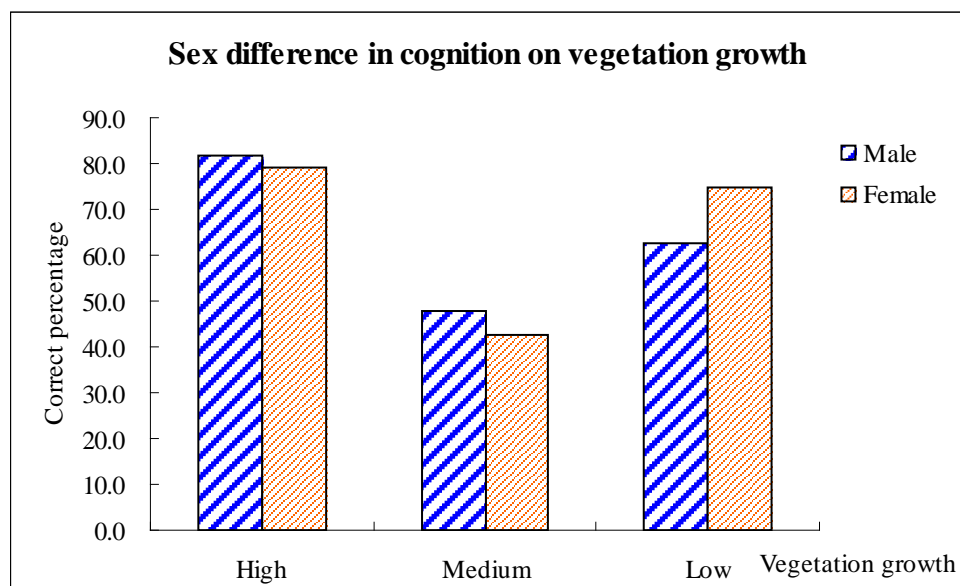
Figure 3.6 Sex differences in the cognition on feature images of different vegetation growth situation
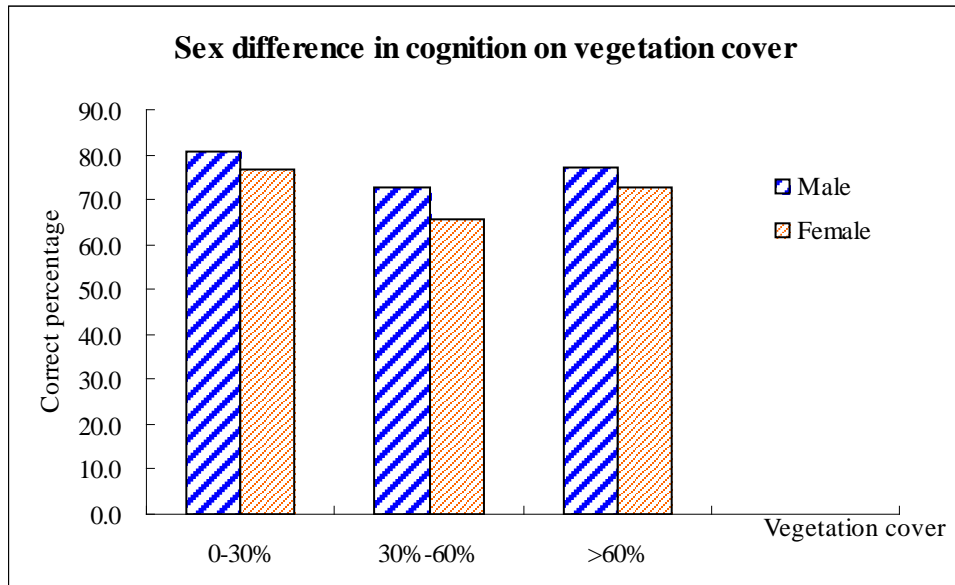
Figure 3.7 Sex differences in the cognition on feature images of different vegetation cover
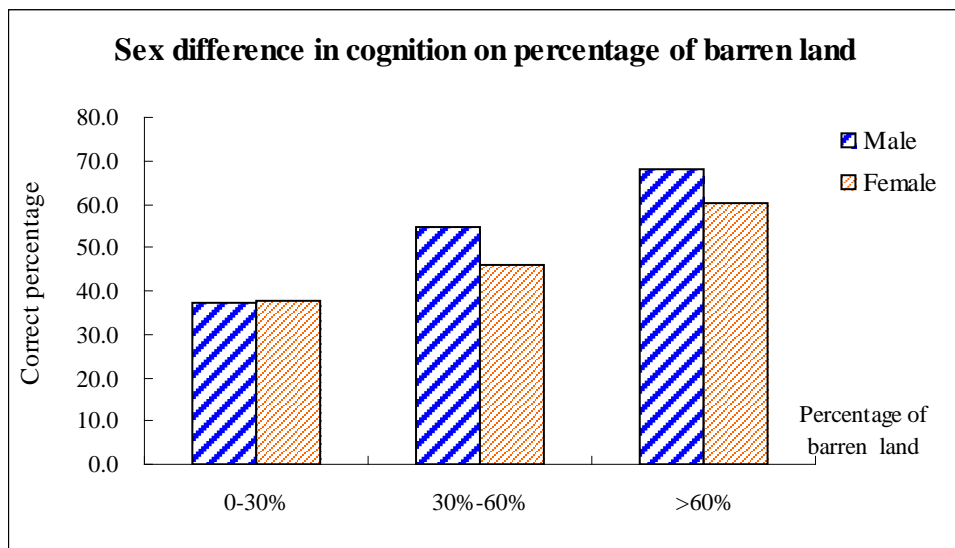
Figure 3.8 Sex differences in the cognition on feature images of different ratio of barren land

The above results imply that experience, age and gender have influences on the visual cognitive abilities on remote sensing images. The experience did make differences in the cognition abilities on feature images of land use types and gender made differences in the cognition on vegetation cover, vegetation growth and the

percentage of barren land in the process of visual manual interpretation on images. The effects of the experience, age and gender on cognitive abilities were different. Therefore, the diagnostic indicators and their threshold values, and the validated samples should be chosen and determined by experienced experts for the application of GEOIC in the extraction of land degradation information. Moreover, local farmers who know well the land degradation situation should participate in the process of selection and determination. It is necessary to combine the results of experts' with farmers' cognition on land degradation for deriving the appropriate indicators and choosing validated samples when the approach of GEOIC is applied. However it is of importance to develop a standardized methodology of image cognition from visual cognition to automatic comprehensive cognition by integrating remote sensing image information, spatial information, geographic information and experience in computer environment. The approach of GEOIC can transform the non-standardized image cognition to the standardized image cognition.

3.5 The approach of GEOIC

3.5.1 The theoretical underpinning of the GEOIC approach

The approach of GEOIC aims at the simulation of the logical and visual cognition of geoscience experts. It includes description, identification, classification and interpretation of land degradation information and mapping of its distribution. Moreover, it also includes mining of implicit land degradation information and geoscience knowledge in remote sensing images and multi-source information for decision making with a combination of various geographic models. Cognition models, which are the core of the GEOIC approach, include models of image pre-processing and analysis, visual cognition on images, logical cognition on images and geo-knowledge mining and decision-making (Luo *et al*., 2001).

The approach of GEOIC is based on theories and methodologies of several disciplines. Earth surface features are reflected in images with the variation of grey level, lightness and spectrum of pixels, which are the physical basis for information extraction. The methods and models of image pre-processing and analysis are based

on mathematic theory, statistics theory, probability theory, remote sensing information theory, and geo-statistics theory, etc. Visual cognition on land degradation using remote sensing images and multi-source information is based on cognition theory, geoscience theory, evolution theory and artificial neural network (ANN) techniques, etc. Logical cognition is also based on geoscience theory, information theory, knowledge processing theory and fuzzy set theory, etc. Mining and decision-making on land degradation information is often based on theories of systematology, cybernetics, catastrophe and operation, and synergetics method, etc. Figure 3.9 shows the underpinning of the GEOIC approach.
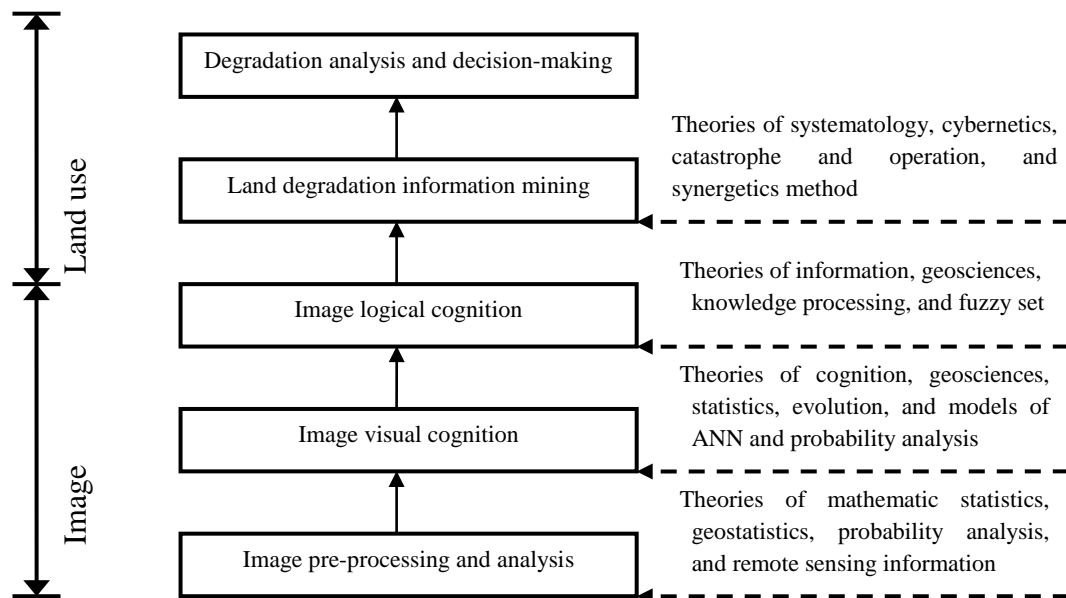
Figure 3.9 Theoretical underpinning of the approach of GEOIC

3.5.2 The model underpinning of the GEOIC approach

For the quantification of ambiguously expressed knowledge from remote sensing imagery and multi-source information, the GEOIC approach is to obtain the features and spatial distribution of land degradation through visual cognition and logical cognition. A series of multi-functional models for the GEOIC should be established to provide functionality of analysis, classification, extraction, simulation, imitation, mining, assessment and decision-making. The underpinning models of the GEOIC approach consist of four layers (see Figure 3.10). The first layer includes the models

of image pre-processing and analysis, which perform functions of basic image pre-processing and analysis for image enforcing, object inspecting, geometry rectifying, texture analysis, shape and color discrimination and basic image classification based on mathematics, statistics, and geo-statistics. It can obtain the primary information of the unknown surface features in feature space domain (Luo 2000).

The second layer includes the models of image visual cognition. Three-dimensional entities are projected into two-dimension images, so images can not represent all information precisely on actual surface objects. Therefore, the aim of image visual cognition on land degradation should interpret more information in a profound level integrating relevant geo-knowledge based on remote sensing images and multi-source information on the basis of cognition models. Image classification models based on ANN, genetic algorithms and statistics models, etc, will simulate visualizing and thinking of visual neuron processing to obtain the complicated non-linear information.

The third layer includes the models of image logical cognition based on knowledge processing models, knowledge discovery models and fuzzy sets models, etc. They are used for extracting and mining land degradation information and detecting change information based on meaningful image objects in a profound level to extract the thematic information that is often expressed ambiguously. With the support of cognition network and geographic knowledge, the precision of processing and analysis on land degradation information will be improved in the process of image logical cognition.

The last layer includes the models of knowledge mining and decision-making analysis, such as models of operational research theory, system theory, mathematics, and statistics. They are used for decision-making analysis on geographical differentiation and land degradation distribution and land use/land cover change.
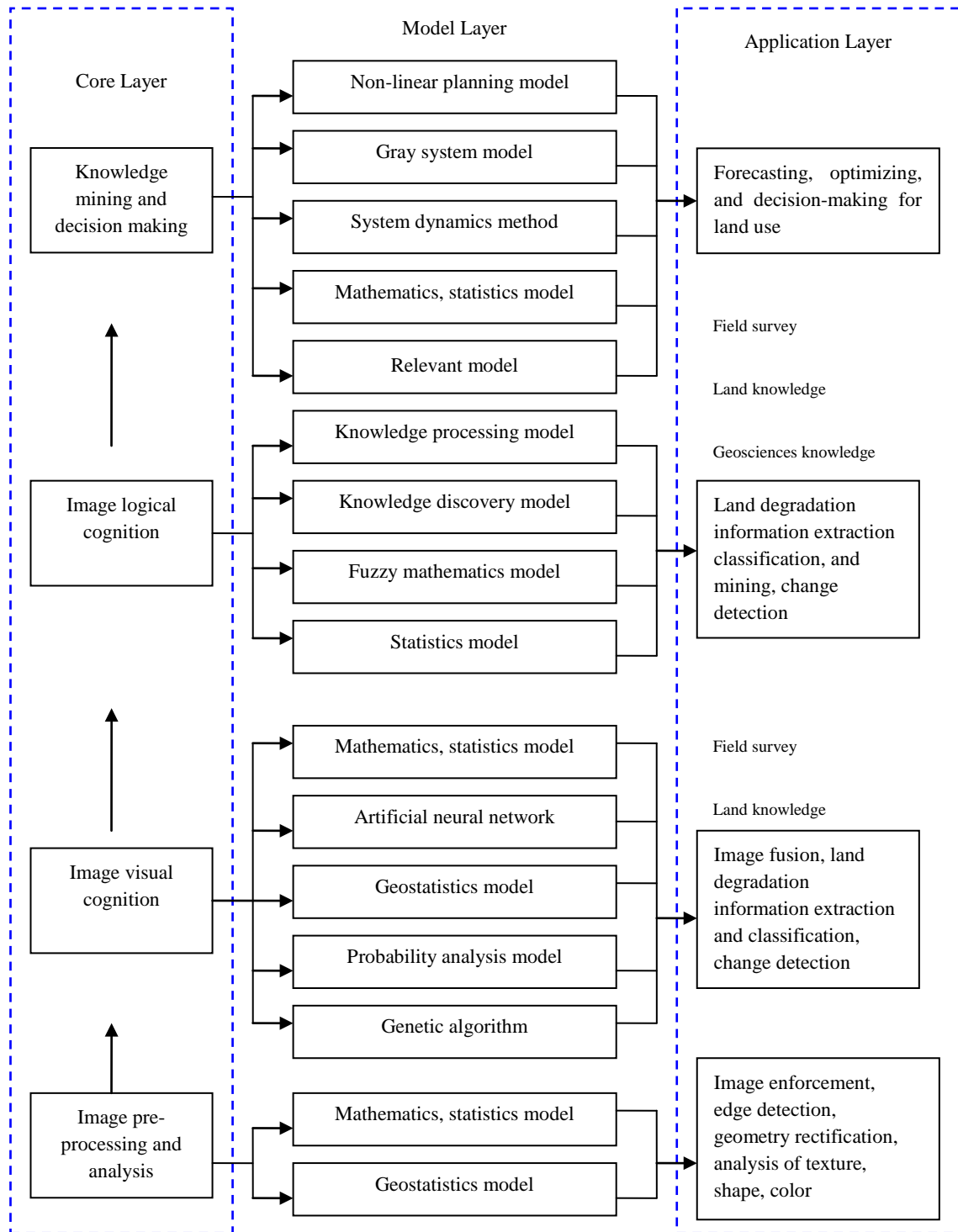
Figure 3.10 Model underpinning of the GEOIC approach

The GEOIC approach is an integrated way involving the methodologies of multi-disciplines. Geographical research indicates that the distribution of natural and human phenomena, such as vegetation, soil, land use, land cover and land degradation, has stochastic and structural characteristics which can be reflected to

some extent by remote sensing information in one or more instance. Statistics is the basic technique for analyzing and processing remote sensing images. The various mathematical and statistical models are used in the process of the GEOIC for the study of land degradation for calculating basic statistics and transformation of statistics of pixel reflectance (such as Fourier transform, wavelet analysis, and principal components analysis), and for the extraction of land degradation information based on statistics (such as regression analysis, trend analysis and hierarchical cluster analysis in supervised classification, discrimination analysis and maximum likelihood classifier and feature analysis, etc). Moreover, some methods of extracting spectrum feature are also based on statistics models. Furthermore the soft classification methods have been proposed to solve the problem of mixed pixel and wrong classified types affecting classification precision, such as fuzzy clustering classification, spatial structure texture classification, ANN, etc. With the development of fuzzy sets theory, knowledge processing models, and robust statistics, the approach of GEOIC has been developed to a new stage by combining fuzzy theory, robust statistics, and spatial analysis and multiple scales analysis integrating geoscience knowledge.

3.5.3 The methodological framework of GEOIC on studying land degradation

Under the conceptual framework of GEOIC on studying land degradation, the methodological framework of GEOIC on studying land degradation was proposed in this study (see Figure 3.11). Firstly, the features of physiognomy, vegetation, soil, and land use and land cover, etc, related to the diagnostic indicators of land degradation are analyzed. The spectral features and spectral responses to these diagnostic indicators are also analyzed. The results from these analyses provide a base for building geoscience knowledge and cognition network. The approach of GEOIC is supported with the so-called cognition networks. A cognition network controls the system of target classes of land degradation and the class definitions as well as the mode of representation. It provides the basis for a rule-based classification system.

The second step is the segmentation of image objects, called as Land Degradation Spectral Response Units (DSRUs). In the GEOIC, the 'image object' is the central element of investigation. The segmentation of DSRUs is realized through integrating various diagnostic indicators, such as remote sensing images, vegetation, soil, DEM, land use, and field survey data, etc. To this end, image segmentation with knowledge-based classification is conjoined.

The third step is building cognition network and rule sets for mining and extraction of land degradation information. Cognition network language used to set up rule sets offers a range of tools and algorithms to address complex target classes. Establishing a rule set is based on a combination of image feature analysis, field survey, geoscience knowledge, and the local knowledge aiming at user's targets. Even if there are methods and techniques to formulate the knowledge and to encapsulate it into rule bases, it is hard to encapsulate the vast intuitive knowledge of a skilled interpreter in a rule system. Transferring existing experience effectively into procedural and structural knowledge remains a challenge.
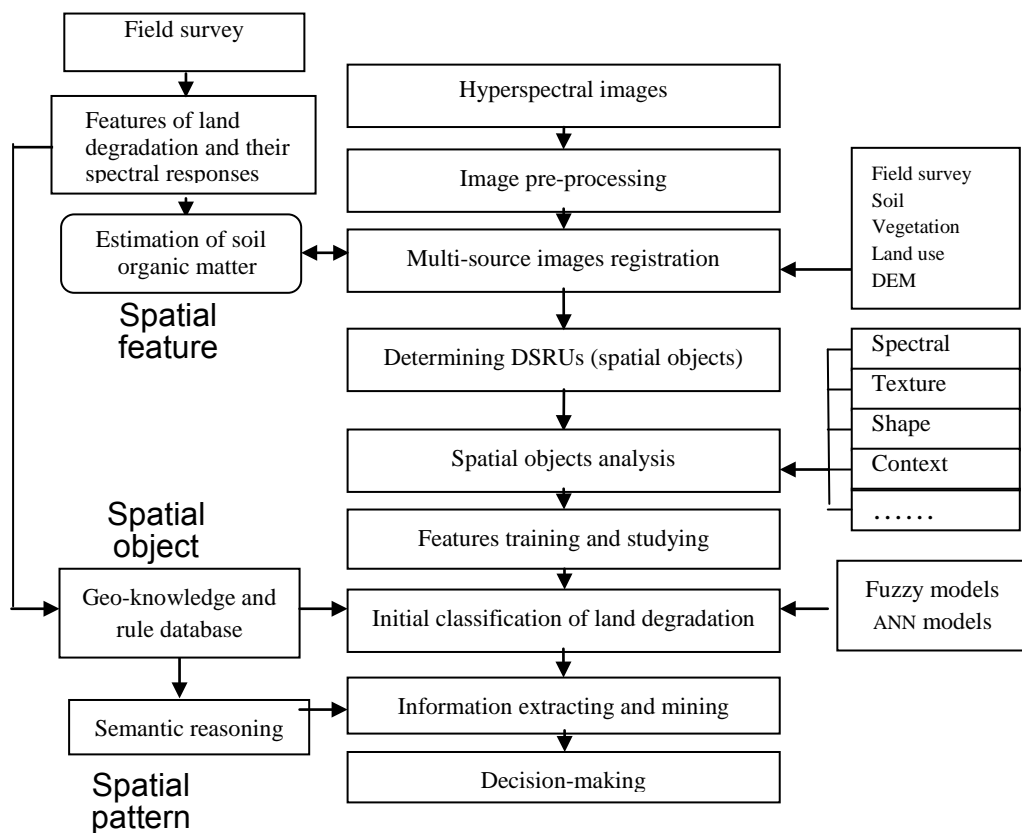
Figure 3.11 Approach of GEOIC on studying land degradation

The last step is the partition of multi-source images into geo-object or meaningful image objects for land degradation classification using fuzzy models and ANN models, etc, under the cognition network and rule sets in software. The meaningful image objects are labeled by rule-based classifiers using the required spectral and geometrical features and spatial relations between image objects. The rule-based classification is the process of associating initial DSRUs (image-objects) to classes of land degradation (geo-objects), based on both the internal features of the objects and their mutual relationships. The distribution of land degradation classes is used for land degradation analysis and decision-making by spatial pattern cognition.

Chapter 4

Test Area and Data Acquisition

This chapter describes the test area, the collection of surface-soil samples and soil reflectance spectra, and acquisition of Hyperion data. In this chapter, the pre-processing method of Hyperion data is discussed in detail, including geometric rectification, radiant correction, and spectrum reconstruction.

4.1 Test area

The test area is in Hengshan County located in the northern part of Shaanxi province, China with latitude from $37^{o}22'$ to $38^{o}74'$ N and longitude from $108^{o}65'$ to $110^{o}02'$ E (Figure 4.1). Hengshan County is in the transitional area from Mu Us Desert in its south to Loess Plateau in its north. The terrain of Hengshan County is characterized by a gradual increase in the altitude from 890 m in the northwest to 1535 m in the southeast. Stratum is leaning to northwest with time aged from east to west. It is in the edge of Loess Plateau, mainly in the south of Wu Ding River. A part of the area is rocky, including erinaceous rock, erinaceous shale and some marl. These sediments are in Oligo-Miocene age. Sandstone is the major rock type there, including fine sandy sediments. A part of that is coarse grain, alternated with sandy marl and conglomerate. This area is designated as "hill". Local names are "Liang" and "Mao". "Liang" and "Mao" mean Loess-hilly slope land and Loess-hilly top land, respectively. The area is in the temperate zone with continental monsoon semi-arid steppe climate. High-pressure center from Siberia affects this area chronically, so the climate is chilliness and desiccation. Precipitation concentrates from July to September each year with an average annual precipitation of 397mm and evaporation of 2085.5mm. The main soil type in the study area is Sandic Entisols, and the

dominant soil structure is physical granule. The average content of organic matter in the agriculture land was 0.68% according to the second soil survey in 1980.

Two large rivers, Wuding River and Lu River, divide the whole county into two geographical parts: one is the north on Wuding River and the west on Lu River, which is in Mu Us desert, suffering from great desertification; the other is the south on Wuding River and the east on Lu River, which is in Loess Plateau, encountering serious water erosion. The test area is in agriculture-pasture mixed area with wind and water erosion and complex physical geographical situation. The area of land degradation accounts for about 2/3 of total area of the county.
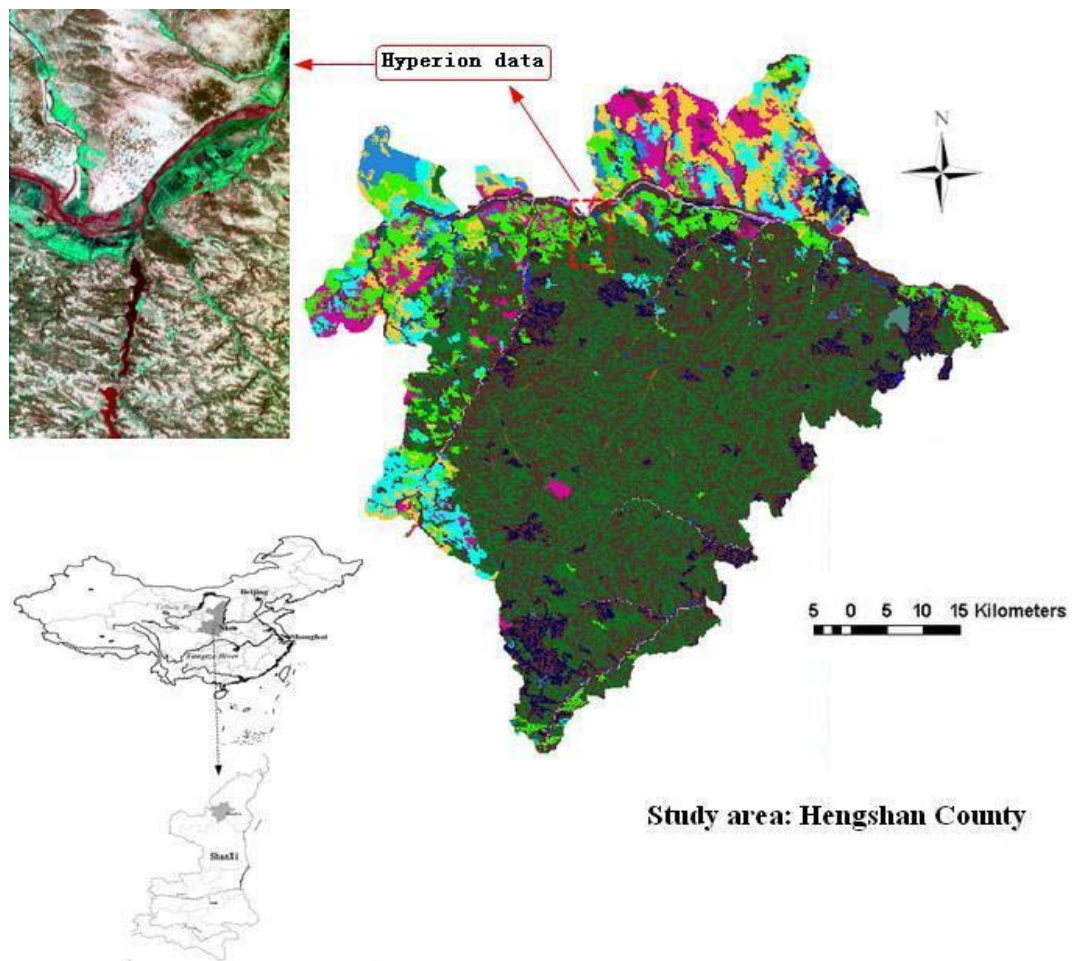
Figure 4.1 Test area: Hengshan County in Shaanxi Province

4.2 Data collection

4.2.1 Soil sample collection

For the study, 84 surface-soil samples in the whole county area were collected in the early June of 2003 (see Figure 4.2). The rectangular frame within the area was covered with Hyperion images with approximately $16km \times 12km$. The sampling sites were selected based on soil, geological and topographic properties so as to cover most of the surface conditions. The sampling sites were positioned with a Trimble Pro XRR GPS receiver. Soil samples were pre-processed and the chemical and physical properties of each soil sample were analyzed. Particle size distribution was determined using the pipette method on Na-saturated samples. SOM was measured by rapid dichromate oxidation technique. Total nitrogen and available nitrogen were measured by Kjeldahl method and steam-distillation method, respectively. Available Phosphorus and Potassium were measured by Mehlich 1 extraction method. Total iron was measured by means of ICP-AES spectrometry. Soil moisture was measured with TDR in-phase flight in June of 2003.
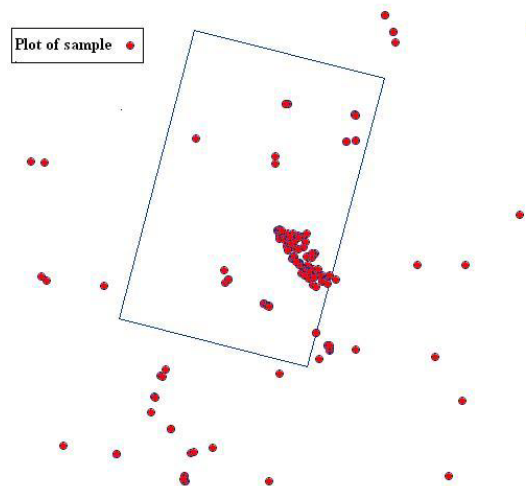
Figure 4.2 Distribution of soil samples in the test area

4.2.2 Spectroscopy collection

Field reflectance spectra was measured and recorded between 10:00 AM and 2:30 PM on a clear sunny day after EO-1 overflight in July of 2003, using a high spectral resolution Analytical Spectral Device (ASD). It operated in visible, near infrared and shortwave infrared bands (0.35–2.5μm). The radiometric measurements were carried out with resolution intervals of 0.01μm between 0.35μm and 1.0μm and 0.02μm between 1.0μm and 2.5μm. A reference panel by Labsphere Incorporated, Sutton, New Hampshire was used as reference before and after each measurement. The reflectance spectra were collected at one meter above the ground with 8% field of view under clear-sky condition. The bidirectional effects of the target reflectance were accounted for by carrying out measurements over a very short time interval and by keeping the viewing angle constant and in vertical position. In addition, the reflectance spectra of the soil samples were measured in the laboratory using ASD. Five individual spectra were averaged for each measured sample.

The nine-point weighted average method was applied to smooth the spectral curve:

$$Y_i = 0.04R_{i-4} + 0.08R_{i-3} + 0.12R_{i-2} + 0.16R_{i-1} + 0.20R_i$$
$$+ 0.16R_{i+1} + 0.12R_{i+2} + 0.08R_{i+3} + 0.04R_{i+4}$$

(4-1)

where Y_i is the weighted reflectance mean of the target for a particular channel, and R is the reflectance measured by the instrument for a particular channel and i is the channel number (Rock *et al.*, 1994).

4.2.3 Hyperion image acquisition

Hyperion is the imaging spectrograph carried by US EO-1 Earth Observatory Satellite. It is a push-broom sensor with one telescope and two spectrographs. The main technical parameters of Hyperion are given in Table 4.1. The 220-channel Hyperion data with 30 m spatial resolution were acquired over the test area on July 23, 2003, covering a ground area of approximately 8×12 km. Land use map in 2002,

soil map at a scale of 1:100 000 and topographic map at a scale of 1:100 000 in Hengshan County were also collected.

Table 4.1 The Technical specifications of Hyperion

Band number	Spectral range	Spectral resolution	Spatial Resolution	Image swath	Radiation accuracy	Quantization Rank	Weight
	μm	nm	M	km	%	Bit	kg
220	0.40-2.50	10	30	7.5	6	12	49

EO-1 is a part of NASA's New Millennium Program, designed to validate new technologies for remote sensing (Ungar, 2003). It was launched from Vandenberg Air Force Base on 21 November 2000 and placed in a sun-synchronous orbit with an altitude of 705 km and a 10:01 AM descending node. Its equatorial crossing time is one minute behind Landsat-7 and the orbit repeatability is 16 days. It is able to image the same location in daylight as many as 5 times every 16 days. The payload is comprised of three instruments: Hyperion, Advanced Land Imager and the Linear Etalon Imaging Spectral Array and Atmospheric Corrector. The Hyperion instrument consists of two push-broom imaging spectrometers with one covering the Visible/Near Infrared (VNIR) and the other Short-Wave Infrared (SWIR). Both spectrometers share a common telescope, producing hyper-spectral images with a spatial resolution of 30 m/pixel and spectral resolution of 10nm/band. A Hyperion image covers 7.5 km in width and typically around 53.6 km (8 s) or 80.4 km (12 s) in along track, which depends on the duration of the data collection. The VNIR spectrometer has 50 calibrated bands, ranging from 0.43 to 0.93 μm, and the SWIR spectrometer has 148 calibrated bands, ranging from 0.91 to 2.4 μm (see Table 4.2). The stability and S/N performance of Hyperion is lower than that of AVIRIS for several technical reasons. Hyperion can, thus, be considered a "moderate-fidelity" instrument in comparison to AVIRIS. A primary goal of the EO-1 program is to provide technical and scientific inputs to future orbital imaging spectrometer missions.

Table 4.2 Summary of Hyperion band wavelengths

Bands	Spectrometer	Calibration	Wavelength range (µm)
1-7	VNIR	Uncalibrated	0.36-0.42
8-57	VNIR	Calibrated	0.43-0.93
58-70	VNIR	Uncalibrated	0.94-1.06
71-76	SWIR	Uncalibrated	0.85-0.9
77-224	SWIR	Calibrated	0.91-2.4
225-242	SWIR	Uncalibrated	2.41-2.58

Peripheral bands with low signal and bands at the spectral overlap of the two spectrometers are uncalibrated, with DNs set to 0 during processing from L0 to L0.5 or L1 data.

4.3 Data pre-processing

Having analyzed the Hyperion data of all 220 bands, we eliminated some bands because of no signal, low signal-to-noise ratio or bad lines. The remaining 133 bands were used for this study. The central wavelength of 133 bands is listed in Table 4.3. Signal-to-Noise Ratio (SNR) gives an indication of data quality (Duggin *et al*., 1986). The homogenous area method was thus selected to calculate SNR values, i.e. use of the scenes in dark and bright locations to calculate signal mean (S) and its standard deviation (N), resulting SNR values. Figure 4.3 shows the SNR values with respect to band numbers for three typical objects: water body, vegetation and sandy land in the study area.

Table 4.3 Central wave length of 133 bands

Band	Central wave length nm	Band	Central wave length nm	Band	Central wave length nm	Band	Central wave length nm
1	467.519989	34	803.299988	67	1213.977036	100	1599.890235
2	477.690002	35	813.479980	68	1225.671375	101	1611.584574
3	487.869995	36	823.650024	69	1237.365714	102	1623.278913
4	498.040009	37	833.830017	70	1249.060054	103	1634.973253
5	508.220001	38	844.000000	71	1260.754393	104	1646.667592
6	518.390015	39	854.179993	72	1272.448732	105	1658.361931
7	528.570007	40	864.349976	73	1284.143072	106	1670.056271
8	538.739990	41	874.530029	74	1295.837411	107	1681.750610
9	548.919983	42	884.700012	75	1307.531750	108	1693.444950
10	559.090027	43	894.880005	76	1319.226090	109	1705.139289
11	569.270020	44	905.049988	77	1330.920429	110	1716.833628
12	579.450012	45	972.989990	78	1342.614769	111	1728.527968
13	589.619995	46	983.080017	79	1354.309108	112	1740.222307
14	599.799988	47	993.169983	80	1366.003447	113	1751.916646
15	609.969971	48	1003.299988	81	1377.697787	114	1763.610986
16	620.150024	49	1013.299988	82	1389.392126	115	1775.305325
17	630.320007	50	1023.400024	83	1401.086465	116	1786.999664
18	640.500000	51	1033.489990	84	1412.780805	117	1798.694004
19	650.669983	52	1043.589966	85	1424.475144	118	1810.388343
20	660.849976	53	1053.689941	86	1436.169484	119	1822.082683
21	671.020020	54	1063.790039	87	1447.863823	120	1833.777022
22	681.200012	55	1073.890015	88	1459.558162	121	1845.471361
23	691.369995	56	1094.089966	89	1471.252502	122	1857.165701
24	701.549988	57	1104.189941	90	1482.946841	123	1868.860040
25	711.719971	58	1164.680054	91	1494.641180	124	1880.554379
26	721.900024	59	1174.770020	92	1506.335520	125	1892.248719
27	732.070007	60	1184.869995	93	1518.029859	126	1903.943058
28	742.250000	61	1194.969971	94	1529.724198	127	1915.637397
29	752.429993	62	1155.505339	95	1541.418538	128	1927.331737
30	762.599976	63	1167.199678	96	1553.112877	129	1939.026076
31	772.780029	64	1178.894017	97	1564.807217	130	1950.720416
32	782.950012	65	1190.588357	98	1576.501556	131	1962.414755
33	793.130005	66	1202.282696	99	1588.195895	132	1974.109094
						133	1985.803434
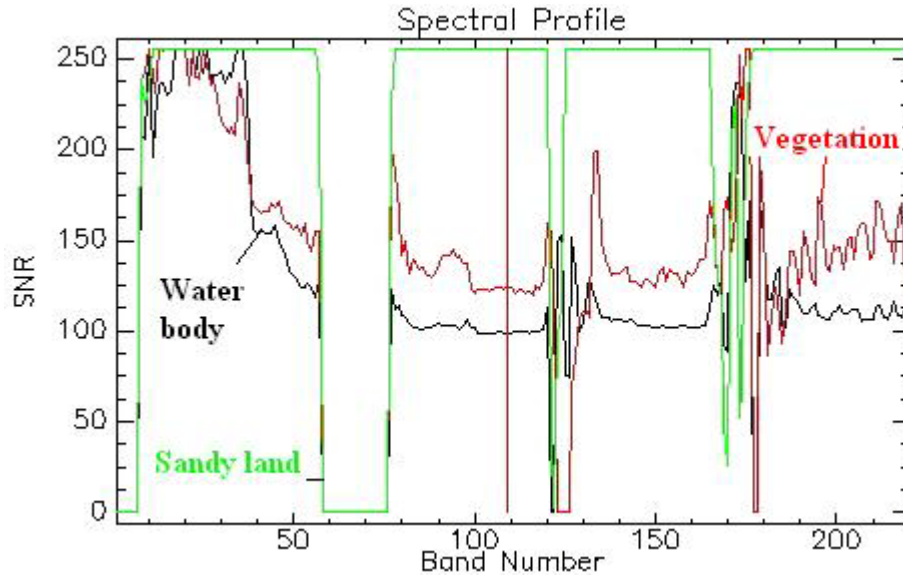
Figure 4.3 Spectral curves of water body, vegetation and sandy land in SNR image

The geometric correction was carried out using the polynomial approach based on 10 ground control points with ENVI software. In our study, accessorial data including land use map were interpreted from SPOT image (resolution 10 m) covering the study area, which was corrected with topographic map at 1:10 0000. The fitting accuracy (Root Mean Square (RMS)) was calculated from the residual errors for 10 control points. The estimated RMS was 0.026364 pixel. The residual errors of each point and corrected image were given in Figure 4.4 and Figure 4.5, respectively.

	Base X	Base Y	Warp X	Warp Y	Predict X	Predict Y	Error X	Error Y	RMS
#1+	1816.75	1634.38	307.55	255.55	307.5794	255.5132	0.0294	-0.0368	0.0471
#2+	1113.25	1565.63	75.69	283.20	75.7239	283.1930	0.0339	-0.0070	0.0346
#3+	1051.25	1611.63	59.00	302.25	58.9752	302.2585	-0.0248	0.0085	0.0262
#4+	1655.25	1979.63	279.78	377.28	279.7517	377.3116	-0.0283	0.0316	0.0424
#5+	1652.67	2044.33	283.48	398.20	283.4705	398.1826	-0.0095	-0.0174	0.0199
#6+	1010.67	1997.67	73.25	428.38	73.2512	428.3718	0.0012	-0.0082	0.0083
#7+	1588.33	2753.33	312.63	629.38	312.6393	629.3870	0.0093	0.0070	0.0117
#8+	2193.33	1215.00	399.79	94.65	399.7900	94.6547	0.0000	0.0047	0.0047
#9+	1660.33	1220.00	227.98	134.02	227.9688	134.0373	-0.0112	0.0173	0.0206
#10+	979.33	2412.33	92.56	562.95	92.5600	562.9503	-0.0000	0.0003	0.0003

Figure 4.4 Residual errors of each control point in geometric correction

Figure 4.5 The geometric corrected image

In order to reduce the influence of atmospheric scatter, water vapour absorption caused by mixed gasses, solar irradiance, and the solar zenith angle, the raw image data were converted to relative reflectance using the method of Internal Average Relative Reflectance (IARR) for image calibration. This is a simple available method for image calibration which is based only on image itself without field spectrum data. Figure 4.6 shows the spectra of vegetation using Hyperion data normalized to reflectance using the IARR method. Resampling was carried out using the nearest neighboring method so as not to severely alter the pixel values.
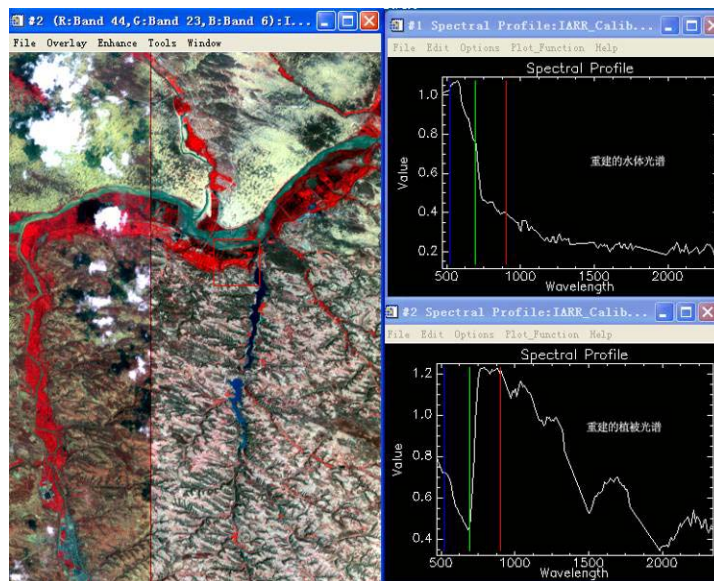
Figure 4.6 The relative reflectance image using the IARR method for image
calibration

Chapter 5

Mapping Soil Organic Matter Using the

GEOIC Approach and Hyperspectral Data

Soil organic matter (SOM) is a solid phase component which is the nutrient storehouse of vegetation. It can not only provide the nutrition for vegetation growing but also improve physical condition and temperature of soil. The SOM is one of the important criteria of soil fertility and also one of important diagnostic indicators related to land degradation. Mapping of SOM provides a base for land degradation evaluation. Soil spectrum and spectral models are the major research topics of image spectroscopy of SOM. As reviewed in section 2.2, numerous studies have been conducted. Although some of the studies have proved to be successful in mapping soil conditions, there exist some problems in the application of the established regression models for the interpretation of multi-spectral or hyperspectral images without any corrections to compensate for the change of scale. Many researchers have attempted to determine the most appropriate up-scaling technique to the models at different scales, but few effective ways have been developed to map soil parameters at a regional scale.

For studying up-scaling problem as mentioned above the GEOIC approach can be an appropriate one. This chapter is to investigate the up-scaling method for mapping SOM with the approach of GEOIC, and to demonstrate its usefulness using the hyperspectral data and multi-source data from the study area. The up-scaling method is developed by setting up the SOM estimation models based on DSRUs.

5.1 Analysis of soil features and spectral responses in the study area

In order to develop the estimation models for mapping SOM using the collected data in the study area (refer to section 4.2) with the GEOIC approach, the soil features and spectral responses were analyzed in detail. The SOM contents were in a range from 0.124% to 1.827%. The values of various soil parameters for different land use types are shown in Table 5.1. Statistical tests indicated that the average content of SOM, total nitrogen (TN), and the ratio of sand particle to clay particle were significantly different among irrigable land, non-irrigable land, and forestry land, abandon arable land, barren grassland, and garden land. The contents of SOM and TN decreased in the following order: irrigable land, non-irrigable land, man-made grassland, garden land, forestry land, barren grassland, other forestry land, and abandon arable land, from 0.77% to 0.22% for SOM and from 0.06% to 0.02% for TN. The cation exchange capacity (CEC) showed a similar decreasing trend with the maximum of 11.37 cmol/kg for irrigable land and the minimum of 8.08 cmol/kg for barren grass land. But the ratio of sand particle to clay particle showed an increasing trend in a similar order with abandon arable land having the maximum ratio of 67.97 and irrigable land having the minimum ratio of 9.29.

Table 5.1 Soil properties of different types of land use

Land type	Sand/Clay	Bulk density	SOM	CEC	SM	TN	Power/Clay
		g/cm^3	%	cmol/kg	%	%	
Irrigable land	9.29	1.32	0.77	11.37	7.77	0.06	1302.6
Non-irrigable land	10.20	1.26	0.53	11.08	6.35	0.04	1582.7
Man-made grassland	13.34	1.34	0.50	11.09	5.96	0.03	2182.2
Forestry land	31.75	1.44	0.43	9.49	7.06	0.03	1357.3
Other forestry land	39.77	1.39	0.32	9.98	4.18	0.02	1228.4
Barren grass land	24.51	1.37	0.42	8.08	4.51	0.03	894.1
Abandon arable land	67.97	1.47	0.22	9.56	3.97	0.02	572.6
Garden land	14.07	1.29	0.48	.	7.26	0.03	354.4
Average	14.03	1.30	0.54	10.77	6.26	0.04	1506.5
Difference level	<0.05	<0.05	<0.05		<0.05	<0.05	No Dif.

The ternary of soil texture was measured in lab according to the international soil texture classification criterion (for clay granule <2 µm, for silt granule = 2-20 µm, for sand granule = 20-2000 µm) (see Figure 5.1). The distribution of the particles

composition of the soil samples centralized relatively with dominant sandy particle, whose content was more than 87.5%. The soil samples were divided into three types: sandy loam soil, loamy sandy soil and sandy soil. Table 5.2 lists the characteristics for each soil type. The contents of SOM, TN, total iron, soil water, total Phosphorus (TP), and CEC decreased from sandy loam soil to loamy sandy soil, and to sandy soil, while the content of total Potassium (TK) increased from sandy loam soil to loamy sandy soil, and to sandy soil. The phenomena may be related to the content of clay grain in soil. The more the clay ingredient is in the soil, the higher the grain's adsorption to the nutrition and water will be.
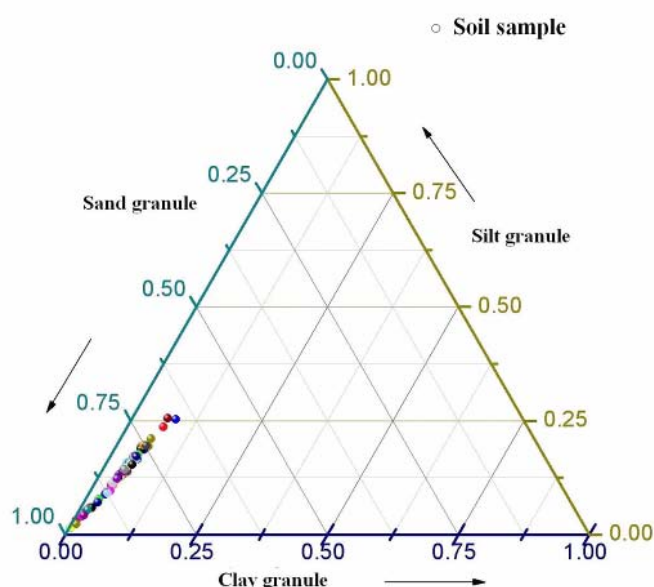
Figure 5.1 Triangle drawing of soil texture

Table 5.2 The soil characteristics in Hengshan county

Soil type	Clay	Silt	Sand	Fe	SOM	TN	Soil moisture
	%	%	%	mg/kg	%	%	%
Loamy sandy	3.27	9.57	87.16	22393	0.674	0.035	10.82
Sandy soil	1.18	3.86	94.97	16094	0.342	0.022	7.48
Sandy loam	4.85	16.37	78.79	23195	0.690	0.048	12.23
soil type	**K**	**TP**	**CEC**	**AN**	**AK**	**AP**	**pH**
	mg/kg	mg/kg	cmol/kg	mg/kg	mg/kg	mg/kg	
loamy sandy	19694	580.75	10.69	93.20	90.19	4.35	7.61
Sandy soil	21321	455.32	8.34	45.73	57.63	4.52	7.60
Sandy loam	19115	630.48	11.51	89.42	85.09	4.64	7.46

The soil spectral reflectance synthetically reflects the physical-chemical characteristics of surface substance. SOM, total iron, silt, sand and mineralogy (quartz, magnetite, kaolinite and smectite) are the most important components influencing the reflectance intensity and the spectral features. They can be used for the characterization and classification of soil. The variation of soil parent materials and changes in vegetation cover and weather can change soil characteristics and its respective spectral reflectance. SOM is one of soil properties that significantly influence the bidirectional reflectance characteristic of soil substrate. Therefore the detection of its change is essential to determine soil degradation and help extract the information on land degradation with remote sensing data. In the study area, the reflectance spectra of 84 soil samples were measured in lab. Figure 5.2 shows the spectral curves of three soil types, which are similar in shape with the spectral reflectance of sandy soil highest and that of loamy sandy soil lowest. Figures 5.3 and 5.4 show the changes in spectral reflectance of soil with various amounts of SOM content, and with different percentages of vegetation cover. One can see from the figures that the reflectance was higher for lower content of SOM, and also for soil with less vegetation cover. These are easy to understand. The average reflectance of soil samples with more than 1% content of SOM was 0.1183 and with less than 1% content of SOM was 0.24. The analysis of the lab spectra for different soil samples shows that SOM had no absorption apex at 0.35-2.5μm. These results are also consistent with the statement by Stoner and Baumgardner (1981) that the SOM content had a negative correlation with the reflectance at visible light band and at 0.62-0.66μm band.
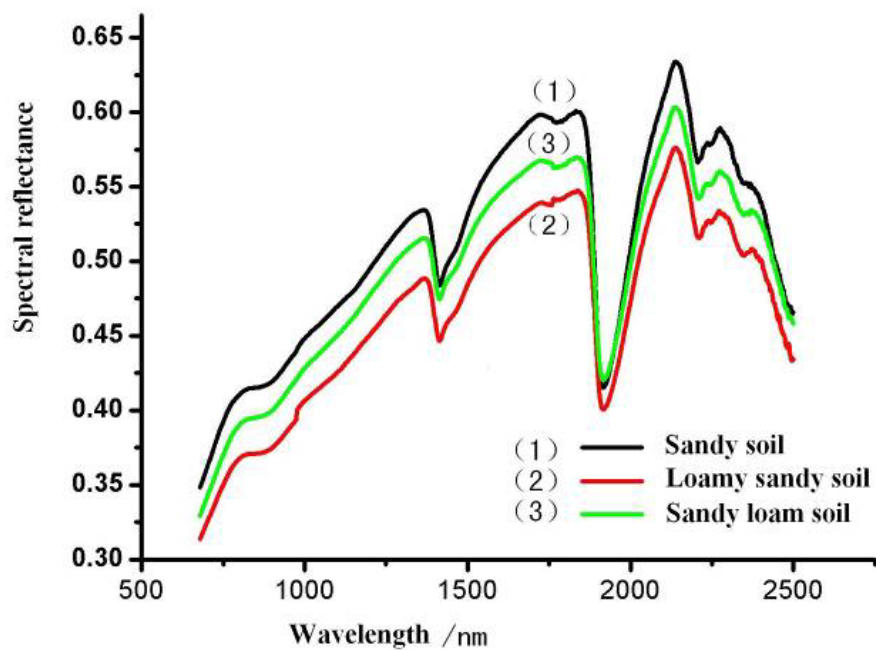
Figure 5.2 Soil spectral curves
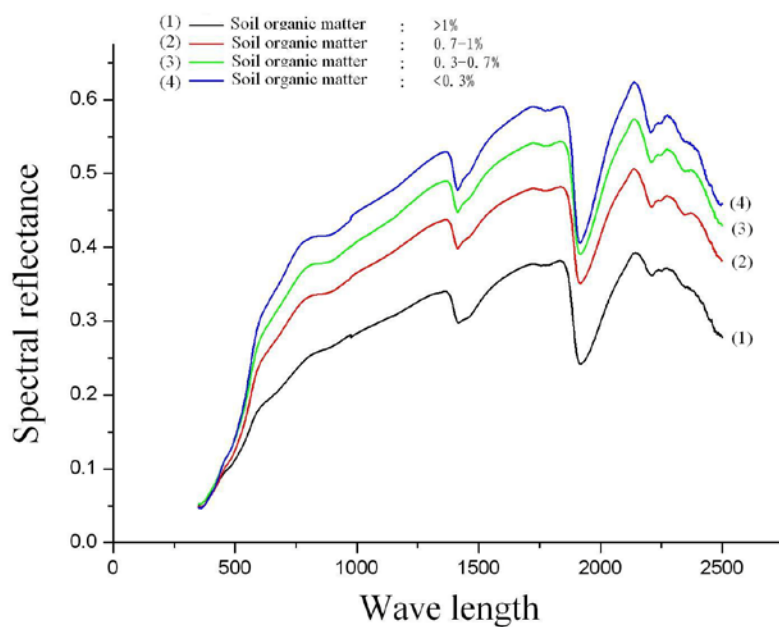
Figure 5.3 The spectral reflectance of soil with various amounts of SOM content
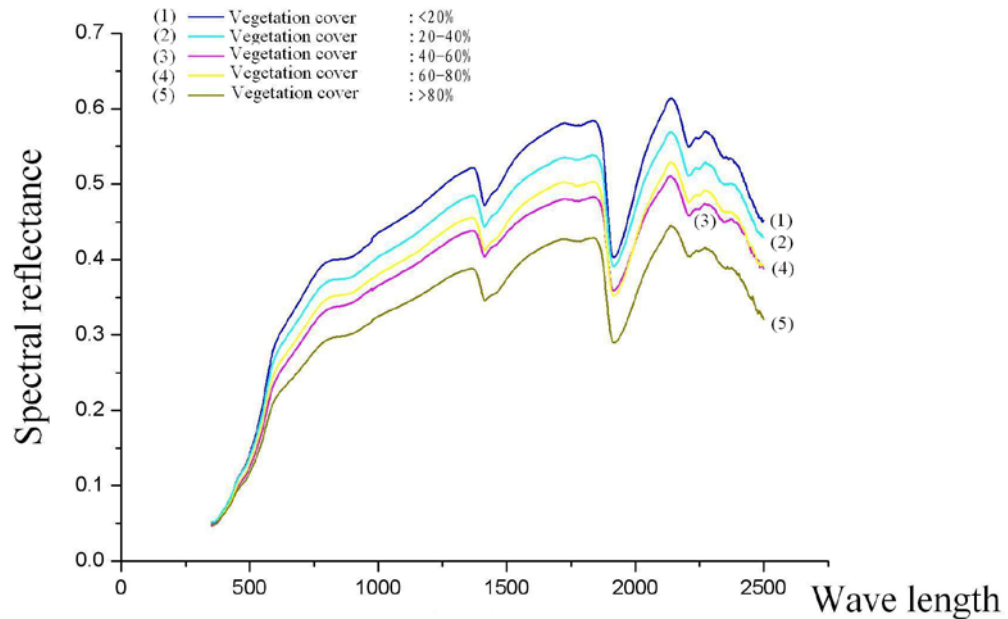
Figure 5.4 The spectral reflectance of soil with different vegetation coverage

5.2 Methods

5.2.1 *In-situ* estimation model of SOM

It is critical to develop an *in-situ* estimation model based on soil parameters and the spectral reflectance of the soil samples measured in laboratory. In this study we develop the estimation models of SOM using the statistics method and the fuzzy estimation method. The detailed procedure is introduced below.

5.2.1.1 Multivariate statistical analysis

Multivariate statistical analysis can be applied in the analysis of soil spectral data using software SPSS 15.0. SPSS provides a powerful statistical-analysis in a graphical environment, using descriptive menus and simple dialog boxes. In this study, the correlation coefficients between the measured soil parameters and the absorption feature parameters at obtained wavelength were calculated. Principal Components Analysis (PCA) was also conducted to transform the relative variables

into the independent variables. Multi-regression between the spectral reflectance and associated soil parameters and analysis of variance were conducted.

A linear regression model expresses the dependent variable (spectral reflectance) as a linear function of independent variables (soil properties):

$$Y_i = \beta_0 + \beta_1 X_{1i} + \beta_2 X_{2i} + ... + \beta_k X_{ki} + e_i \tag{5-1}$$

where β_0 is the intercept or constant term of the regression model; β_j (j=1, 2, …k) are the regression coefficients to be estimated, Y_i is the dependent variable for case i with error e_i; X_{ki} is the kth independent variable for case i.

C_i is caseweight. If caseweight is not specified, $C_i =1$. Let I be the number of distinct cases; p the number of independent variables. Then C is sum of caseweights: $\sum_{i=1}^{I} C_i$.

The regression coefficients of the model are estimated using the least square technique. The outputs include estimated regression coefficients (β), their standard errors, the standardized regression coefficients (*Beta*), statistical quantity t, and test boundary value. Operations start with the correlation matrix **R**. **R** is the sample correlation matrix for $X_{1........}X_p$ and Y:

$$\boldsymbol{R} = \begin{bmatrix} r_{11} & \cdots & r_{1p} & r_{1y} \\ r_{21} & \cdots & r_{2p} & r_{2y} \\ . & \cdots & . & . \\ r_{y1} & \cdots & r_{yp} & r_{yy} \end{bmatrix} \tag{5-2}$$

where $r_{kj} = \dfrac{S_{kj}}{\sqrt{S_{kk}S_{jj}}}$ and $r_{yk} = r_{ky} = \dfrac{S_{ky}}{\sqrt{S_{kk}S_{yy}}}$. In the model, some descriptive statistics are described in the following: S_{kj} is sample covariance for X_k and X_j; S_{yy} is sample variance for Y; S_{ky} is sample covariance for X_k and Y; P^* is number of coefficients in the model. $P^*=P$ if the intercept is not included; otherwise $P^*=P+1$.

The SPSS model summary table reports the strength of the relationship between the model and the dependent variable, including *Multiple R, R square*, adjusted *R square*, and standard error of the estimate. *Multiple R* as the multiple correlation coefficient is the linear correlation between the observed and model-predicted values of the dependent variable. Its large value indicates a strong relationship. *R Square*, the coefficient of determination, is the squared value of the multiple correlation coefficient. It shows that about half the variation in time is explained by the model.

The expression of *Multiple R* is:

$$R = \sqrt{1 - r_{yy}} \tag{5-3}$$

The expression of *R square* is:

$$R^2 = 1 - r_{yy} \tag{5-4}$$

The expression of adjusted *R square* is:

$$R^2_{adj} = R^2 - \frac{(1 - R^2)p}{C - p^*} \tag{5-5}$$

The standard error of the estimate is the mean square residual from the ANOVA table, or expressed as:

$$\sqrt{(SS_e)/(C - P^*)} \tag{5-6}$$

The SPSS analysis of variance table (ANOVA table) is also important in the model. ANOVA tables can be employed to determine how well the model and each parameter fit the data by comparing the mean least square error estimated to the mean pure experimental error and by assuming that the errors are normally distributed. Tests such as the *F* test can then be employed to assess the significance of the fit both for the model as a whole and for the individual parameters of the vector β. This can be expressed in a tabular form as discussed below:

Analysis of Variance	Df	Sum of Squares	Mean Square
Regression	P	SS_R	$(SS_R)/p$
Residual	$C\text{-}p^*$	SS_e	$(SS_e)/(C\text{-}p^*)$

The ANOVA table includes regression and residual sums of squares, mean square, F, and probability of F. The regression row displays the information about the variation accounted for by the model. The residual row displays the information about the variation that is not accounted for by the model. If the regression and residual sums of squares are approximately equal, it means that about half of the variation is explained by the model. The significance value of the F statistic is less than 0.05, which means that the variation explained by the model is not due to chance. While the ANOVA table is a useful test of the model's ability to explain any variation in the dependent variable, it does not directly address the strength of that relationship.

The expression of residual sum of squares (SS_e) is:

$$SS_e = r_{yy}(C\text{-}1)S_{yy} \tag{5-7}$$

with degrees of freedom $C\text{-}p^*$.

The expression of sum of squares due to regression (SS_R) is:

$$SS_R = R^2(C\text{-}1)S_{yy} \tag{5-8}$$

with degrees of freedom p.

The standardized regression coefficients ($Beta_k$) is:

$$Beta_k = r_{yk} \tag{5-9}$$

The standardized error $Beta_k$ is estimated by:

$$\hat{\sigma}_{Beta_k} = \sqrt{\frac{r_{yy} r_{kk}}{C - p^*}} \qquad (5\text{-}10)$$

F-test for *Beta$_k$*:

$$F = \left(\frac{Beta_k}{\hat{\sigma}_{Beta_k}} \right)^2 \qquad (5\text{-}11)$$

with 1 and *C-p** degrees of freedom.

5.2.1.2 Estimation with a fuzzy set approach

The fuzzy set theory is suitable to make decisions in complex systems. It has been commonly used for imprecise information in a non-probabilistic sense and allows an integration of the information on various parameters into modeling and evaluation process. Fuzzy set theory may be regarded as a generalization of classical set theory. A fuzzy set is defined in terms of its membership function. In the classical set theory the membership of a set element is either 1 if it is within a defined boundary, or 0 if outside the boundary. But a fuzzy set is defined in terms of a membership function which maps the domain of interest onto the interval [0, 1]. The membership function for a fuzzy set usually is a curve in shape. The membership function of a set *A* defined over a domain *X* takes the form:

μ_A: $X{\rightarrow}[0,1]$

The set *A* can be expressed as:

$A=\{(\mu_A(X)),x{\in}X,\mu_A(X){\in}[0,1]\}$

In the model estimation process a set of samples is usually divided into two groups: one for modeling and the other for validation. For instance, in the case study described in chapter 4, 84 soil samples were randomly divided into modeling samples and validation samples. The former is about 80% of total samples, and latter

is the rest 20%. Let n be the number of modeling samples, and m the number of modeling indicators. Then the eigenvalue matrix is expressed:

$$X = (x_{ij})_{m \times n} \tag{5-12}$$

where x_{ij} is eigenvalue of sample j with respect to indicator i（the spectral reflectance of jth soil sample to ith indicator）, $i = 1, 2, \cdots, m$, $j = 1, 2, \cdots, n$. The n samples are divided into c classes. The matrix of relative membership degree is expressed:

$$U = (u_{hj})_{c \times n} \tag{5-13}$$

where u_{hj} is the relative membership degree of sample j subject to class h, $h = 1, 2, \cdots, c$. The optimal parameter of the model is calculated by determining the optimal cluster center and the weight of all modeling samples:

$$S^* = (s_{ih})_{m \times c} \tag{5-14}$$

where s_{ih} is eigenvalue standard of class h and indicator i, $0 \leq s_{ih} \leq 1$。

$$W^* = (w_1, w_2, \cdots, w_m), \quad \sum_{i=1}^{m} w_i = 1 \tag{5-15}$$

where w_i is the weight of modeling class i.

The validation samples are classified based on a fuzzy model and the membership degree of the validation samples is computable:

$$u_{hj}^* = \left\{ \sum_{k=1}^{c} \frac{\sum_{i=1}^{m} [w_i (r_{ij} - s_{ih})]^2}{\sum_{i=1}^{m} [w_i (r_{ij} - s_{ik})]^2} \right\}^{-1} \tag{5-16}$$

where u_{hj}^{*} is membership degree of sample j subject to class h.

The optimized matrix of relative membership degree (U^{*}) through the circulation iterative calculation is expressed:

$$U^* = (u_{hj}^*)_{c \times n} \tag{5-17}$$

The class eigenvalue h_j of sample j is calculated by following expression:

$$h_j = (1, 2, \cdots, c) \cdot (u_{1j}^*, u_{2j}^*, \cdots, u_{cj}^*)^T \tag{5-18}$$

The class eigenvalue vector of n samples is calculated by expression:

$$H = (h_1, h_2, \cdots, h_n) \tag{5-19}$$

The relationship model between SOM and soil spectral reflectance can be established based on the fuzzy estimation approach (Li *et al.*, 2003, 2008). The relationship model is as follows:

$$\hat{y} = a + bh \tag{5-20}$$

where $b = \sum_{j=1}^{n}(h_j - \bar{h})(y_j - \bar{y}) / \sum_{j=1}^{n}(h_j - \bar{h})^2$, $a = \bar{y} - b\bar{h}$, $\bar{h} = \dfrac{1}{n}\sum_{j=1}^{n}h_j$, $\bar{y} = \dfrac{1}{n}\sum_{j=1}^{n}y_j$,

y_j is the measured content of SOM, $\hat{y}$ is the estimated content of SOM.

The relative error of the estimated value for the validation samples is expressed as:

$$e_j = (\hat{y}_j - y_j) / y_j \tag{5-21}$$

where e_j is the relative error, y_j measured value, and $\hat{y}_j$ estimated value.

The estimated model is considered satisfactory if the averaged relative error $\bar{e} \leq 20\%$ and if the change in $\bar{e} \leq 20\%$ for selection more modeling samples to set up the estimated model again under the above steps.

5.2.2 Determining optimal spectral bands for the SOM estimation

The development of the estimation models of SOM firstly needs determining the sensitive spectral bands to SOM for an area of interest. In the study area the method of choosing optimal spectral bands by Giorgio *et al*. (2005) was applied. Having analyzed the average reflectance of lab spectra of soil samples, three band regions were divided in view of a small inflexion of the reflectance of spectrum in the 0.35μm to 1.38μm region (Figure 5.5). The negative correlation coefficients between soil spectral reflectance and the SOM content in the study area are higher at bands of $R_{625,}$ R_{740}, and R_{1336} in three regions of 0.35-0.63μm, 0.63-0.84μm, and 0.84-1.38μm, respectively (Figure 5.6). Thus, these 3 bands were considered as the optimal spectral bands for the SOM estimation. The band of 0.74μm was chosen as the most optimal spectral band. This was because not only the negative correlation coefficient of SOM was the highest at band of R_{740}, but also band of R_{740} was maximally influenced by the variations of the correlation coefficient in the visible and in the near infrared range (Latz *et al*., 1984; Krishnan *et al*., 1980).
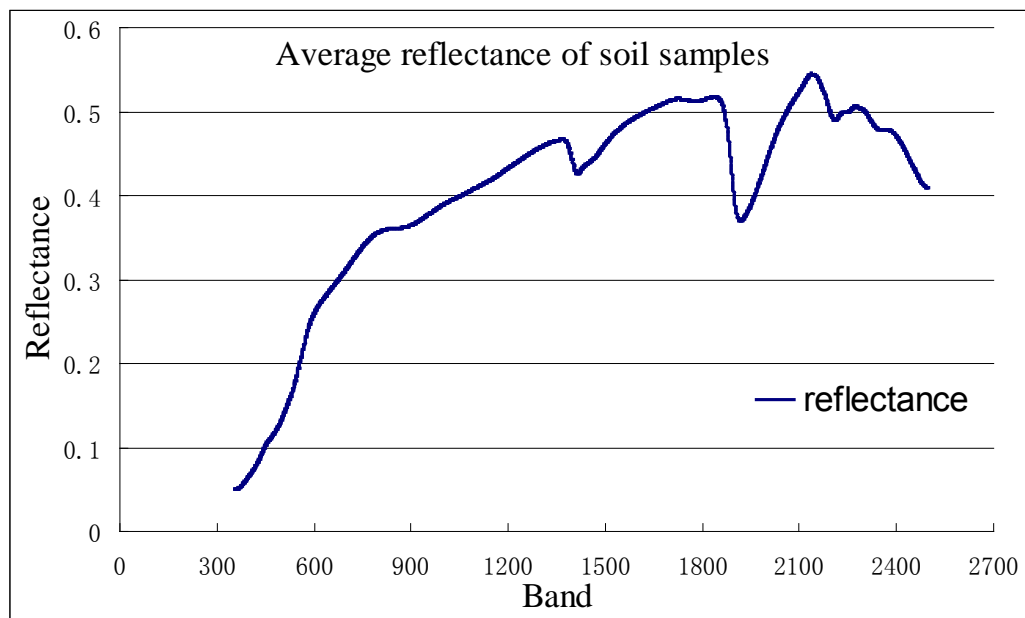
Figure 5.5 Average reflectance of soil sample spectrum
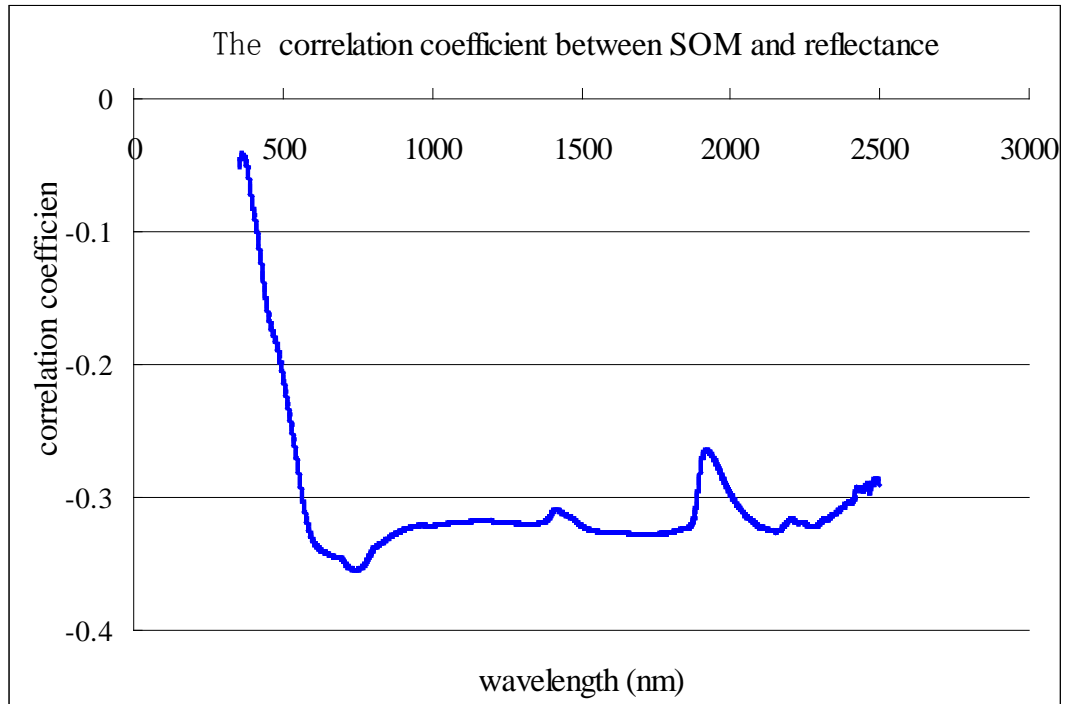
Figure 5.6 Correlation coefficients between contents of SOM and spectral reflectance

To determine the optimal spectral regions for estimating SOM, the correlation coefficients were calculated between the SOM content and the ratio of reflectance in band of 0.74μm as the denominator to one beyond 0.74μm as the numerator. The wavelength with the highest correlation coefficient was chosen. Then these ratios were highly correlated with the SOM content when using a region of 0.43-0.45μm as the numerator. To do a comparison, the correlation coefficients in the range of 0.4-1.2μm as the numerator and 0.74μm as the denominator were also computed. The results showed the relatively highest correlation coefficient was in 0.45μm wavelength. The correlation coefficient was again calculated between the SOM content and the ratios of reflectance in 0.45μm as the denominator to ones beyond 0.45μm as the numerator. It has been demonstrated that the higher correlation coefficients were in bands of 0.44μm band and 0.56μm.

5.2.3 Segmentation of DSRUs with the GEOIC approach

In this study we should segment Land Degradation Spectral Response Units (DSRUs) for the development of the DSRU estimation models of SOM with the developed GEOIC approach. Therefore this section discusses the segmentation of DSRUs with the GEOIC approach using the data/information in the study area (see Chapter 4) as an example.

A land characteristic is an attribute of land that can be measured or estimated. Land units, as determined by soil survey and often derived and updated with physiognomy, soil, vegetation, land use, land cover and remote sensing images, are normally described in terms of land characteristics (Zonneveld, 1989). Determining land units is the basis for SOM mapping for land degradation evaluation at a regional scale. As mentioned above in this study we propose the idea of DSRU It is used not only as the modeling unit of estimation models of SOM, but also as mapping unit at a regional scale using remote sensing techniques. The segmentation of DSRUs is done through integrating different types of data and knowledge under the GEOIC approach, i.e. based on spatial characteristics of physiognomy situation, soil and vegetation, and remote sensing image information.

A basic element in an object analysis is an image object, which is a contiguous region in an image. Each image object has homogeneous characteristic properties. The best segmentation should provide optimal information for further processing (Baatz and Scha¨pe, 2000; Chaudhuri and Sarkar, 1995; Hofmann *et al*., 1998; Laine and Fan, 1996; Mao and Jain 1992). An initial segmentation relies on low-level information, e.g. the pixel values and basic features of the intermediate image objects, and provides the image object primitives with a certain spectral behavior, shape and context. These object features enable a preliminary classification. The classification results can be used as high-level input for segmentation, a so-called classification-based segmentation. Typically, objects of interest are extracted by these iterative loops of classification and processing. Thereby, image objects as processing units can continuously change their shape, classification and mutual relations. This segmentation can be realized as an optimization process. The regions of minimum

heterogeneity, given certain constraints, have to be found. The criteria for heterogeneity, definition of constraints and the strategy for the sequence of aggregation determine the final segmentation results. Multi-scale segmentation results were used to construct a hierarchical network of image objects that simultaneously represented image information in different spatial scales. The image objects were networked, so that each image object "knew" its context (neighbourhood), its super-object, and its sub-objects (see Figure 5.7).
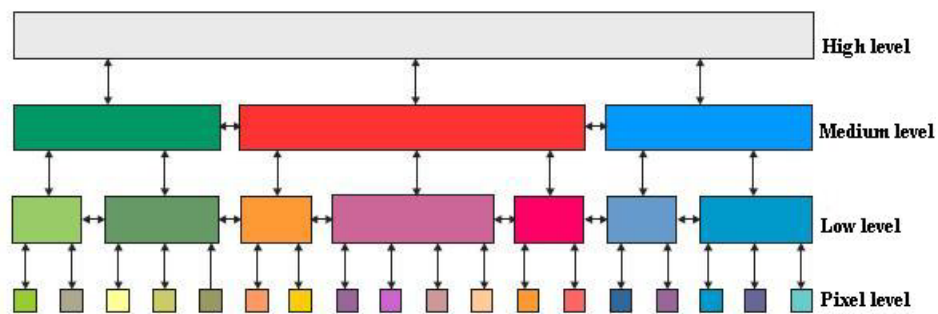
Figure 5.7 Structure of a hierarchical network

The above-mentioned image segmentation method was used for the determination of DSRUs. The segmented image objects are DSRUs using those variables related to land degradation. The climate variable sometimes may not be considered if an area of interest is not large and climate variation could be small, like the study area mentioned in Chapter 4. In this case only layers of physiognomy, vegetation, soil type and image information were used in the process of segmentation of DSRUs.

Vegetation index (Modified Chlorophyll Absorption Ratio Index (MCARI)) derived from Hyperion images were used as the vegetation layer (see Figure 5.8). The expression of MCARI followed Kim *et al*. (1994) and Daughtry *et al*. (2000):

$$\text{MCARI} = [(R_{700}-R_{670})-0.2(R_{700}-R_{550})] (R_{700}/R_{670}) \tag{5-22}$$

where R_{500}, R_{670} and R_{700} represent the reflectance at wavelength of 550nm, 670nm and 700nm, respectively.

Soil map produced from the soil survey in 1980 was collected. Soil map at scale of 1:100 000 (1980) was used as the soil layer for the segmentation of DSRUs. Slope and elevation derived from DEM（30×30 m）was used as the layers of physiognomy characteristics. Hyperion data fusion transformations representing spectral information was the comprehensive response to land use/land cover, soil, vegetation and the effects of human activities. The problem of hyperspectral dimensionality such as the Hughes phenomenon must not be neglected. It was noted that the performance of a classifier is affected by the poor estimates of training statistics beyond about ten features (De Jong and Van Der Meer, 2007). In this study, nine fusion transformations, from first principal component (PCA1) to the ninth principal component (PCA9) calculated from Hyperion hyperspectral bands were used as spectral layers. The weight of each principal component is determined, considering its eigenvalue and spectral information related to above 5 optimal bands. PCA1, PCA2 and PCA3 were with large eigenvalue and contained more information related to the optimal bands, therefore their weights were set 1; while the weights for PCA7, PCA8 and PCA9 were set 0.3. The land use map at scale of 1:100 000 (interpreted from TM images and SPOT 2 4 images in 2001) was used as the thematic layer in the segmentation process (Table 5.3). Its significance is only for the case that any segmentation does not span the polygon border line of vector data in the thematic layer. It is noted that only polygon vector data as the thematic layer could be included in the segmentation process.
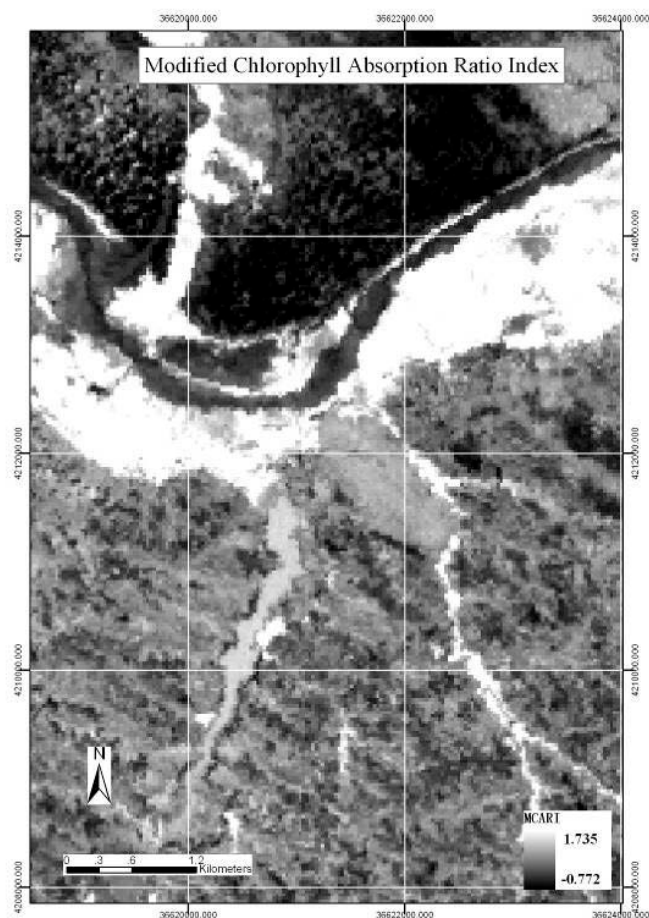
Figure 5.8 Vegetation index (MCARI) derived from Hyperion images

Table 5.3 Segmentation layers and their weights

Layers	Weight
PCA1	1.0
PCA2	1.0
PCA3	1.0
PCA4	0.5
PCA5	0.5
PCA6	0.5
PCA7	0.3
PCA8	0.3
PCA9	0.3
Soil type map	1.0
DEM	1.0
Slope	1.0
MCARI	1.0
Land use map(thematic layer)	1.0

The segmentation used in this study was a bottom-up region-merging approach, starting with one-pixel objects. The segmentation algorithm utilizes spectral information to extract continuous, independent and homogeneous regions or image objects. Spectral or color heterogeneity is defined as:

$$h = \sum_c w_c (n_{merge} \cdot \sigma_c^{merge} - (n_{obj1} \cdot \sigma_c^{obj1} + n_{obj2} \cdot \sigma_c^{obj2})) \qquad (5\text{-}23)$$

where w_c is the weight attributed to each channel and σ_c is the standard deviation of the spectral values in each channel. The standard deviations themselves are weighted by the object sizes n. Object features are calculated after the segmentation using spectral, shape and textural features. The spectral features are the channel means, standard deviations, brightness and maximum difference. Object shape is obtained by calculating object length/width proportion and a shape index. Brightness and shape index are defined as:

$$B = \frac{1}{n_L} \sum_{i=1}^{n_L} \overline{c}_i \qquad (5\text{-}24)$$

$$S = \frac{e}{4\sqrt{A}} \qquad (5\text{-}25)$$

Brightness B is the mean value of the spectral mean values $\overline{c}_i$ of an image object. The shape index S is the border length e of the image object divided by four times the squared root of its area A. Concerning texture, first and second order texture measures are derived from either the Grey-Level Co-occurrence Matrix (GLCM) or the Grey-Level Divergence Vector (GLDV), such as homogeneity, contrast, dissimilarity, entropy, angular second moment, mean, standard deviation and correlation. The GLCM and GLDV are computed for each input channel and in four spatial directions: 0°, 45°, 90°and 135°. To obtain a direction-invariant quantity, all the four directional values are summed up for texture calculation.

In the subsequent step, smaller image objects were merged into bigger ones. Visual interpretation of different image segmentation results showed that it was extremely

beneficial to use DEM, soil type, vegetation index and nine data fusion transformations in the segmentation process.

In this study, the developed GEOIC approach was applied in SOM mapping. DSRUs were partitioned automatically with remote sensing images and multi-source data. Their spatial, spectral, geographic and temporal characteristics were assessed for developing DSRU estimation models of SOM. The eCognition software is regarded as an appropriate tool of the segmentation of DSRUs because it can supply the function of image multi-segmentation. In the segmentation process, a user needs to define several parameters, like scale parameter, layer weight and adjustable criteria for homogeneity or heterogeneity in color and shape. Scale is a crucial factor for image understanding. In software eCognition, the scale parameter is an abstract term which determines the maximum allowable heterogeneity for the resulted image objects. Adjustment of the scale parameter will indirectly influence the average object size: a larger value leads to bigger objects. In this study, different scale parameters were chosen to determine an appropriate one and to study its effect on the precision of estimation models in the study area. Four levels at scale parameters of 25, 50, 100 and 200, representing different size of DSRUs, from smaller to larger, were chosen in the area (Figure 5.9). The homogeneity criterion was set as follows: color 0.8 and shape 0.2 (Table 5.4).

Table 5.4 Four scale parameters for image segmentation

Level	Scale parameter	Spectral heterogeneity		Shape heterogeneity		Number of units
		Color	Shape	Smoothness	compactness	
1	25	0.8	0.2	0.5	0.5	36021
2	50	0.8	0.2	0.5	0.5	9760
3	100	0.8	0.2	0.5	0.5	3180
4	200	0.8	0.2	0.5	0.5	1161
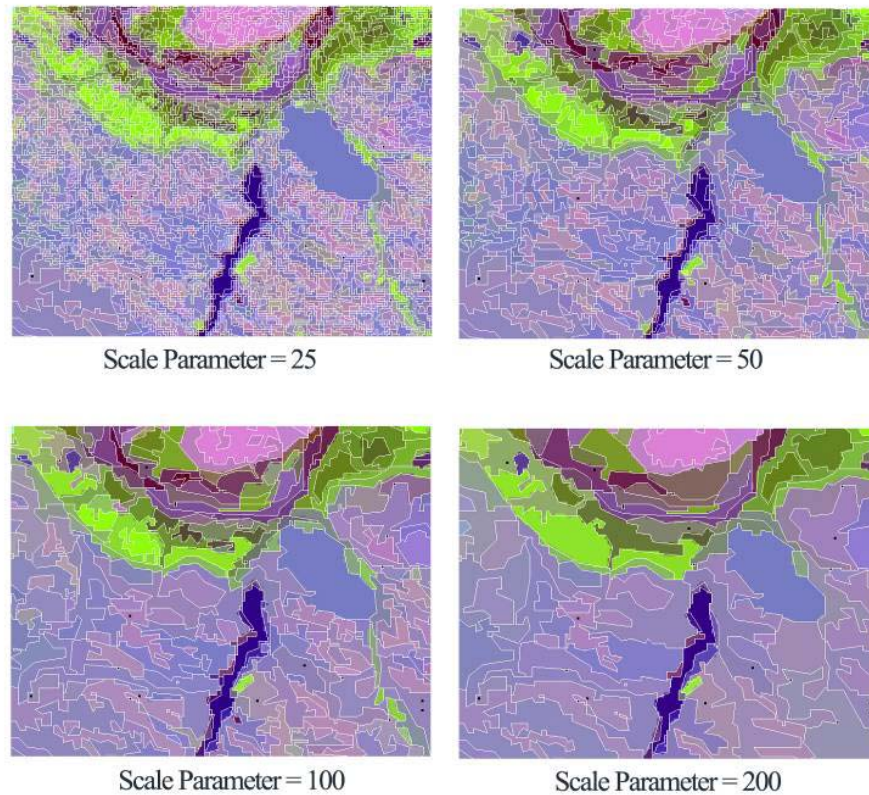
Figure 5.9 The results of segmentation with four scale parameters

5.2.4 Up-scaling method of estimation models for SOM

As mentioned in Chapter 2, the term scaling refers to translating information from one scale to another. Many of the inconsistencies in the results exist when remote sensing data are used to produce thematic maps or as inputs into physical models, without explicitly taking into account the impact of scale.

Remote sensing physical models may be described by the dependence of a parameter $R(l(\omega))$ on the measured radiance $l(\omega)$ at a point ω of the surface. For each ω in a given area Ω, the model R generates a value $R(l(\omega))$, which is usually a density, such as SOM (Figure 5.10). The natural objective of satellite measurements is to obtain the value of R at a regional size. Namely, satellite measurements aim to reach the value:

$$\frac{1}{|\Omega|}\iint_\Omega R(\ell(\omega))d_\omega \tag{5-26}$$

where Ω is one pixel of area; $|\Omega|$ is the definitional domain of Ω, for each point $\omega \in \Omega$. This is the ideal value which would be obtained by computing $R(l\ (\omega))$ using the model and the measurement of l at each point ω of the area Ω (at the same instant) and evaluating the quantity R for the whole area Ω from its value at each ω. For each point $\omega \in \Omega$ at a microscopic scale of the *in-situ* experiment we note the radiances in *n* radiometer channels

$$\ell(\omega) = (\ell_1(\omega),...,\ell_n(\omega)) \tag{5-27}$$

In fact, the actual value given by the model with the satellite measurement is *R(L)*, where *L* is the measured reflectance of the pixel (Figure 5.10). In the following, we consider a perfect sensor, that is, a sensor, with which the impulse response is a squared window. In other words, the reflectance measured by sensor is

$$L = \frac{1}{|\Omega|}\iint_\Omega \ell(\omega)\rho(\omega)d_\omega \tag{5-28}$$

where the given function $\rho > 0$ is the impulse response of the sensor and satisfies (for a perfect sensor, one has $\rho(\omega) = 1$):

$$\frac{1}{|\Omega|}\iint_\Omega \rho(\omega)d_\omega = 1 \tag{5-29}$$
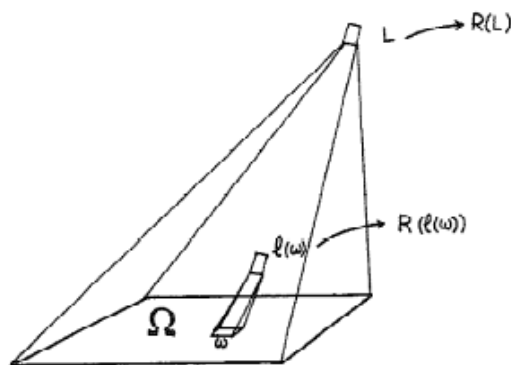
Figure 5.10 The model *R* validated at a local scale, generates a value $R(l(\omega))$ from the radiance $l(\omega)$ at $\omega \in \Omega$. The microscopic area ω is mathematically represented by a point.

As noted by Raffy (1992), there is difference between $\frac{1}{|\Omega|} \int \int_{\Omega} R(l(\omega))\ d\omega,$, which is the exact value of $R(l(\omega))$ integrated over the pixel, and the value obtained from the satellite measurement, *R(L)*. The models used in remote sensing are based on a relationship between the measured radiances and the physical parameters of the soil surface. A number of them are semi-empirical, in the sense that they contain some constants, which were adjusted by taking account of *in situ* models, and generally carried out in a given type of medium. Once validated *in-situ*, these models are applied to large scale areas.

The value $\varphi(\omega)$ is considered to be the `actual' value of a parameter, such as SOM, for $\omega \in \Omega$. A perfect remote sensing model satisfies:

$$\varphi(\omega) = R(\ell(\omega)), \quad \text{for } \omega \in \Omega \tag{5-30}$$

In general the models are not perfect, and the relation between φ and *R* depends on some constant parameters p_i if using multiple linear regression analysis.

$$p = (p_1, ..., p_k) \tag{5-31}$$

Then, for these models, called semi-empirical models, we have

$$\varphi(\omega) \cong R(\boldsymbol{p}, \ell(\omega)), \qquad \text{for } \omega \in \Omega.$$

(5-32)

These models, even validated with *in-situ* experiments, are developed with regional scale data, in order to discover the exact regional value for the parameter Φ:

$$\Phi = \frac{1}{|\Omega|} \int_{\Omega} \varphi(\omega)\, d\omega$$

(5-33)

To approximate Φ, once $\boldsymbol{p}_{\text{loc}}$ is estimated, we deduce

$$\Phi \cong \frac{1}{|\Omega|} \int_{\Omega} R(\boldsymbol{p}_{\text{loc}}, \ell(\omega))\, d\omega$$

(5-34)

Raffy and Gregoire (1998) demonstrated that those constants, appropriate for *in-situ* experiments, were no longer appropriate for a regional scale. For remote sensing applications, these constants must be determined by a new least square cost function.

Remote sensing models are often based on a relationship between a soil-level parameter and the sensor reflectance at a given wavelength. The general practice is to apply these models to the reflectance measured from satellites, without making any correction for the change of scale. The practice, however, can result in arbitrary and erroneous results. Therefore, it is necessary to consider the scale effects in remote sensing. When the model at local scale extrapolated to a larger scale, a general method is proposed to build a new model connected to the one at local scale and connected to the variables at a large scale to compensate for the change of scale.

In the study, an *in-situ* estimation model based on the relationship between the SOM content and soil spectral reflectance of soil samples in field survey is difficult to apply to the images. Therefore the estimation model based on the relationship between the SOM content and the spectral and regional variables of DSRUs was proposed and developed. The estimation model was defined as DSRU model in this study. This model was set up based on a hypothesis that a homogenous DSRU has similar soil properties. A property parameter of a soil sample was regarded as an

attribute of a DSRU where the soil sample was collected. The average parameter value of several soil samples was calculated if a DSRU includes several soil samples.

The flowchart of up-scaling method of SOM estimation models from *in-situ* model to DSRU model is given in Figure 5.11. The laboratory data were used to analyze the features of soil parameters and soil spectral reflectance and spectral responses to soil parameters. The field survey data were used to formulate semi-empirical relationships between soil spectral reflectance and the SOM content at *in-situ* field scale. The features of DSRU, such as color, area, mean and standard deviation of principle components PCA1, PCA2, PCA3, and vegetation index MCARI, and the mean and standard deviation of elevation and slope, and spectral information of sensitive bands were used in DSRU model.
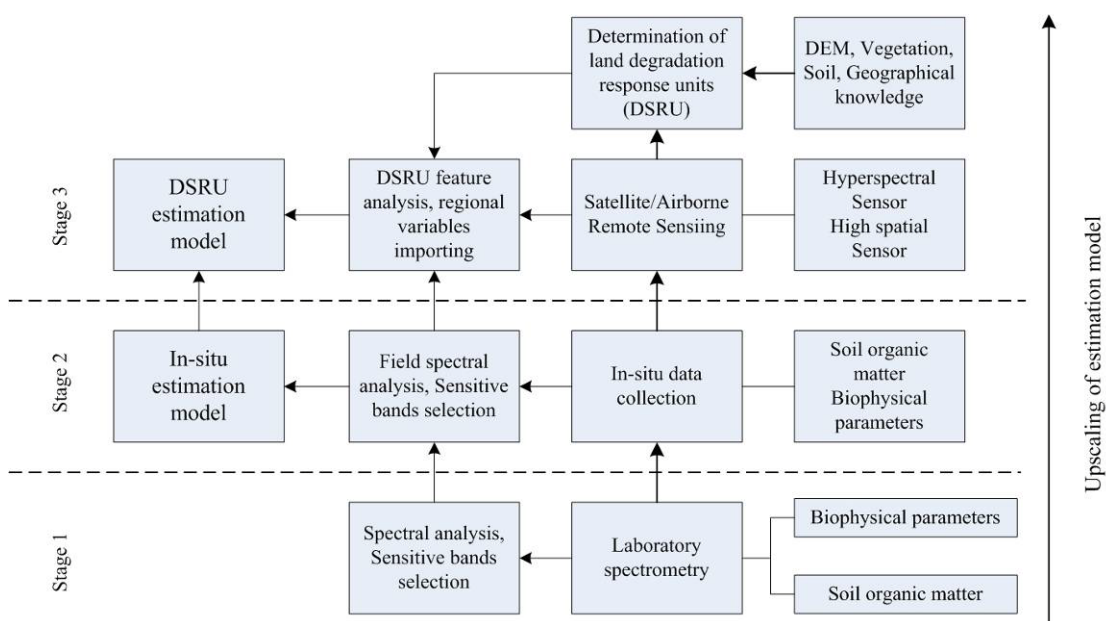
Figure 5.11 Approach flowchart of up-scaling of the SOM estimation model using remote sensing images

5.3 The test results and discussions

5.3.1 *In-situ* model estimation of SOM

The two methods of the multiple regression model (refer to section 5.2.1.1) and fuzzy set model (refer to section 5.2.1.2) were used to develop the *in-situ* models of SOM with the test data. The two different methods were used to validate the consistency of chosen optimal spectral bands for the SOM estimation with the spectral data of soil samples. These bands were used as variables in the model estimation of SOM using Hyperion images.

5.3.1.1 SOM estimation based on multiple statistics analysis

As discussed in section 5.2.2, analysis of the correlation between soil spectra reflectance in lab and the SOM content of soil samples gave 5 optimal spectral bands at the wavelength of 0.44μm, 0.56μm, 0.625μm, 0.74μm and 1.336μm. However, as pointed out by Latz *et al*. (1984) and Krishnan *et al*. (1980), SOM caused a large variation in the reflectance of spectrum from the 0.5μm to 0.8μm region, therefore only four bands of 0.44μm, 0.56μm, 0.625μm and 0.74μm were used for the estimation.

He *et al*. (2004) proved that the transformation of the first differentiation of the logarithm of the reciprocal reflectance could produce a stronger correlation with the SOM content. Let W be the ratio of the first differentiation of the logarithm of the reciprocal reflectance in one band to that in another band, such as $((\log(1/R_{740}))'/(\log(1/R_{440}))')$, $(\log(1/R_{740}))'/(\log(1/R_{560}))'$, $(\log(1/R_{625}))'/(\log(1/R_{440}))'$, and $(\log(1/R_{625}))'/(\log(1/R_{560}))'$, etc. The result for the band of 0.625μm over the band of 0.56μm has the higher correlation coefficient of 0.8948, consistent with the result of Krishnan *et al*. (1980), who demonstrated that SOM content was strongly correlated with the ratio of the first differentiation of the logarithm of the reciprocal reflectance in band 0.623μm to that in band 0.564μm. Therefore different regression models were estimated with W = $(\log(1/R_{625}))'/(\log(1/R_{560}))'$. The results are given in Table 5.5.

Table 5.5 The result of *in-situ* SOM estimation models based on regression analysis

Model types	Estimation equation	adjusted R^2	F value
Linear	Y=23.245w-10.567	0.7457	70.45
Logarithmic	Y=20.446lnw-8.2354	0.7265	69.34
Quadratic	Y=16.466-4.385w+2.668w^2	0.8684	80.34
Power	Y=12.435w$^{3.7232}$	0.6818	66.34
Exponential	Y=0.2563e$^{6.7554w}$	0.6456	65.23

In the table W = (log($1/R_{625}$))'/(log($1/R_{560}$))', R is the reflectance, and Y is the SOM content. The quadratic curve model (y=16.466-4.385w+2.668w^2) was chosen, with the highest adjusted R Squared coefficient (R^2) and F value. The statistical test indicated the equation is significant at $p<0.001$, where p is significant level. The predicted SOM contents with the quadratic model showed a linear relationship with the test values, which suggests the model is appropriate.

5.3.1.2 SOM estimation based on a fuzzy set method

The SOM content and the first differentiation of the logarithm of the reciprocal reflectance for bands of 0.44μm, 0.56μm, 0.625μm, 0.74μm and 1.336μm were input variables in SOM estimation model based on the fuzzy set approach discussed above. Among all the soil samples, 66 samples were used for modeling and 18 samples for validation. In the modeling we set 5 classes and the calculation precision of 10^{-5}. Using the software module developed by Li *et al*. (2003), we got

$$\hat{y} = 0.317h - 0.156 \tag{5-35}$$

where $\hat{y}$ is the estimated content of SOM and h is the class eigenvalue.

The correlation coefficient of the model was 0.9623, and the optimal weight of variables was (0.153, 0.156, 0.208, 0.345, 0.138) for the bands of 0.44μm, 0.56μm, 0.625μm, 0.74μm and 1.336μm, respectively. The result is given in Table 5.6. The average error of estimated SOM content was 10.52%, indicating a higher precision of the model. The stability of the estimation model was tested with different samples for modeling and evaluation. In the test we used 4 samples for validation and 80

samples for modeling. The average error is only a small increase to 11.68%, which suggests the established model is stable.

Table 5.6 The result of *in-situ* SOM estimation model based on fuzzy set analysis

Correlation coefficient	Model parameter		Maximal error	Minimal error	Average error	No. of second validation samples	Second average error
	a	b	%	%	%		%
0.9623	0.317	-0.156	19.03	0.56	10.52	4	11.68

The above results showed that the transformation of soil spectral reflectance is useful to improve the correlation between the SOM content and the spectral reflectance, especially the first differentiation of the logarithm of reciprocal reflectance, consistent with Cloutis's results (Cloutis, 1996). Moreover, the above analyses indicated (1) both multivariate statistical analysis and fuzzy set analysis gave consistent results; and (2) the spectral reflectance of soil samples in bands of R_{440}, R_{560}, R_{625}, R_{740}, and R_{1336} was significantly correlated with the content of SOM. These bands can be used as the variables of estimation model of SOM using Hyperion images.

5.3.2 DSRU models estimation of SOM with the GEOIC approach

To solve the problem of *in-situ* model estimation of SOM, the DSRU estimation models were proposed in this study under the approach of the GEOIC. Through integrating soil spectral knowledge and geographic knowledge, the segmentation of DSRUs was conducted based not only on spatial characteristics of physiognomy situation, soil and vegetation, but also on remote sensing image information. The spectral wavelengths of Hyperion images were not the same as the lab spectral wavelengths collected by ASD. The spectral bands of R_{467}, R_{560}, R_{625}, R_{740}, and R_{1336} in Hyperion images were chosen as optimal ones for the SOM estimation with Hyperion images. The features of DSRUs, such as color, area, the mean and standard deviation of reflectance in bands R_{467}, R_{560}, R_{625}, R_{740}, R_{1336} of Hyperion images, the mean and standard deviation of principle components PCA1, PCA2, and PCA3, vegetation index MCARI of Hyperion images, and the mean and standard deviation

of elevation and slope, were used as the variables to set up the DSRU estimation models at different scale levels of 25, 50, 100, and 200.

The correlation between each of the above variables and the content of SOM of DSRUs was analyzed (see Table 5.7). The results showed that the logarithm of reflectance R_{625} and the logarithm of PCA2, the average of elevation and MCARI, and the quantities of $(1/\log R_{467})/(1/\log R_{625})$, $(1/\log R_{560})/(1/\log R_{625})$, $(1/\log R_{560})/(1/\log R_{740})$, $(1/\log R_{625})/(1/\log R_{740})$, $(1/\log R_{740})/(1/\log R_{625})$ and their reciprocals were significantly correlated with the SOM content for all the scales (at significant level less than 0.01). Color, $(1/\log R_{625})/(1/\log R_{1336})$, the standard deviation of the reflectance in bands of R_{560} and R_{625}, and the standard deviation of MCARI were significantly correlated with SOM content at scale levels of 25 and 50, while the average reflectance in bands of R_{1336}, R_{467} and R_{560}, $(1/\log R_{467})/(1/\log R_{560})$, and $(1/\log R_{560})/(1/\log R_{467})$ were significantly correlated with SOM content at scale levels of 100 and 200. These suggested that the standard deviations of the variables were significantly correlated with SOM at smaller scale levels, while the averages of the variables were at larger scale levels. This can be explained by the result that every scale reveals the information specific to its level of observation (Marceau, 1999). Scale refers to the spatial dimension at which entities, patterns, and processes can be observed and characterized. No single scale is sufficient for assessing the varying sized, and spatially arranged components on the planet, a society, or in any complex system (Hay and Marceau, 2004).

Table 5.7 Correlation significance of SOM content with various variables estimated by DSRU models at four scale levels

	Scale parameter			
	25	50	100	200
COLOR		*		
Log (R_{467})		*	**	**
Log (R_{560})	*	**	**	**
Log (R_{625})	**	**	**	**
Log (PCA2)	**	**	**	**
MEAN R_{1336}			**	
MEAN R_{467}		*	**	**
MEAN R_{560}		*	**	**
MEAN R_{625}	*	**	**	**
MEAN elevation	**	**	**	**
MEAN MCARI	**	**	**	**
MEAN PCA2	**		**	
MEAN PCA3		**	**	*
Standard deviation R_{560}	*			
Standard deviation R_{625}	**			
Standard deviation MCARI	**			**
$(1/logR_{1336})/(1/logR_{625})$	*			
$(1/logR_{467})/(1/logR_{560})$		**	**	**
$(1/logR_{467})/(1/logR_{625})$	**	**	**	**
$(1/logR_{467})/(1/logR_{740})$	**	**	**	
$(1/logR_{560})/(1/logR_{467})$		**	**	**
$(1/logR_{560})/(1/logR_{625})$	**	**	**	**
$(1/logR_{560})/(1/logR_{740})$	**	**	**	**
$(1/logR_{625})/(1/logR_{1336})$	*			
$(1/logR_{625})/(1/logR_{467})$	**	**	**	**
$(1/logR_{625})/(1/logR_{560})$	**	**	**	**
$(1/logR_{625})/(1/logR_{740})$	**	**	**	**
$(1/logR_{740})/(1/logR_{467})$	**	**	**	
$(1/logR_{740})/(1/logR_{560})$	*	**	**	**
$(1/logR_{740})/(1/logR_{625})$	**	**	**	**

** **:** significant level < 0.01; ***** **:** significant level < 0.05

At scale levels of 25, 50, 100, and 200, the number of DSRUs used for modeling was 82, 71, 48 and 24, respectively. The results showed that the stepwise multiple regression models at scale levels of 25, 50 and 100 were statistically significant at significance level less than 0.01, with the determinative coefficients (R^2) of 0.562, 0.721 and 0.722, respectively. The sum of squares and mean square at scale level of 100 was the lowest (see Table 5.8). This displays the information about the variation accounted for by the model. The determinative coefficient (R^2) at scale level of 50 was similar to that at scale level of 100. The model at scale level of 200 had no statistical significance. It was probably due to too few statistical samples. However, the determinative coefficients of DSRU models were lower than those of *in-situ* models. This scaling effect may be partly caused by the inability of the satellite

imagery to detect small scale heterogeneity. Field sampling is able to detect small-scale changes, and the spectral averaging process of DSRU results in a decrease in pixel variation. The spectral averaging effect is likely to be the main reason for the low range of image spectral reflectance and the dominance of low values of DSRUs. Meantime, a potential cause for pixel signal heterogeneity may be due to the vegetation distribution pattern. In the study area, the vegetation distributes sparse, and the distribution pattern of vegetation was similar. Therefore, this potentially increased signal heterogeneity within each pixel while decreasing heterogeneity within each DSRU in Hyperion images.

The type of DSRU estimation model of SOM at different scales was:

$$Y= B_0+B_1X_1+B_2X_2+B_3X_3+ \cdots +B_nX_n \qquad (5\text{-}36)$$

Where Y is the SOM content of DSRU, and $X_1, X_2, X_3, \cdots, X_n$ is DSRU features. B_0 is the constant of regression model. $B_1, B_2, B_3, \cdots, B_n$ are the coefficients of independent variables of $X_1, X_2, X_3, \cdots, X_n$.

Table 5.8 Parameters of regressions estimated by DSRU estimation models at four scales

		Scale parameter			
		25	50	100	200
R		0.750	0.849	0.849	0.988
R Squared		0.562	0.721	0.722	0.977
Adjusted R Squared		0.43	0.56	0.419	0.724
Std. Error of the Estimate		0.208	0.183	0.183	0.191
Sum of Squares	Regression	3.482	3.883	2.001	3.09
	Residual	2.715	1.502	0.772	0.073
	Total	6.196	5.385	2.773	3.163
Df	Regression	19	26	25	22
	Residual	63	45	23	2
	Total	82	71	48	24
Mean Square	Regression	0.183	0.149	0.08	0.14
	Residual	0.043	0.033	0.034	0.036
F value		4.253	4.474	2.384	3.86
Significance level		.000	.000	.010	.226

The meaning of each independent variable is: X_1 = the mean of MCARI, X_2= the mean of elevation, X_3= the mean of slope, X_4= the mean of R_{467}, X_5= the mean of R_{560}, X_6= the mean of R_{625}, X_7= the mean of R_{1336}, X_8= the standard deviation of MCARI, X_9= the standard deviation of elevation, X_{10}= the standard deviation of slope, X_{11}= the standard deviation of R_{467}, X_{12}= the standard deviation of R_{560}, X_{13}= the standard deviation of R_{625}, X_{14}= the standard deviation of R_{740}, X_{15}= the standard deviation R_{1336}, X_{16}= $LogR_{467}$, X_{17}= $(1/logR_{467})/(1/logR_{560})$, X_{18}= $(1/logR_{740})/(1/logR_{560})$, X_{19}= $(1/logR_{560}) / (1/logR_{740})$, X_{20}= $(1/logR_{625})/(1/logR_{560})$, X_{21}=$(1/logR_{740})/(1/logR_{467})$, X_{22}=$(1/logR_{560})/(1/logR_{467})$, X_{23}= $(1/logR_{625})/(1/logR_{1336})$, X_{24}= $(1/logR_{1336}) / (1/logR_{625})$, and X_{25}= $(1/logR_{1336})/(1/logR_{560})$.

The estimated regression models at scale levels of 25, 50, and 100:

$Y=-706.113 -0.078X_1 +0.004X_3 -1.045X_8 -0.015 X_9 + 0.004 X_{10} -0.001X_{11} +0.003X_{12} -0.002X_{13} -0.001X_{14} +354.993X_{18}+351.054X_{19}$ (5-37)

$Y=-302.41 +0.116X_1 +0.008X_3 -0.003X_5 -2.43X_8 + 0.005X_9 +0.032X_{10} -0.002X_{11} -0.005X_{12} +0.006X_{13} +30.050X_{16} +59.642X_{20} -2.04 X_{21} -53.126 X_{22} +85.771X_{23} +117.687 X_{24}$ (5-38)

$Y= 37.022 -0.898X_1 +0.002X_2 -0.008X_3 -0.002X_4 + 0.003X_6 -0.003X_7 -3.519X_8 -0.003X_9 +0.064X_{10} -0.002X_{14} +0.004X_{15} -77.032 X_{17} +56.177 X_{20} -9.392 X_{21} -7.895 X_{25}$ (5-39)

In the model at scale level of 25, the standardized coefficients showed that the effect of independent variables on dependent variable of Y was in the following decreasing order: $(1/logR_{560}) / (1/logR_{740})$, $(1/logR_{740})/(1/logR_{560})$, and the standard deviations of R_{560}, R_{625}, R_{467}, and R_{740}. The tests on each independent variable showed that $(1/logR_{560})/(1/logR_{740})$, $(1/logR_{740})/(1/logR_{560})$, and the standard deviations of R_{560}, R_{625}, and R_{740} all had significant effect on dependent variable of Y. In the model at scale level of 50, the standardized coefficients showed that the effect of each independent variables on dependent variable was in the following decreasing order: $(1/logR_{1336})/(1/logR_{625})$, $(1/logR_{625})/(1/logR_{1336})$, $LogR_{467}$, the mean of R_{560}, the standard deviations of R_{560}, and R_{625}, $(1/logR_{625})/(1/logR_{560})$, the standard deviations

of R_{467}, and $(1/\log R_{560})/(1/\log R_{467})$. The tests on each independent variable showed that $(1/\log R_{1336}) / (1/\log R_{625})$, $(1/\log R_{625})/(1/\log R_{1336})$, and $\log R_{467}$ had significant effect on the dependent variable. In the model at scale level of 100, the standardized coefficients showed that the effect of the independent variables on the dependent variable was in the following decreasing order: the means of R_{625} and R_{467}, $(1/\log R_{625})/(1/\log R_{560})$, the mean of R_{1336}, $(1/\log R_{467})/(1/\log R_{560})$, the standard deviation of R_{740}, and $(1/\log R_{1336})/(1/\log R_{560})$.

The DSRU estimation models of SOM at different scale levels included different independent variables. The combined independent variables by the sensitive bands in R_{467}, R_{560}, R_{625}, R_{740} and R_{1336} were also included into DSRU estimation models and had significant effects on the dependent variable at different scale levels. The standard deviations of R_{467}, R_{560}, R_{625}, and R_{740} were included into the DSRU estimation models at small scale level and had significant effects on the dependent variable. On the other hand, the means of R_{467}, R_{560}, R_{625}, and R_{740} were included into the DSRU estimation models at large scale level and had significant effects on the dependent variable. This difference may be partly caused by the spectral averaging process that results in the decrease in pixel variation from scale level of 25 to scale level of 100.

Moreover, the means of MCARI and slope and the standard deviations of MCARI, elevation and slope had significant effects on the DSRU estimation models at the scale levels of 25, 50 and 100; while the mean of elevation had a significant effect on the estimation model at large scale level. It was found that the environmental variables of elevation, slope and vegetation index (MCARI) were major factors affecting the distribution of SOM at a regional scale, and therefore should be introduced into the DSRU estimation models. It also demonstrated the impact of scale on modeling SOM using remote sensing techniques. Remote sensing provides the possibility of conducting empirical studies to understand the behavior of variables when changing scale, and derive appropriate rules for scaling. The study result was consistent with the results by other researchers about scale effects on modeling and scaling methods through introducing some regional variables or scale invariant variables into models by a change of scale in different fields (Raffy, 1992;

Friedl *et al.*, 1995; Turner *et al.*, 1996; Friedl, 1997). Raffy (1992) proposed a method to reduce the error introduced by a change of scale when linking a ground parameter. Friedl *et al.* (1995) demonstrated that Normalized Difference Vegetation Index (NDVI) is not scale invariant. Turner *et al.* (1996) conducted a study to determine the effects of spatial scale on the results obtained from a spatially distributed biogeochemical model. Their results clearly indicated the differences in the inputs and outputs because of low spatial resolution

A comparison of the measured SOM of the check samples with the estimated values using the DSRU estimation models indicated that the SOM can be reliably obtained from fusing Hyperion imagery and multi-source data through the segmentation of DSRUs at an appreciate scale with the GEOIC approach. The estimated results by the DSRU models at scale levels of 50 and 100 were tested using DSRU samples. The results showed a linear relation between the measured values and the estimated values of SOM.

The fractions of vegetation and water body were first derived by linear spectral mixture model in Hyperion images. The information on the flourishing vegetation with MCARI>0.05 was then derived from the above vegetation fraction. The Hyperion images were processed by masking the information on flourishing vegetation and water body. These processed Hyperion images were used to map the distribution of SOM at scale levels of 50 and 100 by the DSRU models. The results are plotted in Figure 5.12 and Figure 5.13. The figures showed that the irrigated land and dike field contained higher contents of SOM, while the Loess-hilly top land, Loess-hilly slope land and sandy land contained lower contents of SOM. This was in agreement with the field survey results, showing a gradual decrease in the SOM contents from the irrigated land, dike field, terrace, Loess-hilly top land, and to Loess-hilly slope land and to the sandy land. Furthermore, the distribution of SOM was close to the results with the Kridge interpolation of soil samples (Figure 5.14). But one should note that the distribution of SOM using Hyperion images was only relative, and the mapping results only showed spatial variation of SOM in the study area.
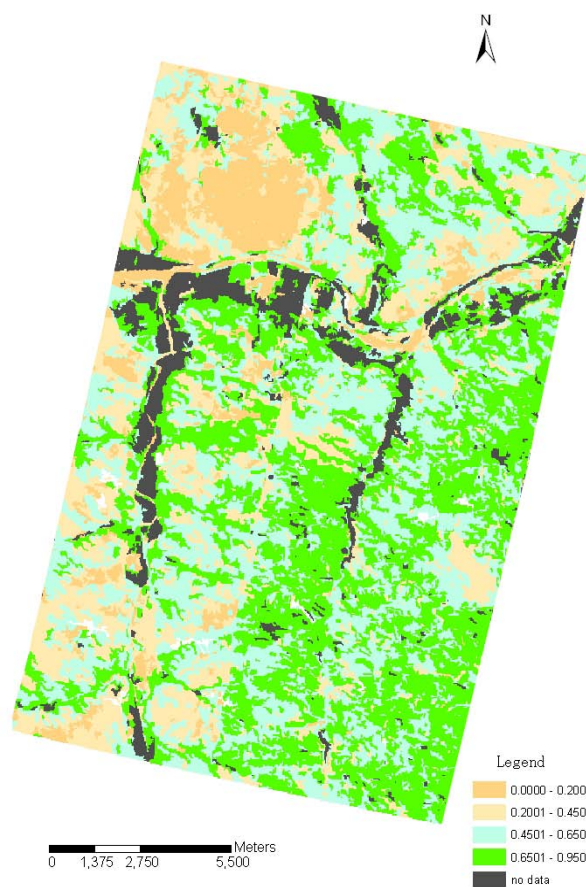
Figure 5.12 SOM mapping based on the DSRU models at scale level of 50 with
Hyperion images
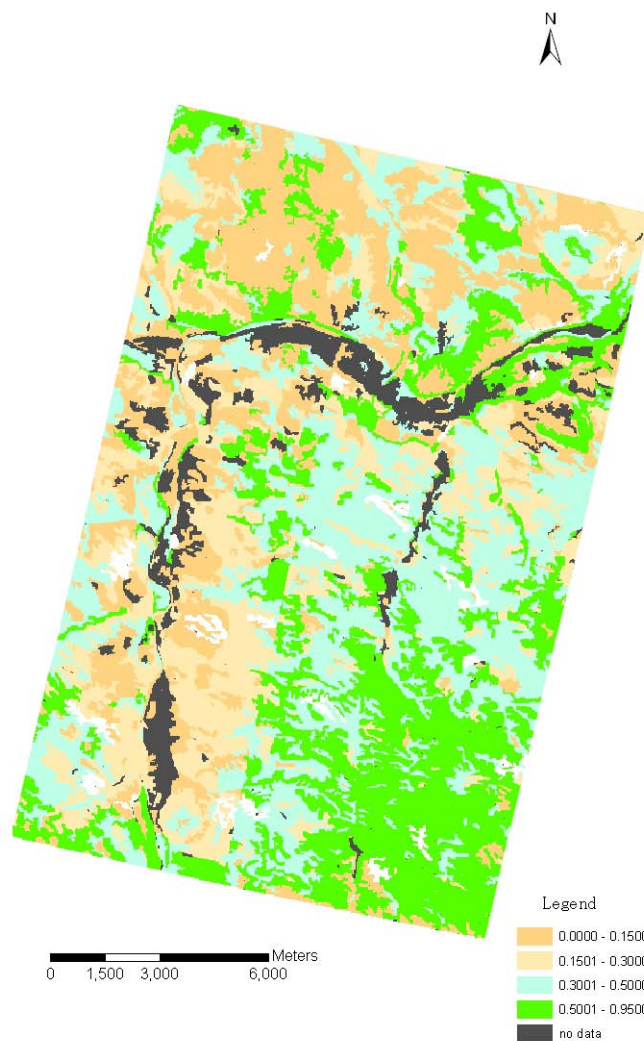
Figure 5.13 SOM mapping based on the DSRU models at scale level of 100 with Hyperion images
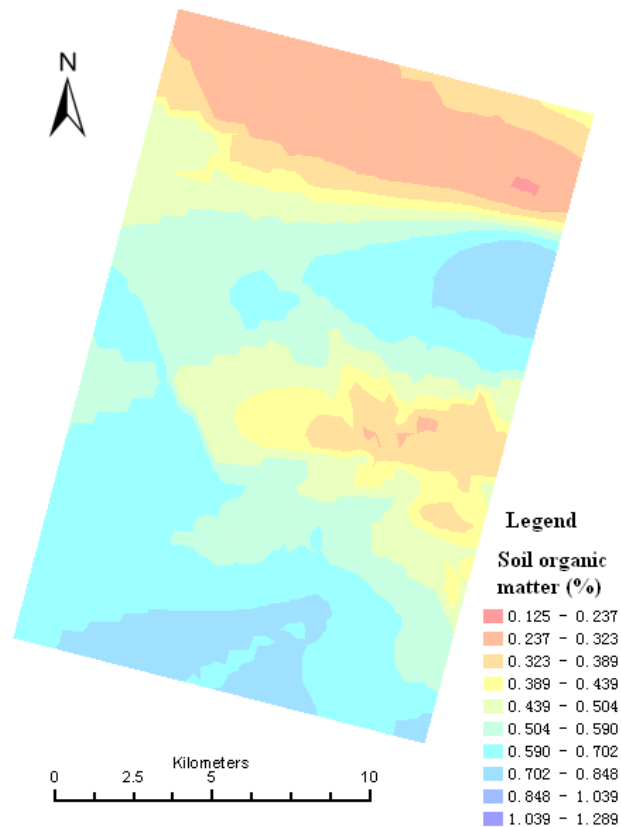
Figure 5.14 SOM content estimated by the Kridge interpolation method

The SOM content seems to have a negative correlation with soil reflectance. The land with a high content of SOM was gray black in the image, while that with a low content of SOM was shiny white. This is because the organic material contains a substance called humic acid which can decrease the reflectance of soil spectral. With a decrease in organic matter, the influence of humic acid to soil spectrum is decreased (Baumgardner *et al*., 1985). The result of the study agreed to Xu (1986) who pointed out that the soil reflectance would increase after the organic material removed.

By application of the GEOIC approach, the DSRU estimation models based on the relationship between the SOM contents and features of spectral and regional variables of DSRU were able to accurately estimate the SOM at a regional scale. The DSRU estimation model is not only based on some variables in *in-situ* model, but also considers some environmental variables to compensate for the change of scale.

The results from our method using the GEOIC approach were consistent with the previous study results by Raffy (1992) and Hay and Marceau (1998).

The method of DSRU estimation model is an application example of the GEOIC approach for soil parameters mapping. It has two main advantages in SOM mapping: (1) the method can overcome the pixel by pixel spectral variation and the SOM variation in a homogenous area, (2) it integrates different types of geo-data into an object-based analysis process and introduces different environmental variables into the estimation models. The presented GEOIC approach for the SOM estimation combines spectral information and texture information with soil types, vegetation, land use information, and *in-situ* information from field surveys. This case study demonstrated the GEOIC approach is valid for monitoring and evaluation of soil quality with hyperspectral images.

However, some problems must be identified and overcome for the application of Hyperion image data to map SOM. Hyperspectral data directly collected in the field or acquired with remote sensing techniques might be affected by the natural soil surface conditions (e.g., roughness, moisture, stoniness, etc), the atmosphere, and the illumination conditions. These effects should be further studied and corrected on the basis of an extended spectral data set collected directly in the field together with ancillary data. In addition, the accuracy of SOM mapping with this approach should be further improved. However, the implementation of DSRU estimation models for SOM mapping seems to be complicated in areas where physical and geographical situations are very complex and fragmentized. A potential solution might be the coupling of the current approach using hyperspectal images of high spatial resolution and DEM at scale of 1:10 000 or 1:50 000 together with ancillary data and larger number of soil samples.

A further improvement of this study can be obtained by a careful analysis of the dependence of accuracy on natural site conditions, integration of other additional data (such as LIDAR data), and a more efficient usage of ancillary information and local knowledge. The GEOIC approach should be applied in other areas to validate the reliability of the approach.

5.4 Summary of the GEOIC application in SOM mapping

Based on the above discussions the flowchart for SOM mapping with the GEOIC approach is given in Figure 5.15.
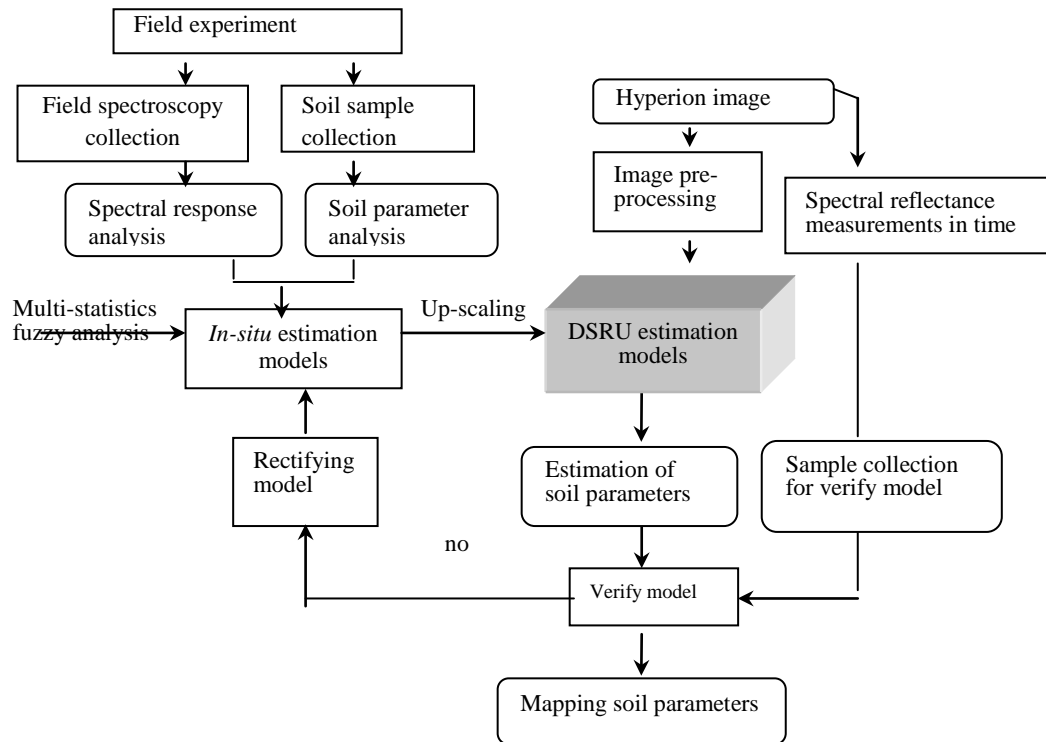
Figure 5. 15 The technical flowchart for mapping soil parameters using hyperspectral data

Analyzing the test data showed that the spectral reflectance of soil samples in bands R_{467}, R_{560}, R_{625}, R_{740}, R_{1336} were significantly correlated to the SOM content. The *in-situ* estimation models based on the relationship between the SOM content and the transformation of the spectral reflectance in bands R_{467}, R_{560}, R_{625}, R_{740}, and R_{1336}, developed using the multiple regression method and the fuzzy set method, were valid to estimate the SOM of soil samples. The five sensitive bands can be used for the SOM estimation using Hyperion images. However, the *in-situ* estimation models were difficult to be applied to images because of less correction applied to compensate the change of scale. Under the approach of GEOIC, the DSRU estimation models were developed based on the relationship between the SOM

content and the spectral and regional variables of DSRUs. The models developed with the stepwise multiple regression method were valid to estimate the SOM content using Hyperion images. The determinative coefficient (R^2) of the model increased from 0.562 at scale level of 25, to 0.721 at scale level of 50, and to 0.722 at scale level of 100. The mean square of regression models at scale level of 100 was lowest. The variables of combination of sensitive bands in R_{467}, R_{560}, R_{625}, R_{740} and R_{1336} were included into the DSRU regression models and had significant effects on dependent variable of SOM at different scale levels. The environmental variables of elevation, slope and vegetation index (MCARI) were also included in the DSRU models. The result of SOM mapping based on the DSRU estimation models using Hyperion images is compatible to the field survey results. It is also close to the result of the Kridge interpolation on SOM using soil samples. Mapping SOM can be done cost-effectively and in a timely manner instead of collecting and measuring large amount of soil samples in large areas.

The method of DSRU estimation model is an application example of the GEOIC approach. It has two main advantages in SOM mapping: overcoming the pixel by pixel spectral variation and the SOM variation in a homogenous area; and integrating different types of geo-data into an object-based analysis process and also introducing different environmental variables into the estimation models. The method provided a useful tool for mapping soil features at a regional scale by combining field data, remote sensing images and regional variables.

Advances in hyperspectral technology have enabled the remote acquisition of the detail information on vegetation and soil over large areas. Although the use of hyperspectral remote sensing images has gained considerable momentum in vegetation mapping, there are some limitations in the application for soil mapping. We explored in this study the applicability of Hyperion data and the GEOIC approach for SOM mapping at a regional scale. We demonstrated how the GEOIC approach applied in SOM mapping compensates for the change of scale of estimation models. The object-based integration of Hyperion imagery with environmental variables holds immense potential for soil parameter mapping in a heterogeneous landscape.

There are some problems in the application of remote sensing images for mapping SOM. The regression models between the spectral reflectance and the SOM content based on experimental data in the test area may have limitations to be applied in other areas because of different variables of estimation models. But the up-scaling method for estimation model to compensate the change of scale can be applicable in most areas. On the other hand, hyperspectral data directly collected in the field or acquired with remote sensing techniques might be affected by the natural soil surface conditions (e.g., roughness, moisture, stoniness, etc), the atmosphere, and the illumination conditions. These effects should be further studied and corrected on the basis of an extended spectral data set collected directly in the field together with ancillary data. Moreover, a comparison of other approaches, such as neural networks or other mathematics/statistics methods with the regression method in integrating multi-source data for developing the estimation models should be conducted to see if they are useful to further improve the accuracy of estimation models.

Chapter 6

Application of the GEOIC Approach in the

Extraction of Land Degradation

Information Using Hyperion Images

Extraction of land degradation information is important for the assessment of land degradation situation. Land degradation can sometimes be estimated or measured directly, but often be indirectly estimated by land characteristics and/or diagnostic criteria (Olderman, 2000), such as land characteristics, soil characteristics, vegetation, land use/land cover, climate, and human activities, or function of them. The evaluation unit is one of the major factors affecting the accuracy of the extraction of land degradation information. It is an ecologically homogeneous tract of land at a scale. It describes the characteristics of the most obvious (mappable) land attributes. Several studies have shown that it is difficult to quantify land degradation due to several issues, such as the ambiguously expressed knowledge, and benchmark, diagnostic indicators, unit, and methodologies to be used, and method for scaling of land degradation evaluation, and influencing factors on land degradation process (FAO 2002; Wang, 2006; Sivakumar and Ndiangui, 2007; Chen and Rao, 2008; Gao and Liu, 2008).

With the development of OBIA methodology, the approach of GEOIC has been developed which was discussed in Chapter 3. The GEOIC approach not only integrates remote sensing information, geographic information, and the knowledge on land resources, but also takes into account the spectral, texture, shape, and spatial relation between pixels based on fuzzy logic methods. For the ambiguously

expressed knowledge on land degradation and complex ecosystems, like the study area described in Chapter 4, the GEOIC approach is more appropriate and can significantly enhance the role of remote sensing technique for the extraction of land degradation information. Little however, has been done in this research area. This chapter is to explore the applicability of Hyperion data and the GEOIC approach for extracting land degradation information through land type classification. The GEOIC approach is realized by the segmentation of DSRUs using Hyperion images, geographic information, vegetation, soil parameters, DEM and local information. The approach is also compared with the Spectral Angle Mapping (SAM) method and the Degraded Soil Line Index (DSLI) method. In this chapter, we demonstrate how the GEOIC approach significantly improves the accuracy of land degradation classification. Furthermore we illustrate how the systematic approach can quantify ambiguously expressed information of land degradation. The above-mentioned three approaches are tested in the study area described in Chapter 4.

6.1 Features of land types and spectral response to land degradation

In this study we should know well the features of land types and spectral response to land degradation for a comprehensive grasp of the geoscience knowledge using the GEOIC approach in the study area. Therefore this section briefly discusses the features of land types and spectral response to land degradation.

The values of various soil parameters for different land types are shown in Table 6.1. The content of SOM ranged from 0.124% to 1.827%, with the average of 0.618%±0.284%. The statistical tests showed that the average contents of SOM, total nitrogen (TN), available nitrogen(AN) and physical clay content are significantly different among irrigated land, dike field, terrace, Loess-hilly top land, Loess-hilly slope land and sandy land. The contents of SOM and TN gradually decreased in the order of irrigated land, dike field, terrace, Loess-hilly top land, Loess-hilly slope land, and sandy land. AN, available potassium (AK) and clay content showed a decreasing trend in similar to that for SOM and TN, while available phosphorus (AP) did not.

These results were generally in agreement with local farmers' perception of land quality.

Table 6.1 Contents of nutrients and clay in the soils of different land types

Types	SOM	TN	AN	AP	AK	Clay
	%	%	%	mg/kg	mg/kg	%
Irrigated land	0.960	0.068	125.17	8.94	133.04	11.30
Dike field	0.711	0.053	105.13	4.89	135.48	10.81
Terrace	0.648	0.048	108.84	5.12	114.19	10.78
Loess-hilly top land	0.542	0.044	98.57	4.47	127.48	8.74
Loess-hilly slope land	0.437	0.036	90.03	3.66	87.30	9.38
Sandy land	0.202	0.017	71.57	5.09	79.36	2.89
F value	18.28**	15.92**	3.39**	8.78**	4.89**	7.99**

** Distinct difference in level of significance less than 0.01

The mean values of various soil parameters for different degraded land types are shown in Table 6.2. The statistical tests indicated that the average contents of SOM, TN, and AK are significantly different among the highly, moderately, and slightly degraded grassland and non-degraded grassland. The average contents of SOM, TN, and AP, total iron, and soil moisture are significantly different between non-degraded arable land and degraded arable land. The average contents of SOM and TN are significantly different between highly-degraded forestry land and slightly degraded forestry land. The average contents of AP and AK in non-degraded forestry land are higher than those in degraded forestry land.

Table 6.2 Comparison of the means of soil characteristics at different types of land degradation in the study area

Land use type	Degradation degree	Fe mg/kg	SOM %	TN %	Soil moisture %	CEC cmol/kg	AK mg/kg	AP mg/kg
Grassland	Slight wind erosion	18850	0.75	0.05	11.93	7.50	95.59	6.30
	High wind erosion	16071	0.12	0.02	8.83	8.31	37.48	2.34
	Slight water erosion	23902	0.76	0.04	10.06	9.60	106.83	3.70
	Moderate water erosion	22291	0.57	0.04	10.90	11.56	78.02	2.51
	High water erosion	22075	0.43	0.04	11.87	13.25	75.90	13.58
	No degradation	24923	0.80	0.04	8.80	17.00	111.92	2.44
	Difference level	No Dif.	<0.001	<0.05	No Dif.	<0.05	<0.05	No Dif.
Arable land	Slight wind erosion	19398	0.35	0.02	8.38	10.55	47.67	2.81
	High wind erosion	18232	0.37	0.02	6.92	8.70	63.19	7.41
	Slight water erosion	23474	0.62	0.07	7.96	11.84	72.47	4.31
	Moderate water erosion	24116	0.61	0.04	8.28	10.51	86.66	4.03
	High water erosion	21612	0.45	0.04	8.07	8.98	79.69	6.84
	No degradation	23453	0.90	0.05	19.64	12.05	92.91	4.71
	Difference level	<0.001	<0.001	<0.001	<0.05	No Dif.	<0.05	No Dif.
Forestry land	Slight wind erosion	11815	0.18	0.01	6.50	6.69	31.55	2.24
	High wind erosion	11409	0.14	0.01	7.75	6.08	48.98	2.86
	Slight water erosion	20659	0.73	0.05	8.25	10.54	79.00	4.21
	Moderate water erosion	22079	0.72	0.03	8.86	10.74	82.26	6.16
	High water erosion	20683	0.37	0.03	7.97	10.87	63.70	4.13
	No degradation	21500	0.65	0.04	10.97	10.23	107.59	6.08
	Difference level	No Dif.	<0.05	<0.001	No Dif.	No Dif.	<0.05	<0.05

The soil spectral reflectance synthetically indicates the physical-chemical characteristics of surface substance. In the study area, the reflectance spectra of 84 soil samples were measured in the lab. The results indicated that the reflectance spectra for non-degraded land, slightly degraded land, moderately degraded land and highly degraded land were different. The reflectance of soil was higher for the moderate and high wind erosion lands than for the non-degraded land and slight wind erosion land (see Figure 6.1).The field survey results indicated 90% of the area of the high wind erosion land was bare, with only one to three individual plants of watermelon, bean, potato and broomcorn per squared meter. On the other hand, scattered desert artemisia distributed on the high wind erosion grassland with only less than 10% vegetation cover. The soil spectra showed that the reflectance decreased from the high wind erosion soil, to the moderate wind erosion soil, and to the slight wind erosion soil and non-degraded soil, while the reflectance of the slight wind erosion soil and non-degraded soil was similar (Figure 6.1). These results

demonstrated that the reflectance of soil is positively correlated to the degree of degradation.

The reflectance of soil was higher for the high water erosion land than for the non-degraded land and slight and moderate water erosion lands (Figure 6.2). The 80% of the area of high water erosion arable land was bare, with three to four individual plants of potato per squared meter, while scattered clover distributed on the high water erosion grassland with less than 10% of vegetation cover. The soil spectra also showed that the reflectance of soil was higher for the high water erosion land than for the moderate and slight water erosion lands and non-degraded land. However, the reflectance for the moderate water erosion land, slight water erosion land, and non-degraded land was similar (Figure 6.2).
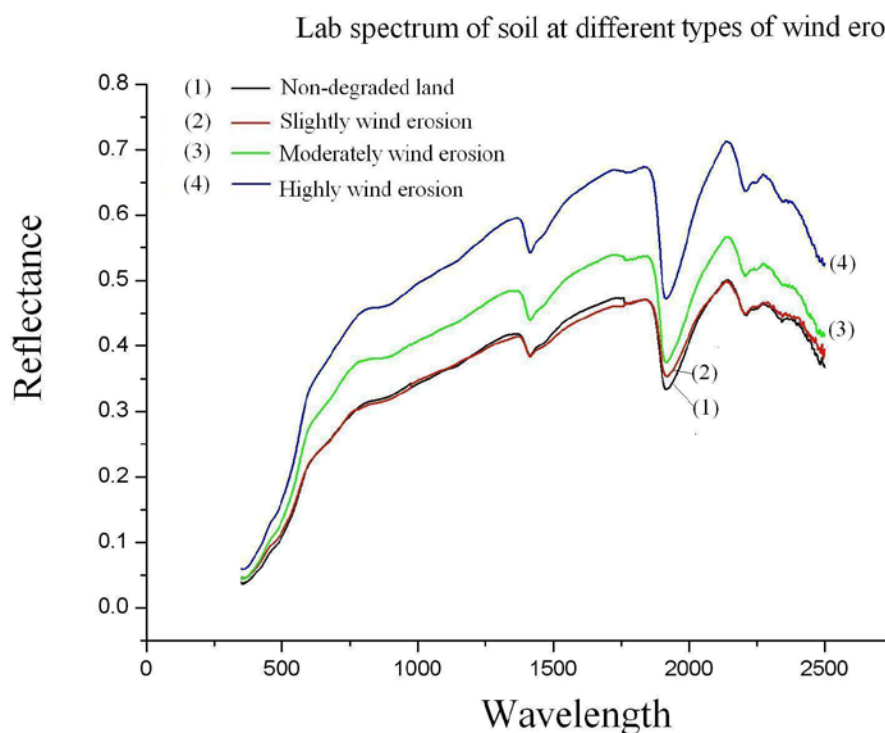
Figure 6.1 Lab spectrum of soil at different degree of wind erosion in Hengshan County
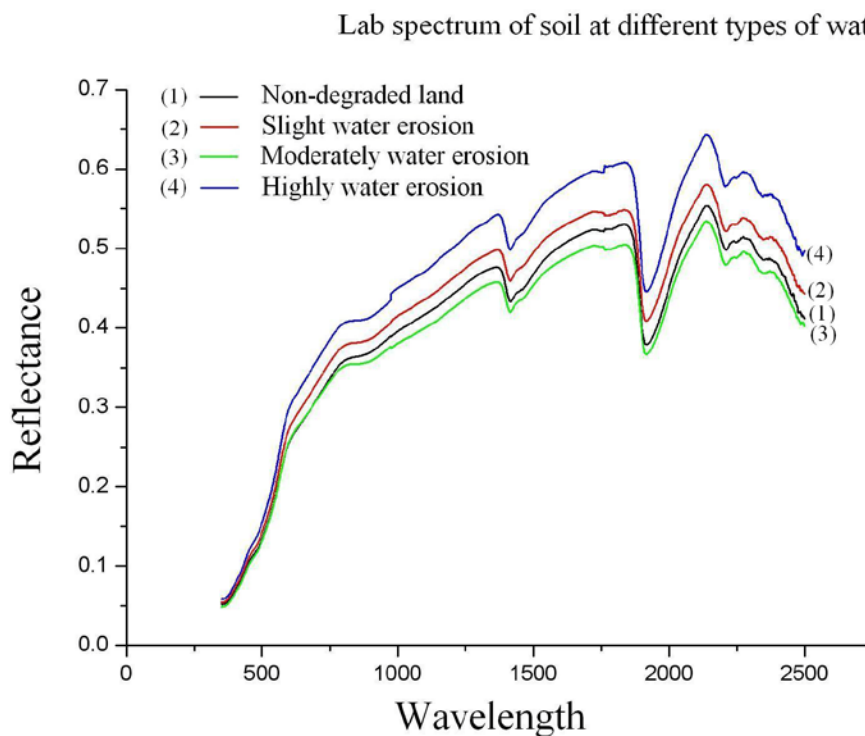
Figure 6.2 Lab spectrum of soil at different degree of water erosion in Hengshan County

6.2 Methodologies

6.2.1 Land degradation classes and land types

Land degradation classes must be first defined for an area of interest. In the study area the land degradation was divided into 4 classes: highly degraded land, moderately degraded land, slightly degraded land and non-degraded land (see Figure 6.3).

Non-degraded land: no topsoil is lost. The land by a river, irrigated land, dike field land, and wood land and farmland with high vegetation cover in fertile soil belong to this class.

Slightly degraded land: small amount of the surface soil is lost due to over-farming and water flow. Orchard land and agricultural land in terrace are in this class.

109

Moderately degraded land: large portion of topsoil is lost due to rills and extensive agricultural activities and moderate water erosion. In this class are Loess-hilly top land, part of arable land and barren grassland with a small quantity of vegetation in slope areas with low fertile soil.

Highly degraded land: most of the topsoil and part of subsoil or substratum are lost due to severely water erosion and wind erosion. This class includes wind-erosion soil (desertification) land and land in steep hillsides with sparse vegetation and lower fertile.

None   Slight   Moderate   High

Figure 6.3 Different types of land degradation

A survey of land quality and land degradation with farmers' perceptions was carried out in 107 household's fields in 2003. The 'Participatory Rural Appraisal (PRA) Technology' played a very important role in the study. PRA is a participatory method for the analysis of the problems and potentialities of a given issue and to identify potential solutions with the direct stakeholders involved. The PRA can thus be used to analyze the major agricultural and environmental systems we identified in more detail. The PRA is an intensive, systematic, semi-structured learning process carried out in a community with the help of a multi-disciplinary team. In this study, semi-structural discussion and questionnaire survey were used to get detailed information about land quality and land degradation. Local farmers classified the land into eight types: irrigated land, dike field, terrace, Loess-hilly top land, Loess-hilly slope land, sandy land, residential land and water body (see Table 6.3). The results of the survey indicated that the farmers were competent in the assessment of land quality and land degradation with some diagnostic indicators, such as topographic characteristics, soil characteristics, agricultural managements, yield, and amount of fertilizer, crop performance, sandy erosion degree, and water erosion

degree. Each type of land except residential land and water body was attributed to one of the six land quality levels and one of the four land degradation classes, as given in Table 6.3.

Table 6.3 Land types, quality levels, and degradation classes in Hengshan County by the farmers' survey

Degradation type	Land quality level by PRA	Land Types	Description
Non -degraded	First level	Irrigated land	Higher productivity with high fertile soil, in the flatness and wide area and in lower elevation area, in convenient irrigation and traffic area, higher covered vegetation
	Second level	Dike field	High productivity, in the flatness and narrow area with high fertile soil, in convenient irrigation and non- convenient traffic area, in low to high elevation area, highly covered vegetation
Slightly Degraded	Third level	Terrace	Moderate productivity, short cultivation time, less nutrient and lower maturity, in high elevation area, in un-convenient irrigation and traffic area, moderately covered vegetation
Moderately Degraded	Forth level	Loess-hilly top land	Low productivity, moderate water erosion, in slope area with low fertile soil, in relative flatness area, in higher elevation area, in un-convenient irrigation and traffic area, moderately covered vegetation
Highly degraded	Fifth level	Loess-hilly slope land	Lower productivity, severely water erosion, in steep slope area with lower fertile soil, in high elevation area, in un-convenient irrigation and traffic area, lower covered vegetation
	Sixth level	Sandy land	Severely wind erosion, lower productivity, not as major agricultural land, in the flatness area with lower fertile soil, in low elevation area, in convenient irrigation and traffic area, lower covered vegetation
	/	Residential land	Much of the land occupied by man-made structures
	/	Water body	Lakes, reservoirs and rivers

6.2.2 GEOIC approach for studying land degradation

According to the results of the farmers' survey, there are four classes of land degradation corresponding to different land types. In the study, we used the GEOIC approach for extracting land degradation information by land type classification based on the segmentation of DSRUs. The land types were classified using eCognition Professional 7.0 by combining the images at different scale levels, including layers of nine fusion transformations of Hyperion images, vegetation index (MCARI), slope, elevation, SOM and land use map and their different combinations. The classification process involved the following four steps (see Figure 6.4), as discussed below.

6.2.2.1 Segmentation of DSRUs

In this study, we use DSRU as a land unit for land degradation evaluation using remote sensing technique. The conception of DSRU and the method of segmentation of DSRUs were described in Chapter 5. DSRU is an ecologically and geographically and spectrally homogeneous area with similar characteristics of physiognomy, vegetation, soil and image spectral information. The segmentation of DSRUs is not only based on spatial characteristics of topography, soil and vegetation, but also the features of land degradation represented in remote sensing image information. In the process of the segmentation of DSRUs, variables or diagnostic indicators related to land degradation were as input layers. The climate variable was not considered due to a small variation in the study area. Thus, layers of physiognomy, vegetation, and soil, and image information were chosen for the segmentation of DSRUs. Vegetation index (MCARI) derived from Hyperion images were used as the indicator of yield and crop performance. SOM interpreted by Hyperion images was used as the indicator of soil characteristics and soil fertilizer. The distribution of SOM was estimated by the DSRU estimation models using Hyperion images (as discussed in Chapter 5). The slope and elevation derived from a DEM（30×30 m）were used to indicate topographic characteristics. Nine fusion transformations from first principal component (PCA1) to the ninth principal component (PCA9) calculated from Hyperion hyperspectral spectral bands were used as spectral indicators. The land use map (at scale of 1:100 000) (interpreted from TM images and SPOT 2 4 images in 2001) was used as thematic layer in the segmentation process (Table 6.4).
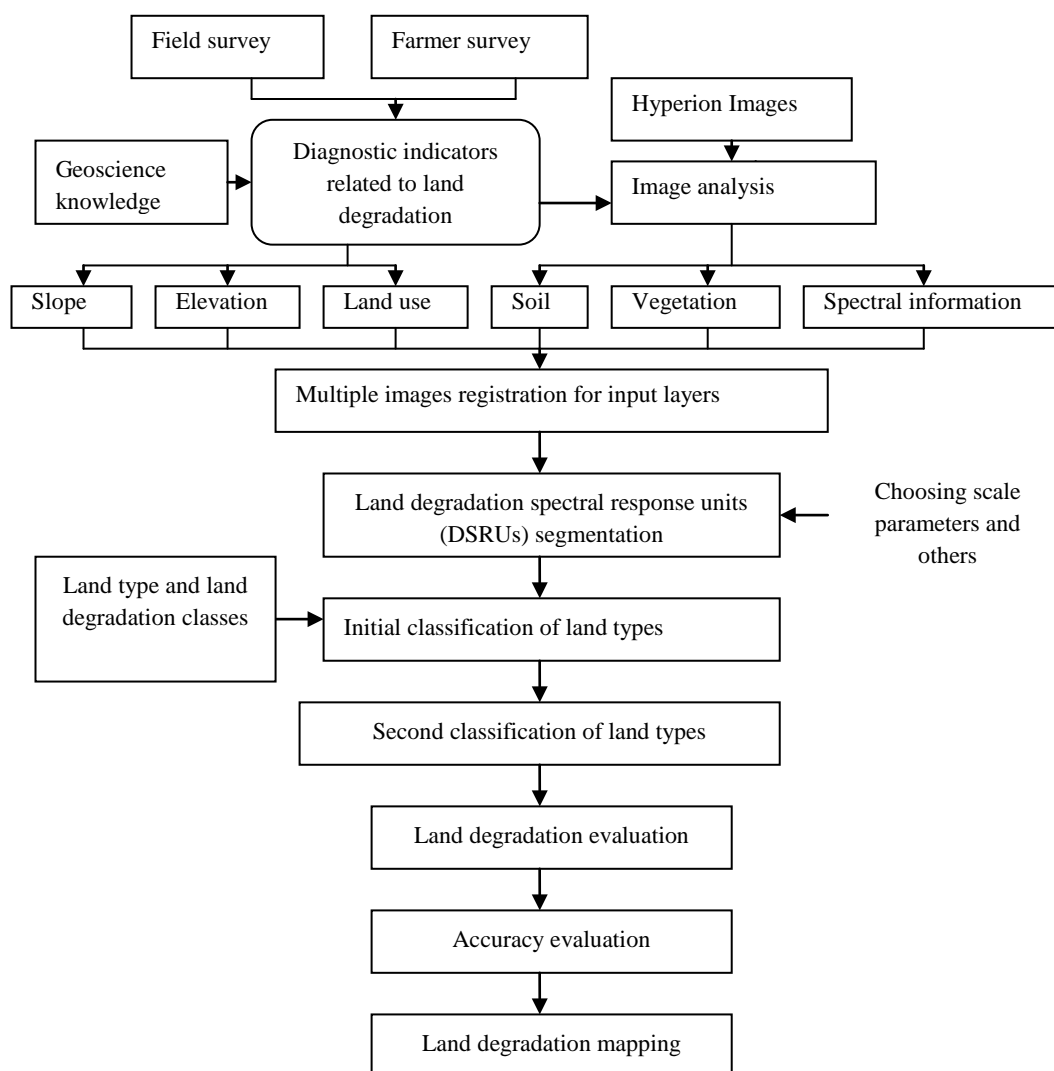
Figure 6.4 Flowchart of the extraction of land degradation information using the GEOIC approach

The different combinations of these diagnostic indicators as input layers were chosen for the segmentation of DSRUs (see Table 6.4). The different combinations of input layers (spectral indicators from PCA1 to PCA9, topographic indicators including elevation and slope, vegetation indicator of MCARI, and soil indicator of SOM, and land use map as the thematic layer) determined by their weights were used for determining the appropriate diagnostic indicators for the extraction of land degradation information.

Table 6.4 Layers used in the segmentation process and their weights in eight types of combinations

Layers	Hyperion+ Elevation+ Slope+ MCARI+ SOM	Hyperion+ Elevation+ Slope+ MCARI	Hyperion+ Elevation+ Slope+ SOM	Hyperion+ Elevation+ SOM	Hyperion+ Elevation+ Slope	Hyperion+ Elevation+ MCARI	Hyperion+ Elevation	Hyperion
PCA1	1.0	1.0	1.0	1.0	1.0	1.0	1.0	1.0
PCA2	1.0	1.0	1.0	1.0	1.0	1.0	1.0	1.0
PCA3	1.0	1.0	1.0	1.0	1.0	1.0	1.0	1.0
PCA4	0.5	0.5	0.5	0.5	0.5	0.5	0.5	0.5
PCA5	0.5	0.5	0.5	0.5	0.5	0.5	0.5	0.5
PCA6	0.5	0.5	0.5	0.5	0.5	0.5	0.5	0.5
PCA7	0.3	0.3	0.3	0.3	0.3	0.3	0.3	0.3
PCA8	0.3	0.3	0.3	0.3	0.3	0.3	0.3	0.3
PCA9	0.3	0.3	0.3	0.3	0.3	0.3	0.3	0.3
Elevation	1.0	1.0	1.0	1.0	1.0	1.0	1.0	0.0
Slope	1.0	1.0	1.0	0.0	1.0	0.0	0.0	0.0
MCARI	1.0	1.0	0.0	0.0	0.0	1.0	0.0	0.0
SOM	1.0	0.0	1.0	1.0	0.0	0.0	0.0	0.0
Land use map	1.0	1.0	1.0	1.0	1.0	1.0	1.0	1.0

*Note that the weighting scheme of spectral indicators from PCA1 to PCA9 has been discussed in Chapter 6

Different scale parameters were chosen to determine an appropriate scale parameter and to study the effect of the size of image objects (DSRUs) on the precision of extracting land degradation information in the study area. Scale parameter 1 which means the relatively smallest size of image objects was chosen to represent a scale level similar to pixel level. Four scale levels with scale parameters of 25, 50, 100 and 200, representing the sizes of DSRUs from small to large, were chosen in the study. The image was segmented starting from similar pixel level (scale parameter 1), to low level (scale parameter 25), a medium level (scale parameter 50 and scale parameter 100) and to high level (scale parameter 200).

In this study, based on the visual interpretation of different image segmentation results and the experience, the homogeneity criterion was set as color 0.8 and shape 0.2; and for the shape criterion, smoothness 0.5 and compactness 0.5. The image objects of DSRUs were generated based upon the above adjustable criteria and parameters throughout the segmentation process.

6.2.2.2 Initial classification of land types

The DSRUs from the segmentation at scale level 25 based on one of the indicator combinations were classified into seven classes: cloud (red), cloud shadow (blue

black), irrigated land and dike field (green), dike field and Loess-hilly slope land (sky blue), Loess-hilly top land and sandy land (rose pink), residential land (navy blue), and water (black). The initial classification of land type was conducted by the Neighbour Classifier using the mean and standard deviation of layer values of each DSRU in eCognition (Figure 6.5). The selection of training samples of different land types was based on color composite images of RGB by PCA1, PCA2 and PCA3 of the Hyperion images in eCognition Professional 7.0. Because the Neighbour Classifier with complex distribution in feature space is not based on a continuous Gaussian distribution function, a practical way is to choose a few samples first and then gradually add necessary samples to meet classification needs in the process of choosing training samples.

6.2.2.3 The second classification of land types

Three of the above seven classes in the initial process of classification, i.e. irrigated land and dike field, dike field and Loess-hilly slope land, and Loess-hilly top land and sandy land, were further classified into six types. Each type is defined by a fuzzy set consisting of membership functions of DSRU features. With the results of field survey and visual interpretation, the combined class of the dike field and Loess-hilly slope land was further divided into the dike field and the Loess-hilly slope land. The former has the elevation from 1040 to 1160 m, or MCARI > 0.05 and slope <8°. The combined class of the Loess-hilly top land and sandy land was further divided into the Loess-hilly top and the sandy land with MCARI>-0.3 and <-0.3, respectively. The combined class of the irrigated land and dike field was further divided into the irrigated land and the dike land with MCARI>0.3 and <0.3, respectively. The above thresholds for elevation, slope degree, MCARI were determined by the field survey and visual interpretation based on the knowledge of land type and land degradation. In addition to the features based on spectral and shape information, other features based on contextual information, such as the relation to neighbour objects, were also used in the classification.
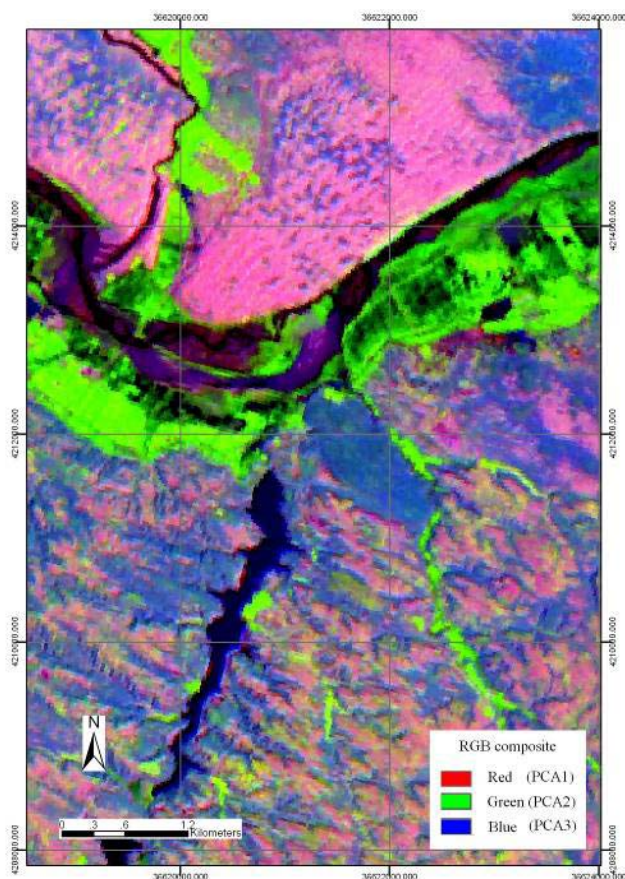
Figure 6.5 False color composite image by RGB as PCA1, PCA2 and PCA3

6.2.2.4 Land degradation evaluation

With the results of the farmers' survey, irrigated land and dike field regarded as high quality land was classified as non-degraded land; terrace as slightly degraded land; Loess-hilly top land as moderately degraded land; and Loess-hilly slope land and sandy land as highly degraded land. Besides, the Loess-hilly slope land and Loess-hilly top land were further classified into the first, second and third sub-classes according to land degradation degree. Each sub-class is defined by a fuzzy set which consists of membership functions of DSRU features using MACRI and SOM. The first class of the Loess-hilly top land has MCARI in the interval of 0.09 to 0.3 or SOM value larger than 0.5, while the third class has MCARI in between -1.0 and -0.2 or SOM value smaller than 0.3. The rest is for the second class. The Loess-hilly slope land was further divided into the first, second, and third class, with SOM value in between 0.5 and 0.95; 0.3 and 0.5; and 0 and 0.3, respectively. The thresholds for

MCARI and SOM were also determined with the field survey and visual interpretation using the knowledge of land degradation.

The images with DSRU resulted from the segmentation at similar pixel level and at scale levels of 50, 100, 200 based on different types of combinations were classified in turn by the above procedures with the same membership function.

6.2.3 Spectral Angle Mapping (SAM)

In this study we compared the developed GEOIC approach with an existing method of the Spectral Angle Mapping (SAM) and the developed method of the Degraded Soil Line Index (DSLI). Therefore the following two sections briefly discuss these two methods.

The SAM method developed by Kruse *et al*. (1993) is a classification approach which determines the similarity between the reference spectrum and the image spectrum that have a common origin by the calculation of the angle θ, treating them as vectors in a space with dimensionality equal to the n number of bands (Kruse *et al*., 1993). The spectral angle is calculated from the following equation:

$$\theta = \arccos(\frac{\vec{t} \bullet \vec{r}}{\|\vec{t}\| \bullet \|\vec{r}\|}) \tag{6-1}$$

where $\vec{r}$ is the reference spectral vector and $\vec{t}$ is the test spectral vector. The attribution of each scene pixel to a given class by the SAM approach is based on the measurement of the angle between the reference spectrum vector and each image vector in the n-dimension space. As we know, the smaller the angle, the higher the similarity will be. The implementation of the SAM approach gives an image with an angle θ for each reference spectrum. Using the θ angle and a pre-set threshold, we can attribute the theme that has smaller θ value than the threshold to each pixel.

6.2.4 Degraded Soil Line Index (DSLI)

The conventional soil line is a synthetic representation of the reflectance spectra of a large number of soils, taken at two spectral bands:

$$\rho_{NIR} = a + b\rho_R \qquad\qquad (6\text{-}2)$$

where ρ_{NIR} is the reflectance determined at a band in the NIR interval of high vegetation reflectance due to the leaf mesophyl structure (>0.76μm), ρ_R is the reflectance measured within the chlorophyll absorption band (0.65-0.68μm), b is the slope of the soil line, and a is the intercept of the line. The above equation is called the "soil line" (Baret $et\ al.$, 1993).

The soil line, a linear relationship between bare soil reflectance observed in two different wavebands, is widely used for the interpretation of remote sensing data. The soil line is a trend line according to the relative spectral reflectance value in the coordinate of red-band and near infred band. The longer the two band interval, the lower the relativity of the reflectance values will be, and the soil line intercept will increase. Because soil reflection spectrums reflect soil color, humidity, roughness, SOM, Fe shadow, etc, the soil line parameters are relevant to the soil chemical and physical characteristics.

The DSLI method is proposed based on the SAM approach and the soil line concept in this study. A slightly degraded bare soil line and a highly degraded bare soil line must firstly be chosen to carry out this method. The definition of these lines requires a collection of points from the pixels of the image itself or derived from ground spectral measurements.

In a bi-dimensional space, any point P representing bare soil is located between the highly degraded bare soil line and that of the slightly degraded soil line (Figure 6.6). The ratio of the tangent of angle α to the tangent of angle β, called the degraded soil line index (DSLI), is carried out for classification after processing of the spectroradiometric data. The method does not limit itself to the choice of specific

bands. Point I is the interception of the two lines. The DSLI can be estimated in a bi-dimensional space by the following equation:

$$DSLI = \frac{\tan \alpha}{\tan \beta} \qquad\qquad (6\text{-}3)$$

The DSLI can be adapted to a n-dimension space, knowing that n is the number of bands. In this case, the highly degraded soil line and the slightly degraded soil line can be defined by using many spectral bands and selecting a single band as reference.

In this test study, the DSLI method was also used for extracting land degradation information directly. The results of the pixel by pixel DSLI and SAM classification methods were used for a comparison with the results of GEOIC approach.
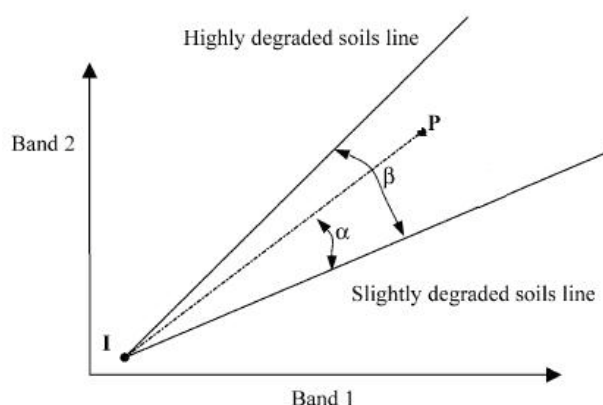
Figure 6.6 Concept of the DSLI approach in a bidimensional space

6.2.5 Ground truthing

The stratified random samples were selected from the field survey data and SPOT5 satellite image and the classified images at different scale levels. The land type of each sample was interpreted from the SPOT5 satellite image and DEM using the visual interpretation method. We randomly selected 40 places in the study area to compare the classification outputs with the interpretation results and the ground-based measurements. Confusion matrices were developed to determine the classification accuracy of land type classification for each classification method.

6.3 The test results and discussions

6.3.1 Determination of diagnostic indicators for GEOIC approach

As mentioned above, the GEOIC approach was used in this study through the segmentation of DSRUs with different combinations of input layers. The DSRUs were classified as different land degradation classes and land types with and without ancillary information. The results were subsequently compared. Different classes of land degradation, i.e. non-degraded land including irrigated land and dike field, slightly degraded land including terrace land, moderately degraded land including Loess-hilly top land, and highly degraded land including Loess-hilly slope land and sandy land were classified. The accuracy of land degradation classification using the GEOIC approach by different combinations of input layers was tested with 40 samples interpreted from the SPOT5 satellite image and DEM using the visual interpretation method. The determination of diagnostic indicators related to land degradation was based on the overall classification accuracy and Kappa coefficients.

The accuracy evaluation results of land degradation classification at four scale levels by different combinations of input layers are showed in Table 6.5. The results showed the overall accuracy of classification was 76.8% at scale level of 50 without additional data, i.e. only with Hyperion images as input layers; but 76.1% with Hyperion images and elevation as the input layers. The overall accuracy was increased with the combination of three indicators, i.e. Hyperion+Elevation+SOM, Hyperion+Elevation+Slope, and Hyperion+Elevation+MCARI. The classification accuracy with Hyperion+Elevation+Slope was higher, with the overall accuracy of 82.9% and Kappa coefficient of 0.80 at the scale level of 200. This implied that the influence of slope layer is more than the layers of vegetation and SOM in the study area. With a combination of four indicators, i.e. Hyperion+Elevation+Slope+MCARI and Hyperion+Elevation+Slope+SOM, the overall accuracy was higher compared with that using the combination of three indicators. At scale level of 50 we achieved the overall accuracy of 83.5% and Kappa coefficient of 0.79. It implied that the vegetation layer is more influential than layer of SOM in the study area. This is due to the importance of vegetation on soil erosion control. With the combination of

Hyperion+Elevation+Slope+MCARI+SOM, the classification accuracy reached the highest, with the overall accuracy of 88.32% and Kappa coefficient of 0.86 at the scale level of 100. The results indicated that the classification accuracy is higher with ancillary information than with Hyperion images only. The overall accuracy was increased by 11.5% when additional data were used. The overall accuracy of classification will increase when a new diagnostic indicator related to land degradation is used. Moreover, one observes that natural site conditions and vegetation condition, especially physiognomy, are more relevant than soil condition for land degradation classification in the study area.

Table 6.5 Accuracy evaluation of land degradation classification at four scale levels by different combinations of input layers

Layers	Scale level of 25		Scale level of 50		Scale level of 100		Scale level of 200	
	Overall accuracy (%)	Kappa Coe.	Overall accuracy (%)	Kappa Coe.	Overall accuracy (%)	Kappa Coe.	Overall accuracy (%)	Kappa Coe.
Hyperion+Elevation+ Slope+MCARI+SOM	82.34	0.7889	83.31	0.8015	88.32	0.861	72.35	0.7235
Hyperion+Elevation+ Slope+MCARI	82.58	0.7830	83.45	0.7920	76.50	0.7090	77.19	0.7150
Hyperion+Elevation+ Slope+SOM	78.26	0.7314	79.26	0.7402	71.26	0.6512	75.70	0.6980
Hyperion+Elevation+ SOM	69.75	0.6498	74.88	0.7052	69.66	0.6438	76.58	0.7260
Hyperion+Elevation+ Slope	69.17	0.6434	74.58	0.7015	69.68	0.6536	82.94	0.7980
Hyperion+Elevation+ MCARI	69.80	0.6500	76.00	0.7180	69.80	0.6450	77.50	0.7350
Hyperion+Elevation	69.55	0.6478	76.07	0.7197	68.86	0.6347	68.98	0.6348
Hyperion	72.65	0.6819	76.82	0.7305	69.40	0.6438	70.78	0.6618

As mentioned above, the results of the farmers' survey indicated that farmers were competent in the assessment of land quality and land degradation with some diagnostic indicators, such as topographic characteristics, soil characteristics, agricultural managements, yield, and the amount of fertilizer, crop performance, sandy erosion degree and water erosion degree (Table 6.6). The farmers' survey result further validated the above accuracy evaluation results of land degradation classification.

Table 6.6 Farmers' indicators for land quality assessment and corresponding criteria

Indicator suite	Indicator	Percentage	Description
Soil attributes	Soil texture	79	Loam soil better than sandy soil
	Soil nutrient	54	The more the better
	Soil depth	17	The deeper the better
	Soil tilth	11	Easy to be ploughed
	Water retention	11	Keeping water for a longer time
	Soil color	3	The darker the better
Topography	Slope gradient	89	Flat lands better than slope lands
	Slope aspect	17	Shady slope better than sunny slope
Agricultural Management	Water availability	81	With irrigation infrastructures or near the river
	Fertilizer input	21	The more the better
	Traffic condition	14	Easy to be connected to road net
	Distance to home	11	The nearer the better
	Farming history	3	The longer the better
Crop performances	Crop yields	40	High quality land with high yields
	Growth status	21	Crop grow more rapidly in high quality land
Environment factors	Wind erosion	20	Low quality land is bad with high wind erosion
	Water erosion	20	Low quality land with gully
Biology indicators	Weed status	11	Low quality land with plenty of weeds
	Indicator species	3	Low quality land with sonchus oleraceus

*Percentage means the percentage of the farmers who used the specified indicator to assess land quality and land degradation.

Therefore, crop performance reflected by vegetation index and topographic factors, such as slope and elevation, were chosen as the diagnostic indicators for extracting land degradation information in the study area. Topographic characteristics and vegetation are two important indicators for monitoring and assessing land degradation. In fact, SOM and texture in topsoil also influenced the process of soil erosion. SOM has significant effects on agriculture management, soil texture and soil nutrients. In the study area, there was no distinct difference in soil texture between sandy loamy soil and loamy sandy soil, but difference between sandy soil and above two types of soil. Thus SOM was chosen as the diagnostic indicator. In addition the remote sensing image which is the comprehensive response of land use and land cover, soil, vegetation and the effects of human activities on land degradation, was also used as the diagnostic indicator in the study area.

6.3.2 Land degradation mapping using the GEOIC approach

In the application of the GEOIC approach, the layers of nine fusion transformations of the Hyperion images, MCARI, slope, elevation, SOM and land use map were used for DSRU segmentation. The land in the study area was classified into irrigated land,

dike field, Loess-hilly slope land, Loess-hilly top land, and sandy land. In addition, the Loess-hilly slope land and top land were further classified into three sub-classes. According to different degrees of degradation, the land is categorized into non-degraded, slightly degraded, moderately degraded, highly degraded.

The classification results at similar pixel level and four scale levels of 25, 50, 100 and 200 give the information on all the objects of a certain subset, e.g. the number of total objects assigned as irrigated land is equal to 240, and the total area of the objects was 21694500 m^2, and the mean area of irrigated land object was 81663 m^2 at scale level of 100. The percentage of each land degradation class out of the total study area was calculated (Figure 6.7 and Table 6.7). For classification at scale level of 100, the total areas of non-degraded and moderately degraded agricultural land were 18.3% and 37.2% of total study area, respectively; while the area of highly degraded agricultural lands was 29.3% (see Table 6.7). The image at scale level of 25 had the majority of image objects in small size with the average size of 7815 m^2 in the scene. The average size of image objects increased from the similar pixel level to scale parameter 200. The classification using the information of the small DSRUs at scale level of 25 resulted in an overestimation of Loess-hilly slope land and Loess-hilly top land in the Loess area. It may be due to the similar spectral properties of vegetation and fragmentized patch. Incorporating the linkage between neighboring objects and relative large DSRUs allows differentiating these types by calculating the standard deviation, shape features, texture measures and classes related features. This resulted in the improved classification results of these types.

In the false color composite image by RGB as PCA1, PCA2 and PCA3, the large amount of sky blue pixels and rose pink pixels indicated that many edges are defined on the right bottom of the image, whereas several large green and sky blue objects did appear on the upper and middle of the image. These low-variance objects were predominantly irrigated land and sandy land.
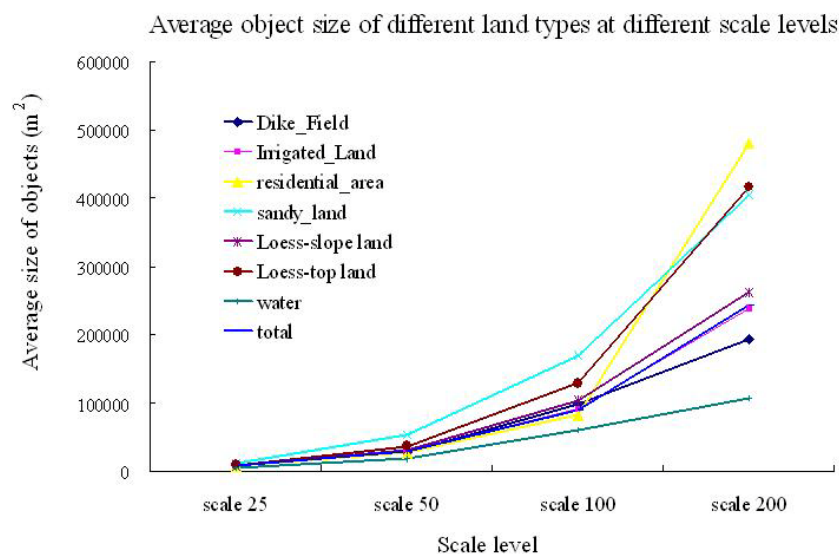
Figure 6.7 Average object size of different land types at four scale levels

Table 6.7 Percentage of the area with different degradation classes in the total area

and objects numbers at four scale levels*

Land degradation	Land type		SL25		SL50		SL100		SL200	
type			NO	Per.	NO	Per.	NO	Per.	NO	Per.
				%		%		%		%
Non-degraded	Irrigated Land		2636	7.11	719	7.38	240	7.71	95	8.02
	Dike Field		2878	7.52	903	8.74	305	10.58	108	7.41
	Sub-total		5514	14.63	1622	16.12	545	18.29	203	15.43
Moderately degraded	Loess-hilly	Top_1	2699	9.32	661	10.19	138	8.50	57	9.47
	top land	Top_2	9085	27.21	2269	25.73	590	26.86	212	32.48
		Top_3	1286	3.82	266	3.19	62	1.85	18	2.23
		Sub-total	13070	40.35	3196	39.11	790	37.21	287	44.18
Highly degraded	Loess-hilly	Slope_1	4865	13.01	1156	11.72	309	8.99	119	7.90
	slope land	Slope_2	4023	11.34	1101	11.72	308	11.79	122	12.92
		Slope_3	1611	4.43	369	4.52	129	5.57	46	4.86
		Sub-total	10499	28.78	2626	27.96	746	26.35	287	25.68
	Sandy land		974	4.12	191	3.58	49	2.94	19	2.73
	Sub-total		11473	32.90	2817	31.54	795	29.29	306	28.41

* SL: Scale level; NO: number of objectives; Per.: percent

The slightly degraded land of terrace land cannot be classified due to the low resolution of Hyperion data at 30×30 m /pixel and DEM data, and the complex physical geographic situation of fragmentized patch in Loess Plateau area. The results also showed that unclassified area and the cloud were 1.4% and 9.1% of total study area at scale level of 100, respectively, while the residential land area and water body area were 0.6% and 4.2% of the study area, respectively.

The classified images of the study area at five scale levels are illustrated in Figure 6.8 to Figure 6.12. They showed that larger structures were formed at the expense of smaller structures. In addition, these classification results revealed an important shift in class membership, particularly the inferior left and right of the images where the Loess-hilly top land and Loess-hilly slope land were shifted to the dike field and irrigated land, and the patches of Loess-hilly top land and Loess-hilly slope land became bigger. Overall, these results indicated that landscape configuration considerably changed from the level at scale of 25 to the level at scale of 200.
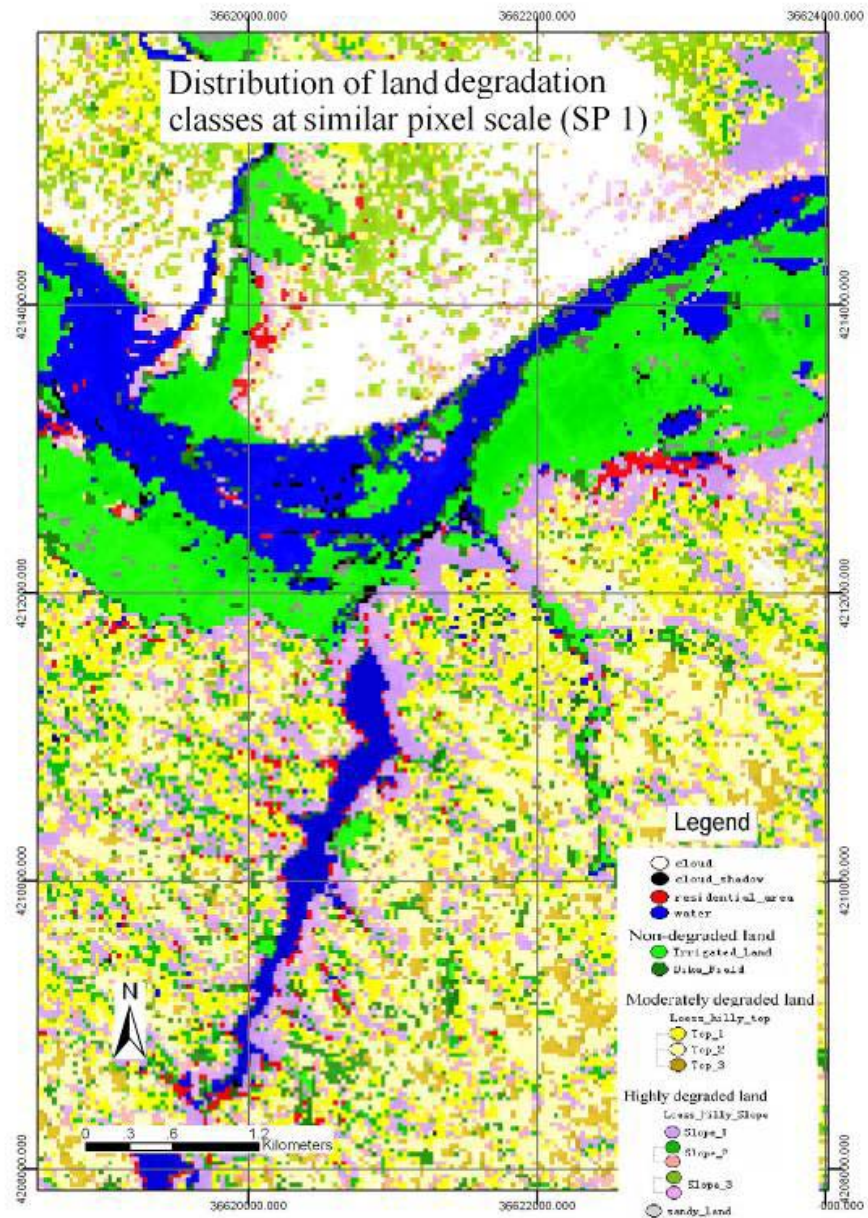
Figure 6.8 Classification of land degradation at similar pixel scale level
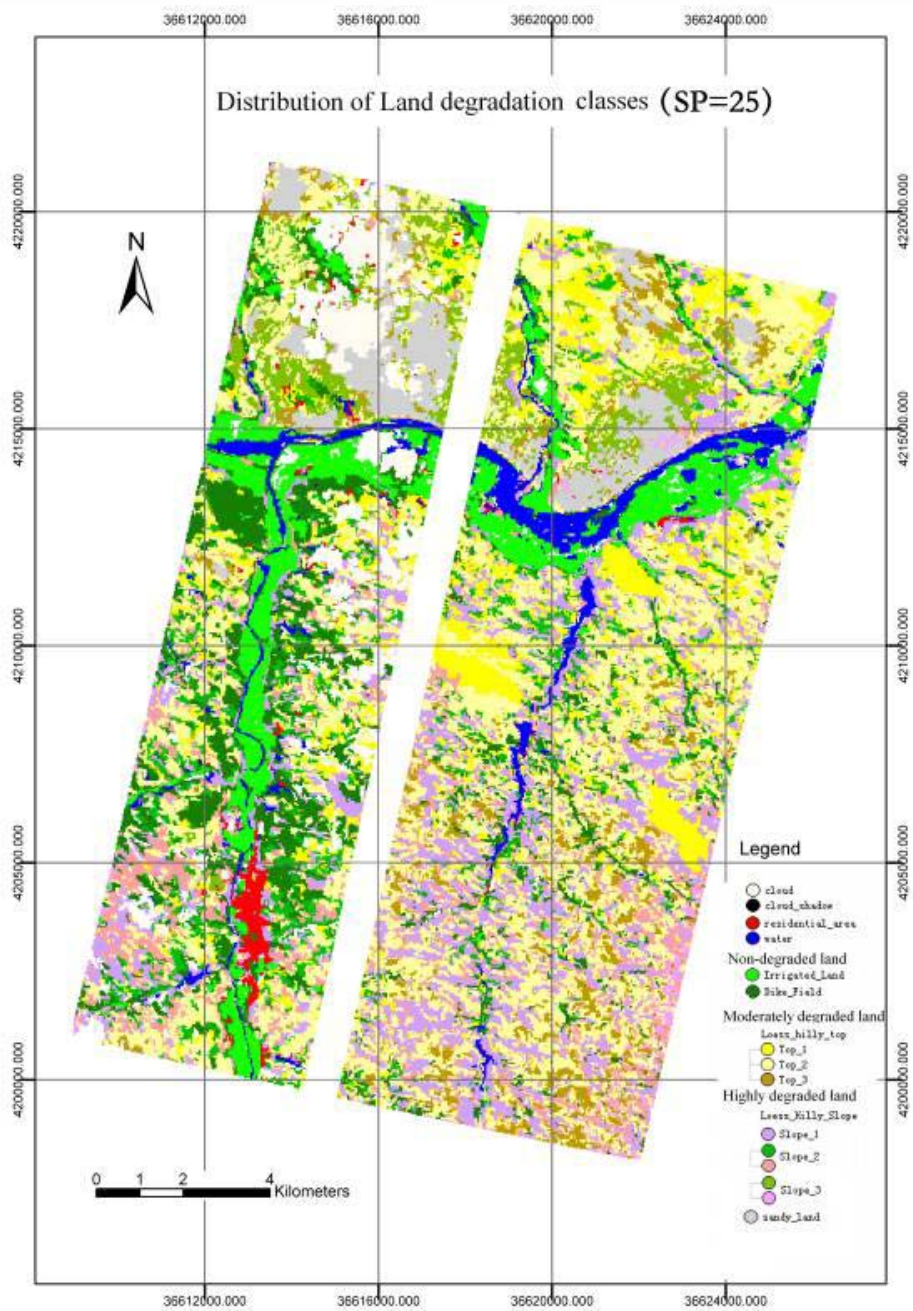
Figure 6.9 Classification of land degradation at the scale level of 25
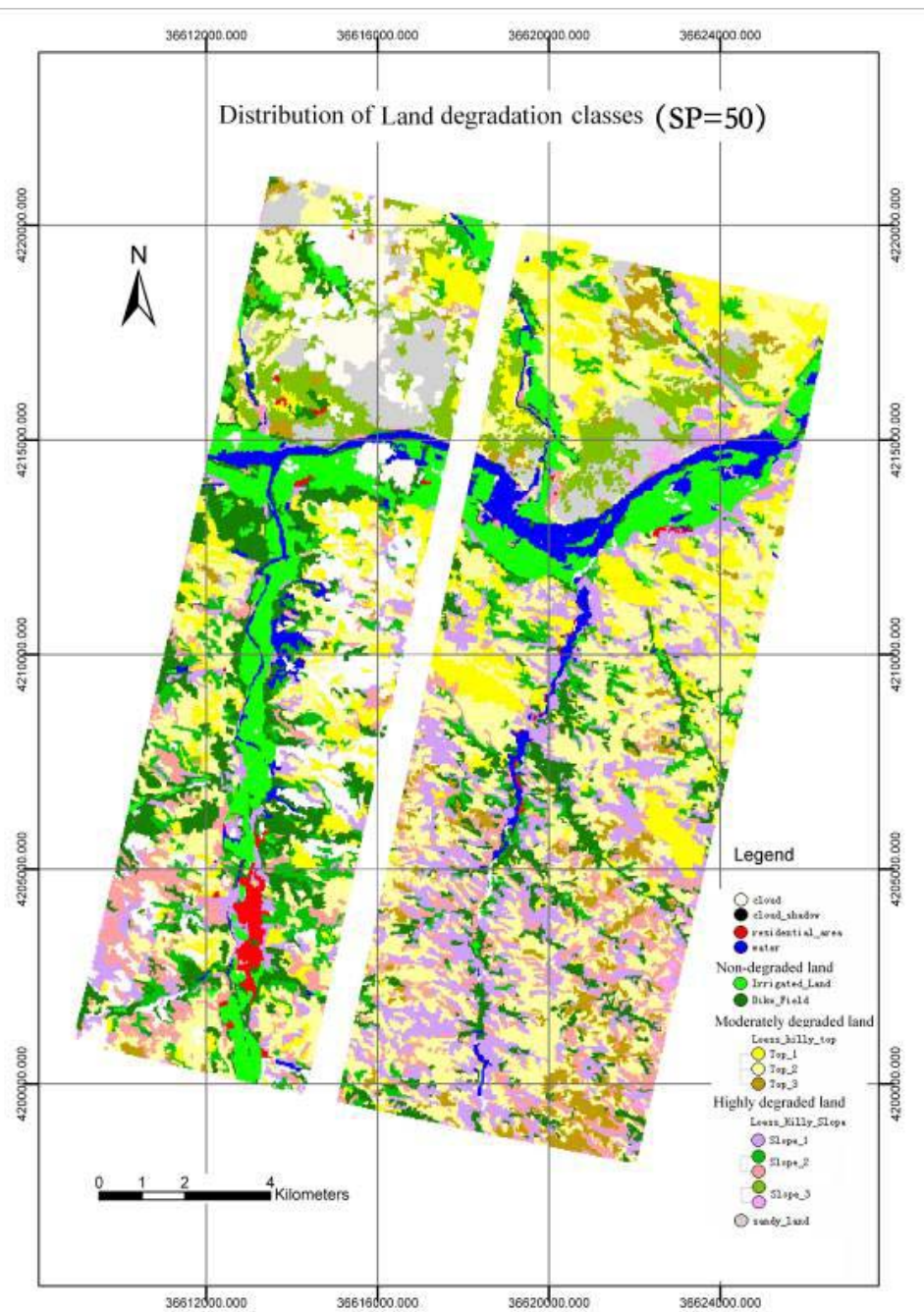
Figure 6.10 Classification of land degradation at the scale level of 50
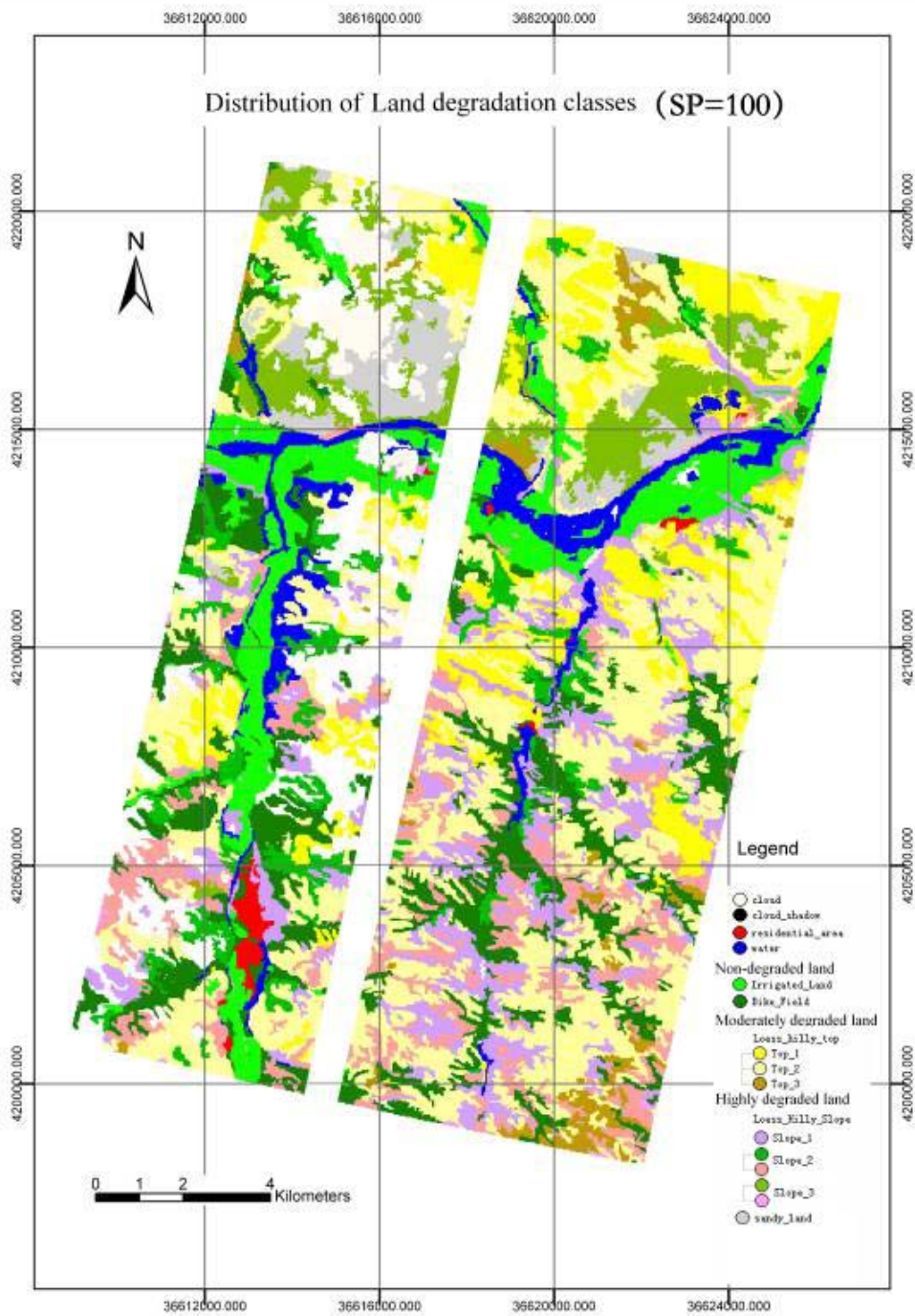
Figure 6.11 Classification of land degradation at the scale level of 100
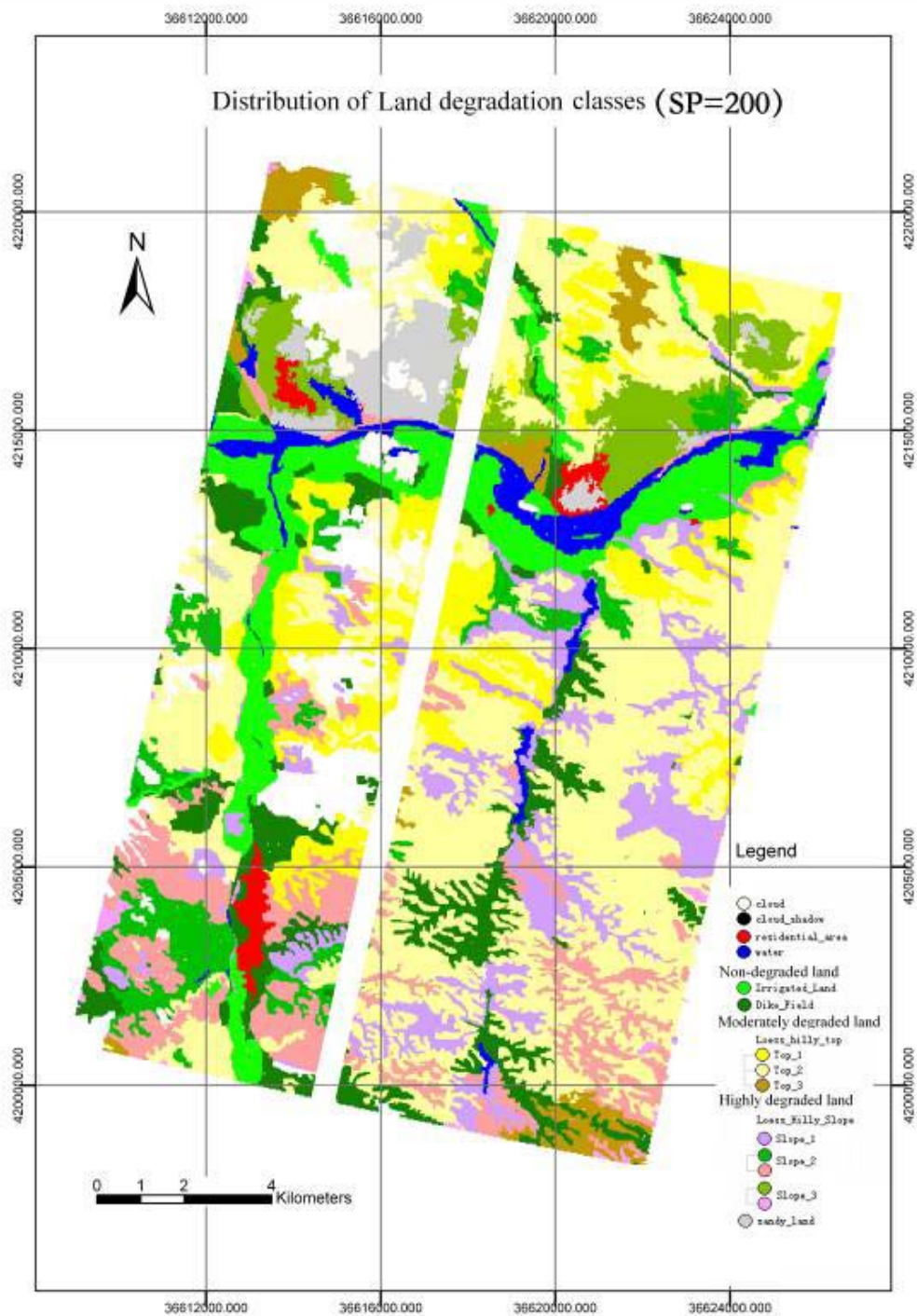
Figure 6.12 Classification of land degradation at the scale level of 200

6.3.3 Land degradation mapping using the SAM approach

The reference spectra were chosen essentially based on the results of the statistical analysis of spectral reflectance data. An angle image θ is produced for each reference spectral signature. The spectral signatures associated with different classes of land degradation were analyzed using the field survey results. The value of 0.15 rad was defined as a threshold for the maximum angle between the image vector and the reference spectrum vector for each degradation class. By regrouping of the similar pixels with θ angle less than 0.15 rad into one class, the state of land degradation classification is presented in Figure 6.13. The classification result from the SAM method is shown in Table 6.10 with an overall accuracy of 67.2% and the error matrix. According to this data, the highly degraded land was mapped with high producer's accuracy (omission error).
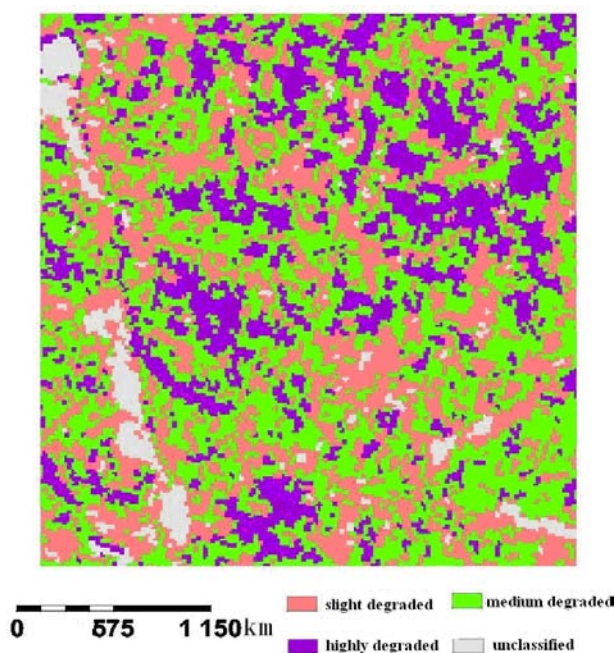
Figure 6.13 Land degradation mapping based on the SAM approach

6.3.4 Land degradation mapping using the DSLI method

The frequency distribution of the result obtained with the DSLI index is presented in Figure 6.14. It can be seen that the highly degraded land was at high DSLI index

value of 0.89 and the slightly degraded land was at a quite low DSLI value of 0.16, and the average value was 0.52 and the standard deviation was 0.21. The application of a threshold to the frequency distribution of the DSLI index may provide well-defined classes. A median filter with a 3×3 window was applied to obtain homogeneous classes and to reduce the presence of isolated pixels. Figure 6.15 shows the result of post-processing. The DSLI map was classified by the Iterative Self-Organizing Data Analysis Technique (ISODATA) method. It is a method of unsupervised classification. The method can split and merge clusters based on an algorithm. User can define threshold values for the parameters. Computer can run the algorithm with iteration until the threshold is reached. In this study, the parameters in the ISODATA method were set as: assumed classes 3, the most iteration times 3, the threshold of change 3% and the least pixel numbers 9. The classification result indicated that the index of the highly and moderately degraded land was more than 60%. Figure 6.16 shows the distribution of land degradation classes based on the DSLI approach.
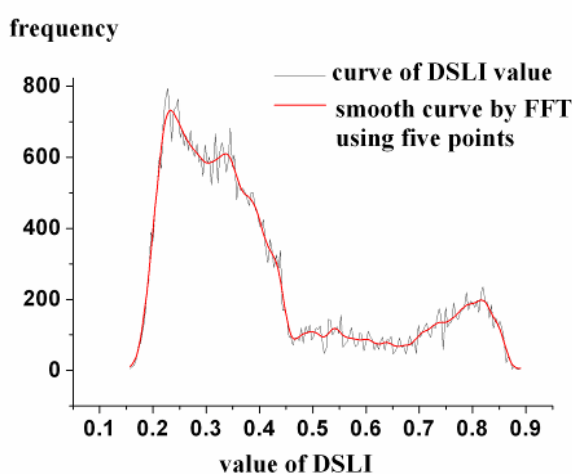
Figure 6.14 Frequency distribution of DSLI index
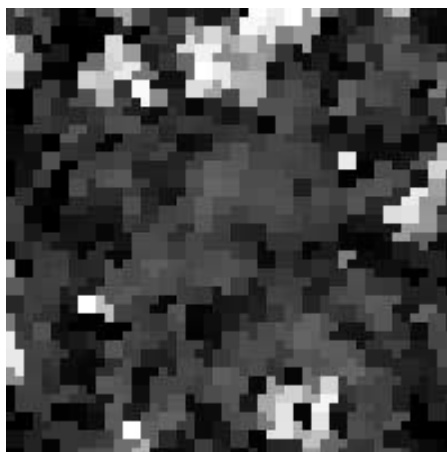
Figure 6.15 DSLI distribution map

slight degraded

medium degraded

highly degraded

0   290 580   1 160 km
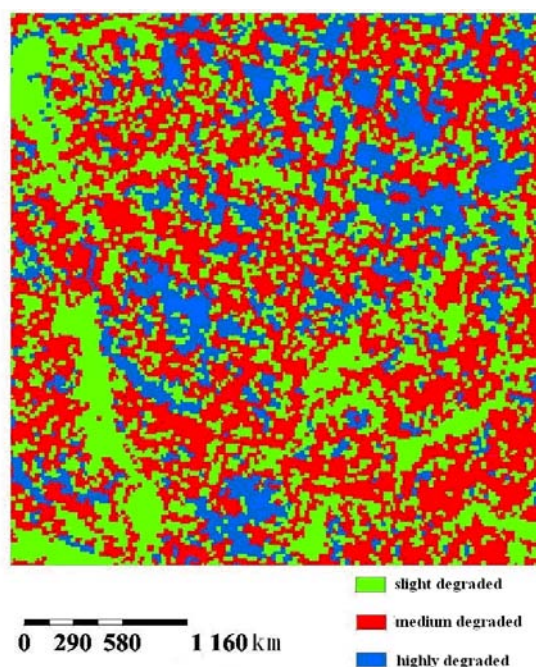
Figure 6.16 Distribution of land degradation classes based on the DSLI approach

6.3.5 Comparison of classification accuracy

6.3.5.1 Classification confusion matrices based on the GEOIC approach

The accuracy of land degradation classification by the GEOIC method was tested by verified samples. The overall classification accuracy is relatively high, ranging from 72.4% to 88.3% (Table 6.8). It can be seen that the classification result at scale level of 100 was effective for mapping land degradation than those at other scale levels,

with an overall accuracy of 88.3% and Kappa coefficients of 0.86. The classification accuracy at scale levels of 25, 50 and 100 was higher than that at the similar pixel level and scale level of 200 using the same training samples and test samples. On the other hand, the overall classification accuracy with the GEOIC method at the similar pixel level was not high, with an accuracy of 73.1% and Kappa coefficient of 0.69. The classes of land type at scale levels of 25, 50, and 100 appear more homogeneous than those at similar pixel level and represent a 9% to 15% increase in the overall accuracy. The detailed confusion matrices based on the GEOIC approach at similar pixel level and scale levels of 25, 50, 100 and 200 were summarized in a bar diagram for each type, enabling a graphical analysis of the classification accuracy of each type (Figure 6.17). According to the error matrix, all types except the sandy land have higher user's (commission error) and producer's accuracy at scale level of 100 than at other scale levels, while the user's and producer's accuracy was lower at scale level of 100 for the sandy land.

It was noted that from similar pixel level to scale level of 200, some bars are partitioned, especially for the dike field and Loess hilly slope land, indicating the emergence from another types. At the similar pixel level, all types except the dike field and Loess hilly slope land had higher user's (commission error) and producer's accuracy; but for the dike field and Loess hilly slope land, the user's (commission error) and producer's accuracy was lower. At scale level of 25, the producer's accuracy is relatively high (more than 79%), except for the dike field and Loess hilly slope land. The Loess hilly slope land was mainly confused with the dike field. This is due to the fact that the Loess hilly slope land, sandy land and Loess hilly top land had similar sparse shrub/crop vegetation, combined with fragmentized pattern of land in the study site. This is also due to the coarse resolution of the DEM data. At the scale level of 100, the irrigated land was well classified. The dike field was also well classified with 10% misclassified as the Loess hilly slope land. The largest errors were observed for the Loess hilly slope land, with classification accuracy of 64%. The errors mainly come from the misclassification as the sandy land (21%) and the dike field (8%). In general, the results were better for all classes at scale level of 100 than at other scale levels.

Table 6.8 Precision evaluation of land degradation classification at five scale levels

land degradation class	land type	SPL[a]	SP25	SP50	SP100	SP200
		Producer's accuracy				
Non-degraded land	Irrigated land	0.800	0.828	0.939	0.999	0.999
	Dike field	0.293	0.525	0.583	0.789	0.107
Moderately degraded	Loess hilly top	0.841	0.909	0.940	0.999	0.999
Highly degraded	Loess hilly slope	0.435	0.651	0.663	0.956	0.622
	Sandy land	0.803	0.839	0.720	0.549	0.195
Non-agricultural land	Residential land	0.800	0.794	0.825	0.860	0.860
	Water	0.976	0.966	0.983	0.999	0.999
		User's accuracy				
Non-degraded land	Irrigated land	0.906	0.936	0.957	0.999	0.999
	Dike field	0.464	0.719	0.545	0.905	0.255
Moderately degraded	Loess-hilly Top	0.785	0.758	0.815	0.876	0.762
Highly degraded	Loess-hilly Slope	0.590	0.604	0.613	0.644	0.382
	Sandy land	0.931	0.996	0.999	0.999	0.999
Non-agricultural land	Residential land	0.971	0.990	0.999	0.999	0.999
	Water	0.966	0.983	0.997	0.999	0.999
Overall accuracy		0.731	0.823	0.833	0.883	0.724
Kappa coefficient		0.685	0.789	0.802	0.861	0.670

a: similar pixel level.
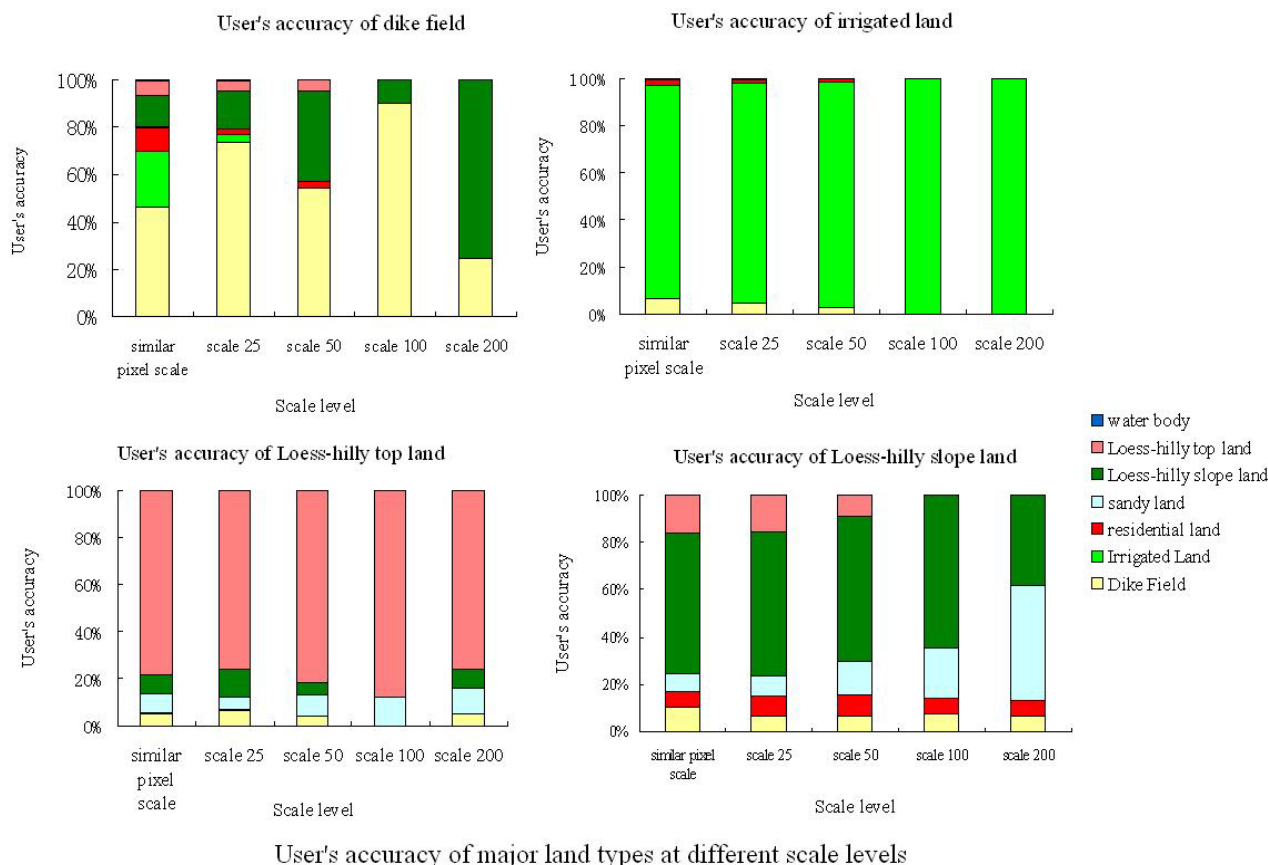
Figure 6.17 User's accuracy of major land types at different scale levels

A comparison of the results with the GEOIC approach with the ground truth indicates that land degradation can be reliably classified with an integration of Hyperion images and multi-source data through the segmentation of DSRUs at an appropriate scale parameter. The classified results at scale level of 100 were validated by 26 field soil samples in the study area. The validation results indicated that the irrigated land and dike field have high content of SOM and the Loess-hilly top land, Loess-hilly slope land and sandy land have low content of SOM. This was consistent with the field survey result, which showed that the content of SOM decreased in the sequence of the irrigated land, dike field, terrace, Loess-hilly top land, Loess-hilly slope land and sandy land. In addition, the map of land degradation at scale level of 100 is closely related to the physico-chemical characteristics of the different classes. Table 6.9 shows that highly degraded land was associated with low SOM, TN, and AN, soil moisture content, and the percentage of small size particles, and high slope gradient. It can clearly be seen that non-degraded land was

characterized by slightly more SOM, TN, and AN, soil moisture content, and the percentage of small size particles.

Table 6.9 Soil parameters statistics of various classes of land degradation at scale level of 100

Lang degradation type	Average slope	Particle <10 um %	Particle <2 um	SOM %	TN %	AN mg/kg	Soil moisture %
Non- degraded	20.4	9.61	0.06	0.59	0.05	115.45	9.46
Moderately degraded	25.2	8.75	0.05	0.44	0.04	92.07	6.18
Highly degraded	29.0	7.89	0.03	0.43	0.03	63.66	4.29
Average	26.6	8.65	0.05	0.49	0.04	88.87	7.07

6.3.5.2 Classification confusion matrices based on the SAM and DSLI methods

The samples of slightly, moderately, and highly degraded land for accuracy assessment were collected in color compound images by the field investigation and the visual interpretation. The results of classification accuracy for the SAM method and DSLI method are presented in Table 6.10. It can be seen that the DSLI method seems to provide more accurate result for mapping land degradation than that with the SAM method, with an overall accuracy of 80.8% for the DSLI and 67.2% for the SAM. According to the error matrix, the slightly degraded land were mapped using the DSLI method with higher user's (commission error) and producer's accuracy than using SAM method, but for highly degraded land with lower user's (commission error) and producer's accuracy than using the SAM method.

Table 6.10 Confusion matrix of classification based on SAM and DSLI methods

Types		Number of pixels					
		Slightly degraded	Moderately degraded	Highly degraded	Unclassified	Total	Short (%)
SAM	Slightly degraded	469	18	11	102	636	20.6
	Moderately degraded	175	413	44	4	600	37.17
	Highly degraded	0	0	603	0	603	0
	Unclassified	0	128	0	956	1084	11.81
Total		644	559	658	1062	2923	
Error (%)		37.31	35.35	8.36	9.98		
Producer's accuracy (%)		67.17	53.22	91.64			
User's accuracy (%)		74.96	63.36	100			
Overall accuracy (%)		67.16					
Kappa		0.6109					
DSLI	Slightly degraded	432	16	2	12	462	6.49
	Moderately degraded	200	379	65	14	658	42.4
	Highly degraded	12	100	517	37	666	22.37
	Unclassified	0	0	0	595	595	0
Total		644	495	584	658	2381	
Error (%)		32.92	23.43	11.47	9.57		
Producer's accuracy		67.08	76.57	88.53			
User's accuracy		93.51	57.6	77.63			
Overall accuracy (%)		80.76					
Kappa		0.7443					

The validation of the result obtained with the DSLI index was carried out by using additional 12 soil samples. Table 6.11 shows that highly degraded class is associated with low SOM and AP, and high slope gradient and sand particle percentage. It indicated that the non-degraded and slightly degraded classes are characterized by a low percentage of sand particles and more SOM.

Table 6.11 Soil parameter statistics of various degradation types based on the DSLI method

Land degradation type	Average slope	Clay	Silt	Sand	SOM	TP	AP
		%	%	%	%	mg/kg	mg/kg
Slightly degraded	15	0.046	54.563	45.391	0.699	814.44	16.4
Moderately degraded	19	0.047	49.479	50.474	0.765	1152.7	8.46
Highly degraded	23	0.047	42.314	57.639	0.214	1291.3	3.45

There is a relationship between land degradation classes and soil reflectance. Non-degraded land generally appears dusty black compared with shiny white of highly degraded land in visibility. This phenomenon indicates that rich SOM content is in negative correlation with spectral reflectance. The reflectance curves of different classes of land degradation also support this point (see Figure 6.18). The highly

degraded land with little content of SOM has the sharpest reflectance while the slightly degraded land has not.
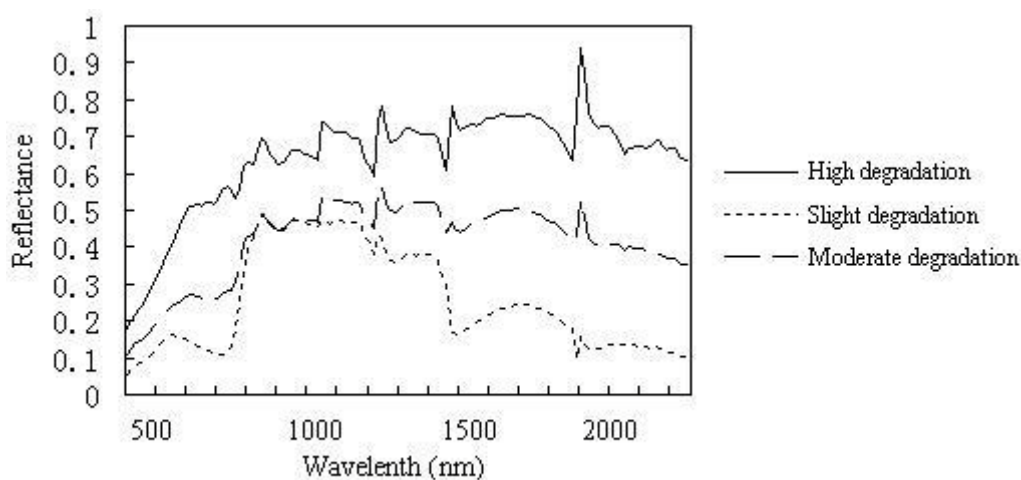
Figure 6.18 Spectral characteristics of different classes of land degradation

6.3.5.3 A comparison of different approaches

From the above accuracy evaluation, it can be seen that the results obtained with three methods are different. The difference between the DSLI and SAM methods is significant. The potential of the DSLI index method for land degradation mapping was revealed. This can be explained by the fact that different degradation types to some extents have different spectral responses. The SAM method has a tendency sometimes to classify the slightly and the moderately degraded classes into one class. The DSLI algorithm is simple and useful for land degradation mapping using hyperspectral remote sensing data. It is easy to carry out and has a potential for evaluating soil degradation and soil surface conditions. However, one should note that the DSLI index calculated from bare soil spectral reflectance is sensitive to the vegetation cover. The method is therefore suitable for the areas of arid to semi-arid environments especially in non-growing season. Although the application of DSLI approach to other regions is feasible if there is a clear contrast between slightly and highly degraded land in the regions, its limitations and uncertainties are obvious. Moreover, the method neglected the other information related to land degradation, i.e.

without integrating remote sensing information and other geographic information and knowledge in the process of land degradation classification.

The test results showed the classification accuracy at scale levels of 25, 50 and 100 was not only higher than that at similar pixel level using the GEOIC approach, but also higher than that of the DSLI method and the SAM method, which are based on pixel by pixel classifiers. Moreover, the GEOIC approach can provide the detail classification of land types compared with the methods of SAM and DSLI. This can be explained by the fact that the approach integrated the information of remote sensing images with the information on vegetation and soil, and physiognomy related to land degradation. However, the overall accuracy and Kappa coefficients at similar pixel level and at scale level of 200 using the GEOIC approach were higher than that with the SAM method, but lower than that with the DSLI method. This is because the GEOIC approach provided the detailed classification of land types corresponding to land degradation classes, while the methods of SAM and DSLI only provided the four classes of land degradation. In spite of that, the problem of "salt and pepper" effect was not solved in the pixel by pixel classification.

The above results showed that the classification accuracy at an appropriate scale level was higher than that with methods based on the pixel by pixel. Wu *et al*. (2006) achieved the overall accuracies of 76.6%, 63.3% and 68.9% and the Kappa coefficients of 0.71, 0.54 and 0.60 for land degradation mapping in the same study area, using the mixed classification method, the spectral angle matching method, and the method of mixture–tuned matching filtering, respectively. Our study not only further validated that the GEOIC approach has great ability for land degradation mapping, but also give the best accuracy.

Furthermore, the GEOIC approach is of advantage over the others for the extraction of land degradation information, because the method can overcome within-class spectral variation and eliminate "salt and pepper" effect in the pixel by pixel classified images, but also can be used to emulate a human interpreter's ability in image interpretation (Yu *et al*., 2006). The advantage is also due to integrating different types of geo-data into an object-based classification process and a fuzzy-

logic-based rule set applied in the classification process. Much higher classification accuracy can be reached with additional data. The heterogeneity of a complex system at different scales is problematic for traditional pixel-based classification techniques. The GEOIC approach, however, produces an accurate representation through the segmentation of DSRUs for the extraction of land degradation information. It extracts land degradation information from the spatial feature perception to spatial object cognition and spatial pattern cognition under the cognition mode of feature-object-pattern. By segmenting DSRUs and grouping homogeneous objects together at different scales, contextual and hierarchical information can be incorporated into the classification process. The segmentation of DSRUs was not only based on spatial patterns of topography, soil and vegetation, but also remote sensing image information related to the features of land degradation. DSRUs have their geographical meanings and are thought to be the result of hydrological and erosion processes related to land degradation. It indicated that the GEOIC approach is of significance for monitoring and assessment on land degradation.

However, the diagnostic indicators of land degradation must be properly selected when the GEOIC approach is applied in other areas. It is extremely important to select the appropriate diagnostic indicators for the assessment of land degradation according to local situation. In this study, some knowledge and the survey results from the local farmers were considered in the selection of diagnostic indicators and the classification of land degradation. These knowledge and results can also be obtained through detailed field surveys and by a reference to local cultivation system, land use history and agricultural history. Another problem must be recognized that the appropriate size of image objects is of importance for the quality of the segmentation and the accuracy of the classification. The determination of scale parameters is very important and challenging in the GEOIC approach. The research on the proper selection of diagnostic indicators and scale parameters should be further conducted in the future.

6.3.6 Scale effects on DSRUs

From Figure 6.9 to Figure 6.12, one can see that the classified images appear very similar at scale level of 50 and scale level of 100. Their visual patterns considerably change compared with that at scale level of 25, which has more textures in Loess hilly slope land and Loess hilly top land, but an increase in the area of dike field in the underside of the scene. The Loess hilly slope land and Loess hilly top land at the underside right of the image changed to dike field and irrigated land. But water and residential land do not change. Moreover, there was a small change in the proportions of different classes. A general trend is that neighboring units tend to be combined into large units, with the larger DSRUs persisting through scale levels at the expense of smaller DSRUs. In addition, a number of DSRUs tend to persist within one or two scale domains, and then suddenly disappear at the next domain. This is apparent in the images at scale levels of 25 and 50 where dike field dispersedly distributed along valley floor in the underside right of the image abruptly mostly appears and is concentrated along valley floor at scale level of 100. Some types of structures emerge at specific scale domains where they did not exist before. This is similar to the results of Turner (1989) that any land cover presenting in less than 50% would ultimately be lost at coarser resolutions by using a larger range of grid cell sizes for testing grain size effects. It suggests that these results related to the sudden shifts in the entire image structure at certain scale domain might correspond to the detection of critical landscape thresholds.

To better understand an appropriate scale parameter and a critical landscape threshold, the accuracy assessment results were analyzed further. The results show that accuracy does vary spatially in relation to these types and their features at different scale levels. It has been proven to be effective for regional land degradation classification with overall accuracy 88.3% and KIA 0.86 at scale level of 100. It implied that the appropriate size of image objects of DSRUs for land degradation mapping in study area was scale parameter 100. The results of the total scene variance from the individual DSRU at different scale levels show that it increased from scale level of 25 to scale level of 200. At scale level of 200, the total scene variance is high, indicating that each DSRU is more heterogeneity. From an object-

specific perspective, a minimum variance threshold has not been reached. Hay *et al.* (2003) demonstrated that the representation at different scale levels corresponds to the objects of interests rather than only referring to statistical measures in an image (Lang and Blaschke, 2003). It is difficult to determine the 'optimal' scales to evaluate the varying sized, shaped, and spectrally distributed image-objects within a scene. As pointed out by Hay *et al.* (2003), there are many optimal scales that are specific to the image-objects that exist/emerge within a scene.

6.4 Conclusions of the GEOIC application

Under the cognition mode of feature-object-pattern, the approach of GEOIC is applied in the extraction of land degradation information through the segmentation of DSRUs with Hyperion images. The GEOIC approach was used in this study with different combinations of input layers for the determination of diagnostic indicators related to land degradation. The method of determining the diagnostic indicators by the comparison of different combinations of the diagnostic indicators and from the local farmer's perception was devised and also validated. The overall classification accuracy and Kappa coefficients showed that the classification accuracy is higher with ancillary information than with the Hyperion images only. The overall accuracy increased when new diagnostic indicators related to land degradation are used. It increased by 11.5% with additional data. With the combination of Hyperion+Elevation+Slope+MCARI+SOM, the classification accuracy reached the highest, with the overall accuracy of 88.3% and Kappa coefficient of 0.86 at the scale level of 100 compared with that of the combination of four indicators and three indicators. The results of the farmers' survey supported the above chosen diagnostic indicators. The topographic factors including slope and elevation, vegetation, SOM, and remote sensing images were determined as the diagnostic indicators for extracting land degradation information in the study area.

In this study, the developed GEOIC approach was compared with the methods of SAM and DSLI. The classification results obtained with the three methods are different. The difference between the GEOIC method and the methods of DSLI and SAM is significant. The potential of the DSLI index method for land degradation

mapping was revealed. The results showed that the DSLI method provided more accurate results for mapping land degradation than those with the SAM method, with an overall accuracy of 80.8% for the DSLI and 67.2% for the SAM. But the DSLI method is suitable for the areas of arid to semi-arid environments especially in non-growing season, and its limitations and uncertainties are obvious. The method neglected the other information related to land degradation, i.e. without integrating remote sensing information and other geographic information and knowledge in the process of land degradation classification. Moreover, the results also indicated that the application of the GEOIC approach is of advantage for the extraction of land degradation information, although the knowledge on land degradation is often expressed ambiguously. The accuracy of the approach at appropriate scale level was much higher than that of the pixel by pixel method. The classification accuracy was higher with the GEOIC approach at all scale levels (72% to 88%), and was lower at the similar pixel level and also with the methods of DSLI and SAM. The classification at scale level of 100 was effective for mapping land degradation with an overall accuracy of 88.3% and Kappa coefficients of 0.86. The user's and producer's accuracy was generally higher at scale level of 100 than at other scale levels. The GEOIC approach with hyperspectral images can be used to study and characterize the state of land degradation without the "salt and pepper" effect. However, the map of land degradation classes is closely related to the physico-chemical characteristics of the different classes.

The developed GEOIC approach also provided a reliable method of integrating the diagnostic indicators related to land degradation through the segmentation of DSRUs. The GEOIC approach can emulate a human interpreter's ability in image interpretation (Yu *et al.*, 2006), and integrate different types of geo-data into an object-based classification process and apply a fuzzy-logic-based rule set in the classification process. Much higher classification accuracy can be reached with ancillary information. The developed GEOIC approach combines remote sensing images with multi-source information and geoscience knowledge, e.g. combining spectral information and texture information with physiognomy, soil characteristics, vegetation, land use information, and information from field surveys and local farmers. The results indicated that the segmentation of DSRUs by integrating SOM,

vegetation index, slope gradient, elevation and Hyperion image information is of significance and advantages. A DSRU is an ecologically and geographically and spectrally homogeneous area with similar characteristics of physiognomy, vegetation, and soil and image spectral information. The size of DSRUs influences the accuracy of the classification of land degradation. The classified images at scale levels of 25, 50, 100 and 200 indicated that larger structure forms at the expense of smaller structure. A general trend is that neighboring units tend to be combined into large units, with the larger DSRUs persisting through scales at the expense of their smaller DSRUs. Scale parameter 100 was observed to be appropriate and effective for regional land degradation classification in this study.

The GEOIC approach based on DSRUs is an attempt for the extraction of land degradation information by integrating remote sensing technique and field survey methods. Meanwhile, it realized the image cognition mode from only the spatial feature perception to comprehensive spatial object cognition and spatial pattern cognition in the process of image cognition on land degradation. This approach is of significance for monitoring and evaluation of land degradation with hyperspectral images, and also for land use management in Loess Plateau areas by providing a tool for remote assessment of land degradation.

The GEOIC approach is capable of land degradation classification. The determination of the diagnostic indicators for land degradation evaluation and selection of suitable function models are important in the process of classification, for they significantly affect the classification accuracy. This approach seems promising, but the accuracy for classifying some land types should be further improved. However, the implementation of automated methods for land degradation classification seems complicated in areas where physical geographic situation is very complex and fragmentized. A potential solution might be coupling of the current approach using hyperspectal images with high spatial resolution and DEM at a scale of 1:10 000.

A further improvement of this study can be obtained by a careful analysis of the dependence of accuracy on natural site conditions, integration of other additional

data (such as LIDAR data), and a more efficient usage of geographic information and local knowledge. The GEOIC approach presented here should be tested in other areas with different soil types and forest types to validate its applicability and reliability. It is also necessary to improve its automated process, so that large areas could be processed cost-effectively and in a timely manner. Moreover, a comparison of different techniques of integrating multi-source data in classification, such as the neural network technique, will be useful for a quality assessment of integration techniques (Baltsavias, 2004).

Chapter 7

Conclusions and Recommendations

7.1 Conclusions

Land degradation is a major problem world-wide. It is estimated that more than one-third of terrestrial land area in China is threatened by land degradation. Land degradation coupled with the population growth has a negative impact on the living conditions for Chinese people. Therefore monitoring and assessment of land degradation is of particular importance, which provides the crucial information for the policy and decision making in terms of sustainable development. The development of hyperspectral remote sensing technique makes possible regularly updating land degradation information by the analysis of precise spectral features and the quantitative retrieval of spectral reflectance of surface features. To improve the accuracy and reliability of land degradation mapping this research has developed the approach of GEOIC for monitoring and assessment on land degradation by integrating remote sensing information, land information and geoscience knowledge. It significantly enriches the theory and methodology in land degradation research. The main conclusions derived from this research are summarized below.

1. This research has developed the approach of GEOIC and determined its conception, connotation, and framework on land degradation based on the methodology of OBIA. The GEOIC is the objectification cognition on remote sensing images and multi-source information using geo-knowledge. It is an extension of the OBIA. The GEOIC approach can not only extract thematic information, but more importantly can mine the information and quantify ambiguously expressed

knowledge. The key objective of GEOIC on studying land degradation is to simulate the functions and processes of the visual interpretation by experts, and extract spatial features, spatial objects and spatial patterns of land degradation under a cognition mode of feature-object-pattern from remote sensing images and multi-source information. It describes the methodology for developing automated methods to partition remote sensing images and multi-source data into DSRUs and assessing their spatial, spectral, geographic and temporal characteristics. It can be employed in wide areas, like land use and land cover classification, vegetation classification, land degradation evaluation, land quality evaluation, soil parameter mapping, and forest development monitoring, etc.

The approach of GEOIC is realized through the segmentation of geo-objects or meaningful image objects using remote sensing information, geographic information, vegetation, soil, and other ancillary information with geoscience knowledge and intelligence. It can emulate a human interpreter's ability in image interpretation, and integrate different types of geo-data in an object-based analysis process with a set of fuzzy-logic-based rules. The approach provides a unified framework for the extraction of land degradation information.

In this research, some issues concerning the approach of GEOIC on studying land degradation, especially the factors affecting human's visual cognition, were discussed, because human's visual cognition on images appears in the whole process of GEOIC. The quantitative analysis of these factors is of significance for the determination and selection of the diagnostic indicators in the application of the GEOIC approach for the evaluation of land degradation. The results of a questionnaire survey showed that the experience, age and gender of a user have influence on the visual cognitive abilities on remote sensing images. The experience affected the cognition abilities on feature images of land use types, while gender did make difference in cognition on vegetation cover, vegetation growth and the percentage of barren land. The effects of the experience, age and gender on cognitive abilities on remote sensing images were different. Therefore, the diagnostic indicators and their threshold values should be chosen and determined by experienced experts if the GEOIC is applied in the extraction of land degradation

information. Moreover, local farmers know well the land degradation situation, and should participate in the process of the selection and determination of the indicators. It is necessary to integrate the results of experts' and farmers' cognition on land degradation for deriving the appropriate indicators. On the other hand, it is of importance to develop a standardized methodology of image cognition from visual cognition to automatic comprehensive cognition by integrating remote sensing image information, spatial information, geographic information and experience in computer environment.

2. This research has developed a reliable method for determining the appropriate diagnostic indicators related to land degradation under the approach of GEOIC with an integration of hyperspectral data with multi-source information. In the cognition mode of feature-object-pattern, DSRUs were segmented with the support of an integration of Hyperion images with multi-source information on various diagnostic indicators based on geoscience knowledge and geographic information. DSRU is an ecologically and geographically and spectrally homogeneous area with similar characteristics of physiognomy, vegetation, soil and image spectral information. It related hydrological and erosion processes to the spectral response of land degradation. It is of significance for the extraction of land degradation information, and for integrating the various diagnostic indicators in land degradation assessment. The tests using the data in the study area validated the data integration techniques and related issues.

The method of determining the diagnostic indicators from the local farmers' perception was proposed and the comparison among various combinations of the diagnostic indicators was made. The test study with different combinations of the input layers for the determination of diagnostic indicators related to land degradation shows the overall classification accuracy was increased by 11.5% when additional data were used. Much higher classification accuracy can be reached if a new layer of diagnostic indicator related to land degradation is used. With the combination of Hyperion+Elevation+Slope+MCARI+SOM, the classification accuracy reached the highest. The results of the farmers' survey supported the above chosen diagnostic indicators. Slope and elevation, vegetation, SOM, and remote sensing images were

determined as the diagnostic indicators for extracting land degradation information in the test area. The results also showed that the determination of the diagnostic indicators and selection of suitable function models are important in this study.

Overall, the GEOIC approach can emulate a human interpreter's ability in image interpretation and integrate different types of geo-data into an object-based classification process. Much higher classification accuracy can be reached with ancillary information. The developed GEOIC approach combines remote sensing images with multi-source information and geoscience knowledge, e.g. combining spectral information and texture information with physiognomy, soil characteristics, vegetation, land use information, and information from field surveys and local farmers.

3. This research investigated the method for mapping soil parameters related to land degradation with hyperspectral images and soil spectral at a regional scale with the approach of the GEOIC. It solved the third key issue mentioned in Chapter 1. The results indicated that the *in-situ* estimation models based on the relationship between the SOM content and the spectral reflectance in bands R_{440}, R_{560}, R_{625}, R_{740}, R_{1336} using multiple regression method and fuzzy set method were valid to estimate SOM of the soil samples. The five sensitive bands could be used for the SOM estimation using Hyperion images. Moreover, the results also indicated that the DSRU estimation models developed based on the relationship between the content of SOM and the spectral and regional variables of DSRUs were valid to estimate the SOM content using Hyperion images. The determinative coefficient (R^2) of the model increased from 0.562 at scale level of 25, to 0.721 at scale level of 50, and to 0.722 at scale level of 100. The mean square of regression models at scale level of 100 was lowest. The DSRU estimation models considered not only some variables in the *in-situ* model, but also some environmental variables to compensate for the change of scale. The mapping results of SOM based on DSRU estimation models using Hyperion images are comparable well with the results of field survey, and close to the results with the Kridge interpolation using soil samples. Mapping SOM could be processed cost-effectively and in a timely manner instead of collecting and measuring large amount of soil samples in large areas. The method provided a useful

tool for mapping soil features at a regional scale by combining field data, remote sensing images and regional variables.

The DSRU modeling of soil parameters was an application of the GEOIC approach. The results obtained in this test study showed the potential and advantages of the GEOIC approach based on DSRU estimation models for soil parameter mapping. The GEOIC approach for SOM estimation combines spectral information and texture information with soil types, vegetation, land use information, and *in-situ* information from field surveys. This has significant implications for land quality management by providing a tool for monitoring soil parameters remotely at a regional scale.

4. This research has demonstrated the approach of GEOIC was successfully applied in the extraction of land degradation information with Hyperion images and multi-source information. It solved the fourth key issue mentioned in Chapter 1. The approach was tested in an agriculture-pasture mixed area in Loess Plateau in China. The developed GEOIC approach was compared with the methods of SAM and DSLI. The differences among the results with the GEOIC method and the methods of DSLI and SAM are significant. The GEOIC approach provided more accurate results at an appropriate scale level for mapping land degradation than those with the SAM method and DSLI method. The results showed that the accuracy with the DSLI method was much higher than that with the SAM method, with an overall accuracy of 80.8% for the DSLI and 67.2% for the SAM. But the DSLI method is suitable for the areas of arid to semi-arid environments especially in non-growing season, and its limitations and uncertainties are obvious. Moreover, the results indicated that the application of the GEOIC approach is of advantage for the extraction of land degradation information, although the knowledge on land degradation is often expressed ambiguously. The accuracy of the approach at an appropriate scale level was much higher than that of the pixel to pixel method. The classification accuracy was higher for the GEOIC approach at all scale levels (72% to 88%). The classification at scale level of 100 was effective for mapping land degradation with an overall accuracy of 88% and Kappa coefficients of 0.86. The user's and producer's accuracy was generally higher at scale level of 100 than at other scale

levels. The GEOIC approach with Hyperion images can be used to study and characterize the state of land degradation without the "salt and pepper" effect. However, the map of land degradation classes in the test area is closely related to the physico-chemical characteristics of the different classes. The GEOIC approach can significantly improve the accuracy of land degradation classification.

The GEOIC approach realized the image cognition mode from the spatial feature perception to comprehensive spatial object cognition and spatial pattern cognition in the process of image cognition on land degradation. This approach is of significance for monitoring and evaluation of land degradation with hyperspectral images. This holds significant implications for land use management in Loess Plateau areas by providing a tool for remote assessment of land degradation.

7.2 Recommendations for further study

Although the developed GEOIC approach seems working well, the following aspects need further study.

(1) It is important to select appropriate diagnostic indicators of land degradation, which should suit well local situation. The selection of appropriate diagnostic indicators should be done by a field detail survey and a reference to local cultivation system, land use history and agricultural history. This issue should be further studied. In addition, some factors such as the methods of DSRUs segmentation, and membership functions need further testing in different environments.

(2) Hyperspectral data directly collected in the field or acquired from remote sensing techniques might be affected by natural soil surface conditions (e.g., roughness, moisture, stoniness, etc), the atmosphere, and the illumination conditions. Their effects should be further studied and corrected using different atmospheric correction methods and other methods on the basis of an extended spectral data set (i.e. larger number of soil samples) collected directly in the field together with ancillary data.

(3) The further improvement of the approach can be done by a careful analysis of the dependence of accuracy on natural site conditions, an integration with other additional data (such as LIDAR data), and more efficient use of geographic information data and local knowledge. The developed GEOIC approach should be applied to other areas, such as soil type classification and forest development monitoring, to test its reliability and applicability. It was also necessary to improve its automation level so that large areas can be processed cost-effectively and in a timely manner. Moreover, a comparison of different techniques for integrating multi-source data for classification, such as neural networks and support vector machines, could be useful for a quality assessment of integrated techniques.

(4) Although the approach of GEOIC on studying land degradation has a great potential, this study only investigated the GEOIC approach through the segmentation of DSRUs for the extraction of land degradation information. This study is the first comprehensive attempt to synthesize the approach of GEOIC and the extraction of land degradation information from an interdisciplinary perspective to a specific type of image processing. The GEOIC approach is an integrated methodology and also develops very rapidly. There are certainly many technical and theoretical issues/problems, which need further investigation.

References

Adejuwon, J. O. and Ekanade, O., 1988. A comparison of soil properties under different land use types in apart of the Nigerian cocoabelt. *Catena*, 15, pp. 319-331.

Al-Abbas, A.H., Swain, P.H. and Baumgartner, M.F., 1972. Relating organic matter and clay content to the multispectral radiance of soils. *Soil Science*, 114, pp. 477–485.

Arsenault, É. and Bonn, F., 2005. Evaluation of soil erosion protective cover by crop residues using vegetation indices and spectral mixture analysis of multispectral and hyperspectral data. *Catena*, 62 (2-3), pp. 157-172.

Atkinson, P. M. and Lewis, P., 2000. Geostatistical classification for remote sensing: an introduction. *Computers & Geosciences*, 26(4), pp. 361-371.

Baatz, B., Hoffmann, C. and Willhauck, G., 2008. Progressing from object-based to object-oriented image analysis. In Blaschke, T., Lang, S. and Hay, G. J. eds. *Object-Based Image Analysis: Spatial Concepts for Knowledge-Driven Remote Sensing Applications*. Heidelberg, Springer-Verlag, pp. 29-42.

Baatz, M. and Scha¨pe, A., 2000. Multiresolution segmentation—an optimization approach for high quality multi-scale image segmentation. In Strobl, J., Blaschke, T. and Griesebner, G. eds. *Angewandte Geographische Informations-Verarbeitung XII*. Wichmann Verlag, Karlsruhe, pp. 12– 23.

Baltsavias, E. P., 2004. Object extraction and revision by image analysis using existing geodata and knowledge: current status and steps towards operational systems. *ISPRS Journal of Photogrammetry & Remote Sensing*, 58, pp. 129-151.

Baret, F., Jacquemoud, S. and Hanocq, J. F., 1993. About the soil line concept in remote sensing. *Advances in Space Research*, 13, pp. 281-284.

Baumgardner, M.F., Silva, L.F., Biehl, L.L. and Stoner, E.R., 1985. Reflectance properties of soils. In Brady, N. Ed. *Advances in Agronomy. vol. 38.* Academic Press, pp.1–44.

Ben-Dor, E. and Banin, A., 1994. Visible and near-infrared (0.4–1.1 μm) analysis of arid and semiarid soils. *Remote Sensing of Environment*, 48(3), pp. 261-274.

Ben-Dor, E. and Banin, A., 1995. Near-infrared analysis as a rapid method to simultaneously evaluate several soil properties. *Soil Science Society of America Journal*, 59, pp. 364–372.

Ben-Dor, E., Inbar, Y. and Chen, Y., 1997. The reflectance spectra of organic matter in the visible, near infrared and short wave infrared region (400–2500 nm) during a control decomposition process. *Remote Sensing of Environment*, 61, pp. 1–15.

Ben-Dor, E., Patkin, K., Banin, A. and Karnieli, K., 2002. Mapping of several soil properties using DAIS-7915 hyperspectral scanner data — a case study over clayey soils in Israel. *International Journal of Remote Sensing*, 23(6), pp. 1043–1062.

Benz, U., Hofmann, P., Willhauck, G., Lingenfelder, I. and Heynen, M., 2004. Multiresolution, object-oriented fuzzy analysis of remote sensing data for GIS ready information. *ISPRS Journal of Photogrammetry and Remote Sensing*, 58, pp. 239-258.

Berberoglu, S. and Akin, A., 2009. Assessing different remote sensing techniques to detect land use/cover changes in the eastern Mediterranean. *International Journal of Applied Earth Observation and Geoinformation*, 11(1), pp. 46-53.

Berberoglu, S., Curran, P.J., Lloyd, C.D. and Atkinson, P.M., 2007. Texture classification of Mediterranean land cover. *International Journal of Applied Earth Observation and Geoinformation*, 9(3), pp. 322-334.

Biard, F. and Baret, F., 1997. Crop residue estimation using multiband reflectance. *Remote Sensing of Environment*, 59 (3), pp. 530-536.

Blaschke, T, Lang, L. and Möller, M., 2005. Object-Based Analysis of Remote Sensing Data for Landscape Monitoring: Recent Developments. In *Anais XII Simpósio Brasileiro de Sensoriamento Remoto, Goiânia, Brasil*. 16-21 abril 2005, INPE.

Blaschke, T., 2003. Object-based contextual image classification built on image segmentation, *IEEE proceedings*, Washington DC, CD-ROM.

Bo, Y.C. and Wang, J.F., 2003. *The Classification for the Uncertainty of Remote Sensing Information and Scale Effect Model*. Geosciences Press. In Chinese.

Boardman, J., 2006. Soil erosion science: Reflections on the limitations of current approaches. *Catena*, 68(2-3), pp. 73-86.

Bocheng, X., Xuzhang, X., Jihua, W. and Guodong W., 2004. Spectral characteristics of brown-humid soil and estimation of soil organic matter content by soil reflectivity. *Chinese Journal of Soil Science*, 35(4), pp. 391-395.

Boschetti, M., Boschetti, L., Oliveri, S., Casati, L. and Canova, I., 2007. Tree species mapping with airborne hyper-spectral MIVIS data: the Ticino Park study case. *International Journal of Remote Sensing*, 28, pp. 1251–1261.

Bowers, S.A. and Hanks, R.J., 1965. Reflection of radiant energy from soils. *Soil Science*, 100, pp. 130-138.

Brandberg, T. and Warner, T., 2006. High resolution remote sensing. In Shao, G. and Reynolds, K. M. eds. *Computer Applications in Sustainable Forest Management*. Dordrecht, Springer Verlag, pp. 19-41.

Burnett, C. and Blaschke, T., 2003. A multi-scale segmentation/object relationship modelling methodology for landscape analysis. *Ecological Modelling*, 168(3), pp. 233-249.

Campbell, J. B., 2002. *Introduction to remote sensing*, 3rd ed. New York, London.

Carleer, A. P. and Wolef, E., 2006. Urban land cover multi-level region-based classification of VHR data by selecting relevant features. *International Journal of Remote Sensing*, 27, pp. 1035-1051.

Castilla, G. and Hay, G. J., 2008. Image objects and geographic objects. In Blaschke, T., Lang, S. and Hay, G. J. eds. *Object-Based Image Analysis: Spatial Concepts for Knowledge-Driven Remote Sensing Applications*. Heidelberg, Springer-Verlag, pp. 90-110.

Chabrillat, S., Kaufmann, H., Merz, B., Hill, J. and Mueller, A. A., 2003. Land Degradation Studies Using Spectroscopic Techniques. *Geophysical Research Abstracts*, 5, pp. 12660

Chaudhuri, B. and Sarkar, N., 1995. Texture segmentation using fractal dimension. *IEEE Transactions on Pattern Analysis and Machine Intelligence*, 17, pp. 72–77.

Chen, S. and Rao, P., 2008. Land degradation monitoring using multi-temporal Landsat TM/ETM data in a transition zone between grassland and cropland of northeast China. *International Journal of Remote Sensing*, 29 (7), pp. 2055–2073.

Chen, S.P. and Zhao, Y.S., 1990. *Geo-analysis on Remote Sensing*. Beijing: Survey Press. In Chinese.

Chen, Y. Q., Nixon, M. S. and Thomas, D. W., 1997. On texture classification. *International Journal of Systems Science*, 28(7), pp. 669-682.

Chica-Olmo, M. and Abarca-Hernández, F., 2000. Computing geostatistical image texture for remotely sensed data classification. *Computers & Geosciences*, 26(4), pp. 373-383.

Civanlar, R. and Trussell, H., 1986. Constructing membership functions using statistical data. *Fuzzy Sets and Systems*, 18, pp. 1–13.

Cloutis, E.A., 1996. Hyperspectral geological remote sensing: Evaluation of analytical techniques. *International Journal of Remote Sensing*, 17 (12), pp. 2215–2242.

Cohen, W. B., Maiersperger, T. K., Yang, Z. Q., Gower, S. T., Turner, D. P., Ritts, W. D., Berterretche, M. and Running, S. W., 2003. Comparisons of land cover and LAI estimates derived from ETM$^+$ and MODIS for four sites in North America: a quality assessment of 2000/2001 provisional MODIS products. *Remote Sensing of Environment*, 88(3), pp. 233-255.

Cozzolino, D. and Morón, A., 2006. Potential of near-infrared reflectance spectroscopy and chemometrics to predict soil organic carbon fractions. *Soil and Tillage Research*, 85(1-2), pp. 78-85.

Curran, P. J., 2001. Imaging spectrometry for ecological applications. International *Journal of Applied Earth Observation and Geoinformation*, 3(4), pp. 305-312.

Cyr, L., Bonn, F. and Pesant, A., 1995. Vegetation indices derived from remote sensing for an estimation of soil protection against water erosion. *Ecological Modelling*, 79(1-3), pp. 277-289.

Dalal, R. C. and Henry, R. J., 1986. Simultaneous determination of moisture, organic carbon, and total nitrogen by near infrared reflectance spectrophotometry. *Soil Science Society of America Journal*, 50, pp. 120–123.

Daughtry, C. S. T., Walthall, C. L., Kim, M. S., Brown De Colsyoum, E. and Mcmurtrey III, J. E., 2000. Estimating corn leaf chlorophyll concentration from leaf and canopy reflectance. *Remote Sensing of Environment*, 74, pp. 229– 239.

De Jong, S. M., 1994. Application of reflective remote sensing for land degradation studies in a Mediterranean environment. *Netherlands Geographical Studies*, KNAG, Utrecht. pp. 240.

De Jong, S. M., Hornstra, T. and Maas, H., 2001. An integrated spatial and spectral approach to the classification of Mediterranean land cover types: the SSC method. *International Journal of Applied Earth Observation and Geoinformation*, 3(2), pp. 176-183.

De Jong, S.M. and Van Der Meer, F.D., 2007. *Remote sensing image analysis: including the spatial domain*. The Netherlands Dordrecht: Kluwer Academic Publishers. pp. 359–365.

De Paz, J. M., Sánchez, J. and Visconti, F., 2006. Combined use of GIS and environmental indicators for assessment of chemical, physical and biological soil degradation in a Spanish Mediterranean region. *Journal of Environmental Management*, 79(2), pp. 150-62.

De Wit, R., Leibreich, J., Vernier, F., Delmas, F., Beuffe, H., Maison, P., Chossat, J.C., Laplace-Treyture, C., Laplana, R., Clavé, V., Torre, M., Auby, I., Trut, G., Maurer, D. and Capdeville, P., 2005. Relationship between land-use in the agro-forestry system of les Landes, nitrogen loading to and risk of macro-algal blooming in the Bassin d'Arcachon coastal lagoon (SW France). *Estuarine, Coastal and Shelf Science*, 62(3), pp. 453-465.

Dehaan, R.L. and Taylor, G.R., 2002. Field derived spectra of salinized soils and vegetation as indicators of irrigation induced soil salinization. *Remote Sensing of Environment*, 80, pp. 406-417.

Demattê, J. A. M., Campos, R. C., Alves, M. C., Fiorio, P. R. and Nanni, M. R., 2004. Visible–NIR reflectance: a new approach on soil evaluation. *Geoderma*, 121(1-2), pp. 95-112.

Doran, J. W. and Parkin, T. B., 1994. Defining and assessing soil quality. In Doran, J.W., Coleman, D.C., Bezdicek, D.F. and Stewart, B.A. eds. *Defining soil quality for sustainable environment*. Soil Sci.Soc. Am. Special publication N. 35, Madison, Wisconsin, US, pp. 3-21.

Dregne, H.E. and Boyadgiev, T.G., 1983. *Provision Methodology for Assessment and Mapping of Desertification*. FAO, Rome.

Duggin, M.J., Rowntree, R., Emmons, M, Hubbard, N., Odell, A.W., Sakhavat, H. and Lindsay, J., 1986. The use of multidate multichannel radiance data in urban feature analysis. *Remote Sensing of Environment*, 20(1), pp. 95-105.

Eals, M. and Silverman, I., 1994. The Hunter-Gatherer theory of spatial sex differences: Proximate factors mediating the female advantage in recall of object arrays. *Ethology and Sociobiology*, 15(2), pp. 95-105.

Escadafal, R., 1994. Soil spectral properties and their relationships with environmental parameters—Examples from arid regions. In Hill, J. and Mégier, J. eds. *Imaging Spectrometry—A Tool for Environmental Observations*. Kluwer Academic Publishers, Amsterdam, pp.71–87.

Escadafal, R., Belghith, A. and Ben Moussa, H., 1995. Strategy for the dynamic study of desertification. *Proceedings of the ISSS International Symposium Ouagadougou*, pp. 19-34.

Escadafal, R., Belghith, A. and He, B.M., 1994. Indices spectraux pourlatele detection dela degradation des milieux naturels en Tunisie aride. *Proceedings of the Sixth International Symposium on Physical Measurements and Signatures in Remote Sensing*, pp. 17–24.

FAO, 1976. *A Framework for Land Evaluation*. Soil Bulletin 32, FAO, Rome.

FAO, 2002. *Land Degradation Assessment in Dry lands*. FAO, Rome. :.

Fischer, A., 1991. Mapping and correlating desert soils and surfaces with imaging spectroscopy. *Proceeding of the Third Airborne Visible/lnfrared lmaging Spectrometer (AVIRIS) Workshop*. JPL Publication 91-28, pp. 23-32.

Frazier, B. E., 1989. Use of Landsat Thematic Mapper band ratios for soil investigations. *Advances in Space Research*, 9 (1), pp. 155-158.

Friedl, M. A., Davis, F. W., Michaelsen, J. and Moritz, M. A., 1995. Scaling and uncertainty in the relationship between the NDVI and land surface biophysical variables: An analysis using a scene simulation model and data from FIFE. *Remote Sensing of Environment*, 54(3), pp. 233-246.

Friedl, M.A., 1997. Examining the effects of sensor resolution and sub-pixel heterogeneity on spetral vegetation indices: implications for biophysical modeling. In Quattrochi, D.A. and Goodchild, M.F. eds. *Scale in Remote Sensing and GIS*. Lewis Publishers, Boca Raton, pp. 113–140.

Galvão, L. S. and Vitorello, I., 1998. Variability of laboratory measured soil lines of soils from southeastern Brazil. *Remote Sensing of Environment*, 63(2), pp. 166-181.

Gao, J. and Liu, Y.S., 2008. Mapping of land degradation from space: a comparative study of Landsat ETM[+] and ASTER data. *International Journal of Remote Sensing*, 29 (14), pp. 4029–4043

Gibson, C. C., Ostrom, E. and Ahn, T. K., 2000. The concept of scale and the human dimensions of global change: a survey. *Ecological Economics*, 32(2), pp. 217-239.

Giorgio, D. A., Gitelson, D., Rundquist, C., Leavitt, B., Barrow, T. and Holz, J. C., 2005. Assessing the potential of SeaWiFS and MODIS for estimating chlorophyll concentration in turbid productive waters using red and near-infrared bands. *Remote Sensing of Environment*, 96(2), pp. 176-187.

Goodchild, M. F., 2001. Metrics of scale in remote sensing and GIS. International *Journal of Applied Earth Observation and Geoinformation*, 3(2), pp. 114-120.

Goovaerts, P., Jacquez, G. M. and Marcus, A., 2005. Geostatistical and local cluster analysis of high resolution hyperspectral imagery for detection of anomalies. *Remote Sensing of Environment*, 95(3), pp. 351-367.

Grainger, A., 1992. Characterization and assessment of desertification process In Chapman G P. ed. *Desertification Grasslands: Their Biology and Management*. London: Academic Press, pp. 17-33.

Gregory, P. A., 2003. Imaging Spectroscopy for Desertification Studies: Comparing AVIRIS and EO-1 Hyperion in Argentina Drylands. *IEEE transactions on geoscience and remote sensing*, 41(6), pp. 1283-1296

Haboudane, Bonn, D. F., Royer, A., Sommer, S. and Mehl, A., 2002. Land degradation and erosion risk mapping by fusion of spectrally based information and digital geomorphometric attributes. *International Journal of Remote Sensing*, 18, pp. 3795-3820.

Halpern, D. F., 2000. *Sex Differences in Cognitive Abilities*. Lawrence Erlbaum Associates Publishers, Mahwah, New Jersey.

Haralick, R. M., Shanmugam, K. and Dinstein, I., 1973. Textural features for image classification. *IEEE Transactions on Systems, Man and Cybernetics*, 3, pp. 610-621.

Hay, G. J. and Castilla, G., 2008. Geographic Object-Based Image Analysis (GEOBIA): A new name for a new discipline. In Blaschke, T., Lang, S. and Hay, G. J. eds. *Object-Based Image Analysis: Spatial Concepts for Knowledge-Driven Remote Sensing Applications*. Heidelberg, Springer-Verlag, pp. 75-90.

Hay, G. J., Blaschke, T., Marceau, D. J. and Bouchard, A., 2003. A comparison of three image-object methods for the multiscale analysis of landscape structure. *Photogrammetric Engineering Remote Sensing*, 57, pp. 27–345.

Hay, G. J. and Castilla, G., 2006. Object-Based Image Analysis: Strengths, Weaknesses, Opportunities and Threats (SWOT). *International Archives of Photogrammetry, Remote Sensing and Spatial Information Sciences*, Vol. No. XXXVI-4/C42

Hay, G. J. and Marceau, D. J., 1998. Are image-objects the key for upscaling remotely sensed data? In *Proceedings of Modelling of Complex Systems*, July 12–17, New Orleans, USA, 88–92.

Hay, G. J. and Marceau, D. J., 2004. Multiscale object-specific analysis (MOSA): an integrative approach for multiscale landscape analysis. In De Jong, S.M. and Van der Meer, F.D. eds. *Remote Sensing and Digital Image Analysis, Including the Spatial Domain*. Remote Sensing and Digital Image Processing, vol.5, Kluwer Academic Publishers, Dordrecht, pp. 71–92.

Hay, G. J., Niemann, K. O. and Goodenough, D. G., 1997. Spatial thresholds, image-objects and upscaling: a multi-scale evaluation. *Remote Sensing of Environment*, 62 (1), pp. 1–19.

He, T., Wang, J., Guo, X.D. and Chen, Y., 2004. Study on Applying Hyperspectral Remote Sensing Technology in Land Quality Monitoring, In Ehlers, M., Posa,

F., Kaufmann, J., Ulrich Michel, U. and De Carolis, J. eds. *Remote Sensing for Environmental Monitoring, GIS Applications,and Geology IV*, Proceedings of SPIE Vol.5574, SPIE, Bellingham, W A, pp. 410-419. SPIE's Remote Sensing 2004, Spain.

Hellden, U., 1991. Desertification-time for an assessment. *Ambio*, 20, pp. 372-383.

Herold, M., Couclelis, H. and Clarke, K. C., 2005. The role of spatial metrics in the analysis and modeling of urban land use change. *Computers, Environment and Urban Systems*, 29(4), pp. 369-399.

Hill, J., Hostert, P. and Tsiurlis, G., 1998. Monitoring 20 years of intense grazing impact on the Greek island of Crete with earth observation satellites. *Journal of Arid Environments*, 39(2), pp. 165-178.

Hill, J., Megier, J. and Mehl, W., 1995. Land degradation, soil erosion and desertification monitoring in Mediterranean ecosystems. *Remote Sensing of Environment*, 12, pp. 237-260.

Hill, J. and Schütt, B., 2000. Mapping complex patterns of erosion and stability in dry mediterranean ecosystems. *Remote Sensing of Environment*, 74(3), pp. 557-569.

Hoffer, R. M. and Johannsen, C. J., 1969. Ecological potentials in spectral signature analysis. In Johnson, P.L. ed. *Remote Sensing in Ecology*. University of Georgia Press, Athens, pp.1–29.

Hofmann, T., Puzicha, J. and Buhmann, J., 1998. Unsupervised texture segmentation in a deterministic annealing framework. *IEEE Transactions on Pattern Analysis and Machine Intelligence*, 20, pp. 803–818.

Hudson, N. W., 1957. Erosion Control Research Progress Report: An Experiment at Henderson Research Station. *Rhodesia Agriculture*. pp.1953–1956.

Hudson, N.W., 1971. *Soil Conservation*. London, Batsford.

Hunt Jr. E. R., Rock, B. N. and Nobel, P. S., 1987. Measurement of leaf relative water content by infrared reflectance. *Remote Sensing of Environment*, 22(3), pp. 429-435.

Imeson, A.C., Cammeraat, L.H. and Perez-Trejo, F., 1995. Desertification response units. In Fantechi, R., Peter, D., Balabanis, P. and Rubio, J.L. eds. *Desertification in a European Context: Physical and Socio-Economic Aspects*. Luxembourg, Office for Official Publications of the European Communities. pp. 263–277.

Imeson, A. C., 2000. Indicators of land degradation in the Mediterranean. In Enne, G., Zanolla, C. and Peter, D. eds. *Desertification in Europe, mitigation strategies, land use and planning*. EUR19390, pp. 47-58.

Ingleby, H.R. and Crowe, T.G., 2000. Reflectance models for predicting organic carbon in Saskatchewan soils. *Canadian Agricultural Engineering*, 42 (2), pp. 57–63.

Jacquin, A., Misakova, L. and Gay, M., 2008. A hybrid object-based classification approach for mapping urban sprawl in periurban environment. *Landscape and Urban Planning*, 84(2), pp. 152-165.

Jarvis, C., 1994. Modelling forest ecosystem dynamics using multitemporal multispectral scanner (MSS) data. *Advances in Space Research*, 14(3), pp. 277-281.

Johansen, K., Phinn, S., Lowry, J. and Douglas, M., 2008. Quantifying indicators of riparian condition in Australian tropical savannas: integrating high spatial resolution imagery and field survey data. *International Journal of Remote Sensing*, 29 (23), pp. 7003–7028.

Kamagata, N., Hara, K., Mori, M., Akamatsu, Y., Li, Y. and Hoshino, Y., 2008. Object-based classification of IKONOS data for vegetation mapping in Central Japan. In Blaschke, T., Lang, S. and Hay, G.J. eds. *Object-Based Image Analysis -Spatial Concepts for Knowledge-Driven Remote Sensing Applications*. Heidelberg: Springer-Verlag, pp. 459-476.

Kim, M. S., Daughtry, C. S. T., Chappelle, E. W., Mcmurtrey III, J. E. and Walthall, C. L., 1994. The use of high spectral resolution bands for estimating absorbed photosynthetically active radiation. *Proceedings of the 6th Symposium on Physical Measurements and Signatures in Remote Sensing*, pp. 299–306.

Kim, M., Madden, M. and Warner. T., 2008. Estimation of optimal image object size for the segmentation of forest stands with multispectral IKONOS imagery. In Blaschke, T., Lang, S. and Hay, G.J. eds. *Object-Based Image Analysis -Spatial Concepts for Knowledge-Driven Remote Sensing Applications*. Heidelberg: Springer-Verlag, pp. 459-476.

Kosko, B., 1992. *Neural networks and fuzzy systems, a dynamical systems approach to machine intelligence*. Prentice Hall International, Englewood Cliffs NJ 07632 .

Krishnan, P., Alexander, J.D., Butler, B.J. and Hummel, J.W., 1980. Reflectance technique for predicting soil organic matter. *Soil Science Society of America Journal*, 44, pp. 1282–1285.

Kruse, F.A., Lefkoff, A.B., Boardman, J.W., Heidebrecht, K.B., Shapiro, P.J. and Goetz, A.F.H., 1993. The spectral image processing system (SIPS)-interactive visualisation and analysis of imaging spectrometer data. *Remote Sensing of Environment*, 44, pp. 145–163.

Laine, A. and Fan, J., 1996. Frame representations for texture segmentation. *IEEE Transactions on Image Processing*, 5, pp. 771–779.

Laliberte, A.S., Fredrickson, E.L. and Rango, A., 2007. Combining decision trees with hierarchical object-oriented image analysis for mapping arid rangelands. *Photogrammetric Engineering and Remote Sensing*, 73 (2), pp. 197–207.

Lam, N. and Quanttrochi, D. A., 1992. On the issues of scale, resolution and fractal analysis in the mapping sciences. *Professional Geographer*, 44, pp. 88-98.

Lang, S., 2005. *Image Objects and Landscape Objects – Interpretation, Hierarchical Representation and Significance* – unpublished PhD thesis, Salzburg

Lang, S., 2008. Object-based image analysis for remote sensing applications: modeling reality – dealing with complexity. In Blaschke, T., Lang, S. and Hay, G. J. eds. *Object-Based Image Analysis: Spatial Concepts for Knowledge-Driven Remote Sensing Applications*. Heidelberg, Springer-Verlag, pp. 3-28.

Lang, S. and Blaschke, T., 2003. Hierarchical Object Representation: Comparative Multi-Scale Mapping of Anthropogenic and Natural Features. In *ISPRS Archives*, Vol XXXIV, Part 3/W8, pp. 181-186.

Lang, S. and Langanke, T., 2005. Multiscale GIS tools for site management. *Journal for Nature Conservation*, 13(2-3), pp. 185-196.

Lang, S. and Tiede, D., 2007. *Conditioned Information For GMES Applications*. Presentation at the Definiens GMES Research Award 2007, March 29.

Latz, K., Weismiller, R. A., Van Scoyoc, G. E. and Baumgardner, M.F., 1984. Characteristics variations in spectral reflectance of selected eroded Alfisols. *Soil Science Society of America Journal*, 48, pp. 1130–1134.

Leone, A. P. and Sommer, S., 2000. Multivariate analysis of laboratory spectra for the assessment of soil development and soil degradation in the Southern Apennines. *Remote Sensing of Environment*, 72, pp. 346-359.

Lewinski, S.T. and Polawski, Z.F., 2005. The comparison of interpretation possibility of RGB composite of LISS-III and ETM$^+$ scanner. Proceedings of the 24th Symposium of European Association of Remote Sensing Laboratories, New strategies for European Remote Sensing, 25-27 May 2004, Dubrovnik, Croatia, Oluic. Millpress.

Li, X.C., Wang, J. and Li, Y.H., 2008. Estimation of soil parameters with hyperspectral data based on fuzzy setanalysis.*Geography and geographic information science*, 24(4), pp. 25-28. In Chinese.

Li, X.C., Zong, X.C. and Li, J., 2003. Models of fuzzy analysis and forecast and their application. *Journal of Shandong Agricultural University*, 34(2), pp. 267-271. In Chinese.

Linn, M. C. and Pulos, S., 1983. Male-female differences in predicting displaced volume: Strategy usage, aptitude relationships, and experience influences. *Journal of Educational Psychology*, 75 (1), pp. 86-96.

Liu, W.D., Baret, F., Gu, X.F., Tong, Q.X., Zheng, L.F. and Zhang, B., 2002. Relating soil surface moisture to reflectance. *Remote Sensing of Environment* 81(2-3), pp. 238-246.

Lu, X. J., Qing, C. Z., Zhang, H. Y. and Chen, W. M., 2005. Spatial cognitive mode and its application. *Journal of Remote Sensing*, 9(3), pp. 277-285. In Chinese.

Luo, J. C., 2000. Remote-Sensing Intelligent Geo-Interpretation Model and its Geo-Cognition Issue. *Progress in Geography*, 19(4), pp. 289-296. In Chinese.

Luo, J. C., Zhou, C. H. and Yang, Y., 2001. Land-cover and land-use classification based on remote sensing intelligent Geo-interpreting model. *Journal of Natural Resources*, 16(2), pp. 179-183. In Chinese.

Ma, A. N., 1997. *Remote Sensing Information Model*. Beijing: Beijing University Press. In Chinese.

Maccoby, E. and Jacklin, C. N., 1974. *Psychology of Sex Differences*. Stanford: Stanford Univesity Press.

Mallinis, G., Koutsias, N., Tsakiri-strati, M. and Karteris, M., 2008. Object-based classification using Quickbird imagery for delineating forest vegetation polygons in a Mediterranean test site. *ISPRS Journal of Photogrammetry & Remote Sensing*, 63, pp. 237–250.

Manakos, I., Scheneider, T. and Ammer, U., 2000. A Comparison Between the ISODATA and the eCognition Classification Methods on Basis of Field Data. *IAPRS 2000*, 33 (Supp. B7), pp.133-139.

Mao, J. and Jain, A., 1992. Texture classification and segmentation using multi-resolution simultaneous autoregressive models. *Pattern Recognition*, 25 (2), pp. 173– 188.

Marceau, D. J., Howarth, P. J. and Gratton, D. J., 1994. Remote sensing and the measurement of geographical entities in a forested environment: the scale and spatial aggregation problem. *Remote Sensing of Environment*, 49(2), pp. 93-104.

Marceau, D.J., 1999. The scale issue in the social and natural sciences. *Canadian Journal of Remote Sensing*, 25 (4), pp. 347–356.

Mathieu, R., Pouget, M., Cervelle, B. and Escadafal, R., 1998. Relationships between Satellite-Based Radiometric Indices Simulated Using Laboratory Reflectance Data and Typic Soil Color of an Arid Environment. *Remote Sensing of Environment*, 66(1), pp. 17-28.

Matinfar, H.R. and Sarmadian, F., 2007. Comparisons of object-oriented and pixel-based classification of land use/land cover types based on Lansadsat 7 spectral bands. *Journal of Agriculture and Environment*, 2 (4), pp. 448-456.

Menenti, M., Azzali, S. and Boss, M., 1999. *Early warning on desertification and land degradation*. Report for the 3d meeting of the EC/MS expert group on desertification, Brussels, 7 Apr 99, The Netherlands

Mohamed Chikhaoui, Bonn, F. and Bokoye, A. I., 2005. A spectral index for land degradation mapping using ASTER data: Application to a semi-arid Mediterranean catchment. *International Journal of Applied Earth Observation*, 7(2), pp. 140-153

Mougenot, B. and Cailleau, D., 1995. Identification par télédétection des sols dégradés d'un domaine sahélien au Niger. *Proceedings of the ISSS International Symposium Ouagadougou*, working groups RS and MD, pp. 169-179.

Mulders, M., 2001. Advances in the application of remote sensing and GIS for surveying mountainous land. *International Journal of Applied Earth Observation and Geoinformation*, 3(1), pp. 3-10.

Nasir, M., Khan, V. V., Rastoskuev, Y. S. and Shiozawa, S., 2005. Assessment of hydrosaline land degradation by using a simple approach of remote sensing indicators. *Agricultural Water Management*, 77, pp. 96-109.

Nazzareno, D. and Michele, C., 2004. Multivariate indicator Kriging approach using a GIS to classify soil degradation for Mediterranean agricultural lands. *Ecological Indicators*, 4, pp. 177-187.

Nicholas, J. M., David, S. and Thomas, G., 1997. *World Atlas of Desertification* (second edition). London: Arnold.

Nicholson, S. E., Tucker, C. J. and Ba, M. B., 1998. Desertification, drought, and surface vegetation: An example from the West African Sahel. *Bulletin of the American Meteorological Society*, 79, pp. 1-15.

Okin, G.S., Murray, B. and Schlesinger, W.H., 2001. Degradation of sandy arid shrubland environments: observations, process modeling and management implications. *Journal of Arid Environments*, 47(2), pp. 123-144.

Oldeman, L. R., Hakkeling, R. T. A. and Sombroek, W. G., 1990. *World Map of the Status of Human induced Soil Degradation: An Explanatory Note*. 2nd revised Edn. ISRIC, Wageningen, The Netherlands.

Oldeman, L.R., 2000. *Impact of soil degradation: a global scenario*. In Report 2000/01, ISRIC, Wageningen.

Omuto, C.T. and Shrestha, D.P., 2007. Remote sensing techniques for rapid detection of soil physical degradation. *International Journal of Remote Sensing*, 28 (21), pp. 4785–4805.

O'Neill, E. G., O'Neill, R. V. and Norby, R. J., 1991. Hierarchy theory as a guide to mycorrhizal research on large-scale problems. *Environmental Pollution*, 73(3-4), pp. 271-284.

Oruc, M., Marangoz, A.M. and Buyuksalih, G., 2004. Comparison of pixel-based and object-oriented classification approaches using landsat-7 ETM spectral bands. *Proceedings of ISPRS Conference*, 19-23 July, Istanbul.

Page, N.R., 1974. Estimation of organic matter in Atlantic coastal plain soils with a colour difference meter. *Agronomy Journal*, 66, pp. 652–653.

Pellenq, J., Kalma, J., Boulet, G., Saulnier, G. M., Wooldridge, S., Kerr, Y. and Chehbouni, A., 2003. A disaggregation scheme for soil moisture based on topography and soil depth. *Journal of Hydrology*, 276(1-4), pp. 112-127.

Pierre, G., Geoffrey, M. J. and Andrew, M., 2005. Geostatistical and local cluster analysis of high resolution hyperspectral imagery for detection of anomalies. *Remote Sensing of Environment*, 95(3), pp. 351-367.

Pieters, C. M. and Mustard, J. F., 1988. Exploration of crustal/mantle material for the earth and moon using reflectance spectroscopy. *Remote Sensing of Environment*, 24(1), pp. 151-178.

Raffy, M., 1992. Change of scale in models of remote sensing: A general method for spatialization of models. *Remote Sensing of Environment*, 40(2), pp. 101-112.

Raffy, M. and Gregoire, C., 1998. Semi-empirical models and scaling: a least square method for remote sensing experiments. *International Journal of Remote Sensing*, 19, pp. 2527-2541.

Reeves III, J., McCarty, G. and Mimmo, T., 2002. The potential of diffuse reflectance spectroscopy for the determination of carbon inventories in soils. *Environmental Pollution*, 116 (Supplement 1), pp. S277-S284

Rock, B.N., Williams, D.L., Moss, D.M., Lauten, G.N. and Kim, M., 1994. High-spectral resolution field and laboratory optical reflectance measurements of red spruce and eastern hemlock needles and branches. *Remote Sensing of Environment*, 47(2), pp. 176-189.

Röder, A., Udelhoven, T., Hill, J., Del Barrio, G. and Tsiourlis, G., 2008. Trend analysis of Landsat-TM and -ETM+ imagery to monitor grazing impact in a rangeland ecosystem in Northern Greece. *Remote Sensing of Environment*, 112(6), pp. 2863-2875

Rossi, R. E., Dungan, J. L. and Beck, L. R., 1994. Kriging in the shadows: Geostatistical interpolation for remote sensing. *Remote Sensing of Environment*, 49(1), pp. 32-40.

Schiff, W. and Oldak, C., 1990. Accuracy of Judging Time to Arrival: Effects of Modality, Trajectory, and Gender. *Journal of Experimental Psychology: Human Perception and Performance*, 16(2), pp. 303-316.

Shields, J.A., Paul, E.A., Arnaud, S. and Head, W.K., 1968. Spectrophotometric measurement of soil colour and its relationship to moisture and organic matter. *Canadian Journal of Soil Science*, 48, pp. 271–280.

Shrestha, D.P., Margate, D.E., Van Der Meer, F. D. and Anh, H.V., 2005. Analysis and classification of hyperspectral data for mapping land degradation: An application in southern Spain. *International Journal of Applied Earth Observation and Geoinformation*, 7(2), pp. 85-96.

Sivakumar, M. V. K. and Ndiangui, N. eds. *Climate and Land Degradation*. Heidelberg: springer-Verlag, 2007.

Smith, B., 2001. Fiat Objects. *Topoi*, 20, pp. 31-148.

Smith, B. and Mark, D. M., 1998. Ontology and Geographic Kinds. *Proc. 8th Int. Symp. on Spatial Data Handling (SDH'98)*, pp. 308-320

Smith, G. A. and McPhee, K. A., 1987. Performance on a coincidence timing task correlates with intelligence. *Intelligence*, 11(2), pp. 161-167.

Stein, A., Van Der Meer, F. D. and Gorte, B., 1999. *Spatial Statistics for Remote Sensing*. Dordrecht: Kluwer Academic Publishers.

Stoner, E.R. and Baumgardner, M.F., 1981. Characteristic variation in reflectance on surface soils. *Soil Science Society of America Journal*, 45, pp. 1161–1165.

Stroosnijder, L., 2005. Measurement of erosion: Is it possible? *Catena*, 64, pp. 162-173.

Sun, W. and Li, B.S., 1999. An approach to classification and assessment of desertification. *Geographical Research*, 18(3), pp. 225-230. In Chinese.

Tarr, M. J. and Cheng, Y. D., 2003. Learning to see faces and objects. *Trends in Cognitive Sciences*, 7(1), pp. 23-30.

Thomas, S., Jürgen, B. and Schmidhalter, U., 2006. High resolution topsoil mapping using hyperspectral image and field data in multivariate regression modeling procedures. *Geoderma*, 136(1-2), pp. 235-244.

Thomas, D. S. G. and Middleton, N. J., 1994. *Desertification: exploding the myth*. Chichester: John Wiley&Sons.

Thomasson, J.A., Sui, R. and Atkins, D.C., 2001. Soil reflectance sensing for determining soil properties in precision agriculture. *ASAE Paper vol. 001044*, ASAE, St. Joseph, Michigan.

Tripathy, G.K., 1996. Monitoring of desertification process in Karnataka state of India using multi-temporal remote sensing and ancillary information using GIS. *International Journal of Remote Sensing*, 17(12), pp. 2243-2257.

Turner, B.L., Skole, D. and Sanderson, S., 1995. *Land Use and Land Cover Change: Science/ Research Plan*. IGBP Report No. 35, HDP Report No. 7. Stockholm and Geneva.

Turner, D. P., Dodson, R. and Marks, D., 1996. Comparison of alternative spatial resolutions in the application of a spatially distributed biogeochemical model over complex terrain. *Ecological Modeling*, 90(1), pp. 53-67.

Turner, D. P., Ritts, W. D., Cohen, W. B., Gower, S. T., Zhao, M. S., Running, S. W., Wofsy, S. C., Urbanski, S., Dunn, A. L. and Munger, J. W., 2003. Scaling Gross Primary Production (GPP) over boreal and deciduous forest landscapes in support of MODIS GPP product validation. *Remote Sensing of Environment*, 88(3), pp. 256-270.

Turner, M., 1989. Landscape ecology: the effect of pattern on process. *Annual Review of Ecology and Systematics*, 20, pp. 171-197.

UNCOD, 1977. *Plan of action to stop desertification*. In Report of the UN conference on desertification, vol. A/CONF 74/36, UNEP, Nairobi.

UNEP, 1987. *Sands of Change*. In UNEP Environmental Brief No.2.

Ungar, A.A., 2003. Seeing the Möbius disc-transformation group like never before. *Computers & Mathematics with Applications*, 45(4-5), pp. 805-822.

Vagen, T., Shepherd, K. D. and Walsh, M. G., 2005. Sensing landscape level change in soil fertility following deforestation and conversion in the highlands of Madagascar using VIS-NIR spectroscopy. *Geoderma*, 133, pp. 281-294.

Van Der Meer, F. D., 1997. Mineral mapping and Landsat Thematic Mapper image classification using spectral unmixing. *Geocarto International*, 12, pp. 27–40.

Van Der Meer, F. D., 2001. Basic physics of spectrometry. In Van Der Meer, F.D. and De Jong, S.M. eds. *Imaging Spectrometry*. Dordrecht: Kluwer Academic Publishers. pp. 3–16.

Van Der Meer, F. D., 2006. Indicator kriging applied to absorption band analysis in hyperspectral imagery: A case study from the Rodalquilar epithermal gold mining area, SE Spain. *International Journal of Applied Earth Observation and Geoinformation*, 8(1), pp. 61-72.

Walsh, S. J., Butler, D. R. and Malanson, G. P., 1998. An overview of scale, pattern, process relationships in geomorphology: a remote sensing and GIS perspective. *Geomorphology*, 21 (3-4), pp. 183-205.

Wang, J., 2006. *Methodologies of Remote Sensing Monitoring and Evaluation on Land Resources*. Science Press, Beijing. In Chinese.

Whiteside, T. and Ahmad, K., 2005. A comparison of object-oriented and pixel-based classification methods for mapping land cover in northern Australia. Proceedings of SSC2005 Spatial intelligence, innovation and praxis. *The national biennial Conference of the Spatial Sciences Institute*, Melbourne: Spatial Sciences Institute.

Williams, M. A. and Balling, R. C., 1996. *Interactions of desertification and climate*. London: Arnold.

Wood, E. F., 1994. Scaling, soil moisture and evapotranspiration in runoff models. *Advances in Water Resources*, 17(1-2), pp. 25-34.

Woodcock, C. E and Strahler, A. H., 1987. The factor of scale in remote sensing. *Remote Sensing of Environment*, 21(3), pp. 311-332.

Woodcock, C. E., Strahler, A. H. and Jupp, D.L.B., 1988. The use of variograms in remote sensing: real digital images. *Remote Sensing of Environment*, 25(3), pp. 349-379.

Wu J., He T. and Chen P.G., 2006. Study on land degradation mapping using Hyperion data in Hengshan region in China. *Progress in Geography*, 25(2), pp. 131-138. In Chinese.

Wu, J. G. and Marceau, D., 2002. Modeling complex ecological systems: an introduction. *Ecological Modelling*, 153 (1-2), pp. 1-6.

Xu, B.B., 1986. The correlationship of soil physicochemical characteristics and Reflectance Characteristics. *Journal of soil*. Vol.41. Science Press, Beijing.

Yu, Q.P., Gong, N., Clinton, G., Biging, M.K. and Shirokauer, D., 2006. Object-based detailed vegetation classification with airborne high spatial resolution remote sensing imagery. *Photogrammetic Engineering and Remote Sensing*, 72(7), pp. 799-811.

Zhou, C.H., Luo, J.C. and Yang, X.M., 2001. *The Comprehension and Analysis for Remote Sensing Image Based on Geography*. Science Press, Beijing. In Chinese.

Zhou, W., Troy, A. and Grove, J. M., 2008. Object-based land cover classification and change analysis in the Baltimore metropolitan area using multi-temporal high resolution remote sensing data. *Sensors*, 8, pp. 1613−1636.

Zonneveld, I.S., 1989. The land unit — A fundamental concept in landscape ecology and its applications. *Landscape Ecology*, 3 (2), pp. 67-86.